PROJECTE O TESINA D'ESPECIALITAT

Títol

VFT® - Prefabricated Composite Construction Method

Autor/a

Agnieszka Skalska

Tutor/a

Joan Ramon Casas

Departament

Enginyeria de la construcció

Intensificació

Tecnologia i construcció d´estructures

Data

Juny de 2009

Escola Tècnica Superior d'Enginyers de Camins, Canals i Ports de Barcelona

UNIVERSITAT POLITÈCNICA DE CATALUNYA

Títol

VFT® - Prefabricated Composite Construction Method

Autor/a

Agnieszka Skalska

Tutor/a

Joan Ramon Casas

Especialitat

Tecnologia i Construcció d´Estructures

Data

Juny de 2009

Resum

Este documento describe el método VFT como una solución eficiente y estética para puentes con vanos de corta y media longitud. Actualmente, el método presentado en este informe es un fuerte competidor de los puentes de hormigón. Esta combinación entre un uso económico del acero y del hormigón proporciona numerosas ventajas y hace que sea cada vez más usado. Este informe presenta la idea de las vigas VFT, el proceso de fabricación y la rápida construcción pueden explicar la popularidad de esta tecnología especialmente en Alemania y Polonia.

Para mostrar las diferencias entre un puente mixto y un puente mixto de vigas prefabricadas se propone una estructura de 2 vigas continuas de 50m de longitud (dos vanos: 25,00m + 25,00m) con las siguientes vigas transversales:

- 4 vigas mixtas (acero + hormigón "in situ")

- 4 vigas VFT

Se presentan dos modelos de construcción en FEM (Método de Elementos Finitos), usando el software ROBOT MILLENNIUM, y elementos de dimensionado.

Como resultado del desarrollo de las vigas VFT e investigaciones de conectores continuos se ha creado una nueva técnica VFT llamada Método de Construcción VFT-WIB. Este documento introduce el diseño estático y a fatiga de los conectores continuos VFT-WIB.

Para resumir los métodos descritos, se muestran algunos ejemplos ejecutados en Alemania y Polonia

SUMMARY

This document describes VFT method as an efficient and aesthetic solution for small and medium span bridges. Nowadays, the technology presented in this paper is surely strong competition for concrete bridges. This combination of economic use of steel and concrete materials gives many advantages and causes the number of composite bridges to grow bigger and bigger. This paper presents the idea of VFT girders, manufacturing process and fast assembly which can explain the popularity of this technology especially in Germany and Poland.

To show the differences in design process between typical composite bridges and bridges with composite prefabricated girders, two 50,00m length continuous beams (two spans: 25,00m + 25,00m) have been proposed:

- Cross-section consisting of 4 composite girders (steel + "in-situ" concrete),
- Cross-section consisting of 4 VFT girders.

Two construction models in FEM (Finite Element Method), using ROBOT MILLENNIUM software, and elements of dimensioning have been presented.

Further development of VFT beams and investigations in continuous connectors resulted in the creation of the new kind of VFT technique which is called the VFT-WIB construction method. This paper introduces the static and fatigue design of VFT-WIB continuous shear connectors.

To sum up the methods described, some examples of bridge executing in Germany and Poland have been shown.

UNIVERSITAT POLITÈCNICA DE CATALUNYA

RESUMEN

Este documento describe el método VFT como una solución eficiente y estética para puentes con vanos de corta y media longitud. Actualmente, el método presentado en este informe es un fuerte competidor de los puentes de hormigón. Esta combinación entre un uso económico del acero y del hormigón proporciona numerosas ventajas y hace que sea cada vez más usado. Este informe presenta la idea de las vigas VFT, el proceso de fabricación y la rápida construcción pueden explicar la popularidad de esta tecnología especialmente en Alemania y Polonia.

Para mostrar las diferencias entre un puente mixto y un puente mixto de vigas prefabricadas se propone una estructura de 2 vigas continuas de 50m de longitud (dos vanos: 25,00m + 25,00m) con las siguientes vigas transversales:

- 4 vigas mixtas (acero + hormigón "in situ")
- 4 vigas VFT

Se presentan dos modelos de construcción en FEM (Método de Elementos Finitos), usando el software ROBOT MILLENNIUM, y elementos de dimensionado.

Como resultado del desarrollo de las vigas VFT e investigaciones de conectores continuos se ha creado una nueva técnica VFT llamada Método de Construcción VFT-WIB. Este documento introduce el diseño estático y a fatiga de los conectores continuos VFT-WIB.

Para resumir los métodos descritos, se muestran algunos ejemplos ejecutados en Alemania y Polonia.

UNIVERSITAT POLITÈCNICA
DE CATALUNYA

CONTENT:

Summary

Resumen

1. INTRODUCTION

1.1. Definition of the composite construction

In structural engineering, ***composite construction*** exist when two different materials are bound together so strongly that they act together *as a single unit* from a structural point of view. One common example involves steel beams supporting concrete floor slab. If the beam is *not connected firmly* to the slab, then the slab transfers all of its weight to the beam and the slab contributes nothing to the load carrying capability of the beam. On the other hand, if the slab is *connected positively* to the beam with studs, then a portion of the slab can be assumed to act compositely with the beam. In effect, this composite creates a larger and stronger beam than would be provided by the steel beam alone[1].

Within the European Union, composite constructions are commonly applied to bridges, however to buildings they are applied in Western European countries[2]. The followings composite types are the most popular in bridge engineering:

- concrete (prefabricated) – concrete (in-situ) → Figure 1.1.,
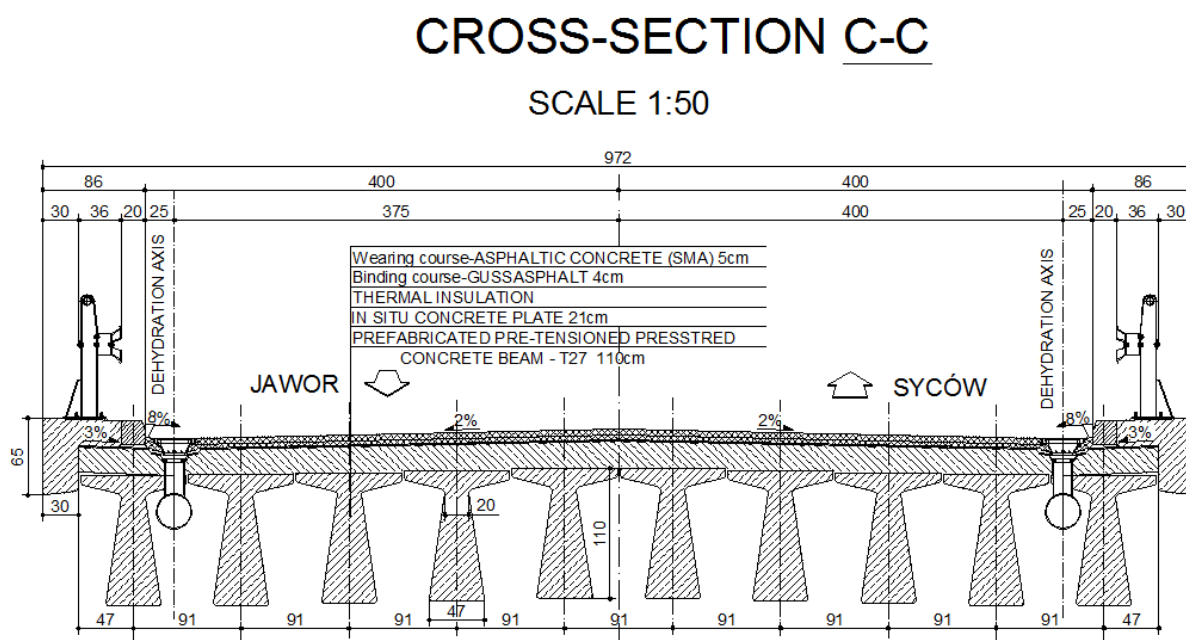- concrete – steel → Figure 1.2.,

Fig. 1.1. Road bridge cross-section.

This document is devoted to steel-concrete composite construction. From the designer's point of view, this kind of structure is complicated, because the majority problems for both steel and concrete construction appear during the design phase. Moreover there are a lot of issues which are typical for the composite construction.
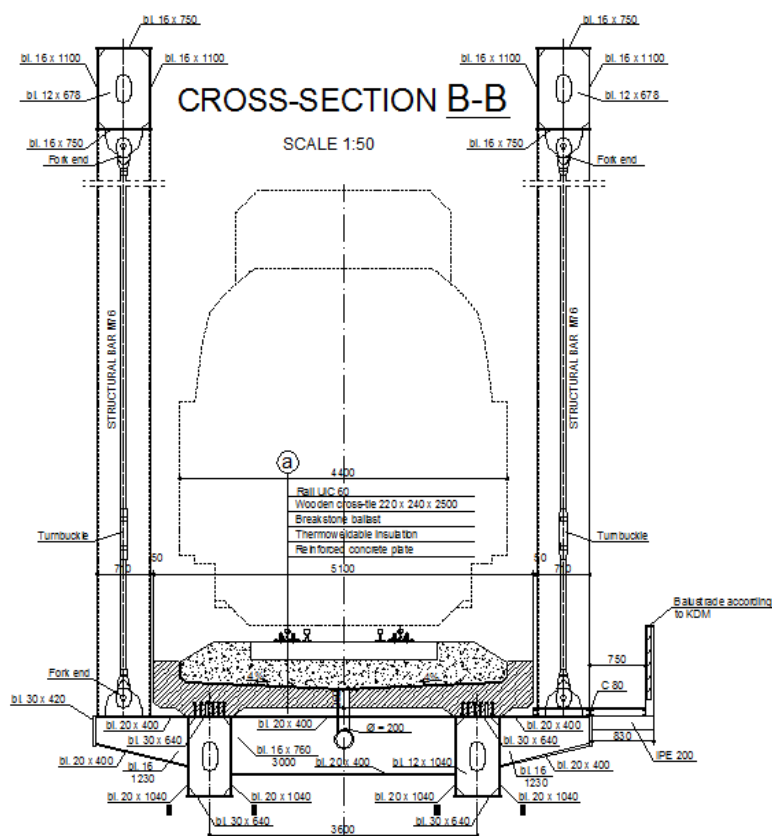
1.2. Railway bridge cross-section.

1.2. Origin and development of VFT technology

Essential changes in economic conditions and technical requirements within the last few years in Germany caused increased interest in composite bridges. Particularly, public investors extended a demand for correct and reliable solutions. The most important factors in the development of composite bridges are:

- exploitation (increased load capacity),
- maintenance (increased durability),
- economy (reduced steel prices) [3].

The number of this type of bridge in public tenders underlined this tendency. These changes also give good reasons to rethink standard construction methods for composite bridges. There is much room for improvement in construction and procedures, particularly in structures with short and medium-sized spans that are built over existing traffic routes.

A new method for economic construction of composite deck bride with a span of 20 to 80 metres has now been developed, and is known as ***the prefabricated composite (VFT®) construction method***. It unites the benefits of conventional composite and prefabricated construction methods and consists of an integral system of prefabricated assembly units.

The starting point for development of the system were two cross section designs for deck bridges with small spans, made up of prefabricated elements and supplementary in-situ concrete slab, which proved very successful on the market:

- Prefabricated prestressed concrete girders,
- Composite cross sections with filigree slabs.

Since the 1970s, multi-web T-beams made of prefabricated prestressed concrete girders with wide flanges have been used as the formwork for

Fig.1.3.VFT-girder.

laying in-situ concrete slabs. Unfortunately, use of the prestressed concrete girder is only limited to railway bridges up to about 30 metres in length and in road bridges up to about 40 metres, since it is itself very heavy. In this span range, the prestressed concrete used for composite construction method is usually superior. The price benefits of prestressed concrete girders are mainly due to the fact that an extensive amount of prefabrication work is involved in the prestressed concrete construction method, reducing the amount of work on the construction site.
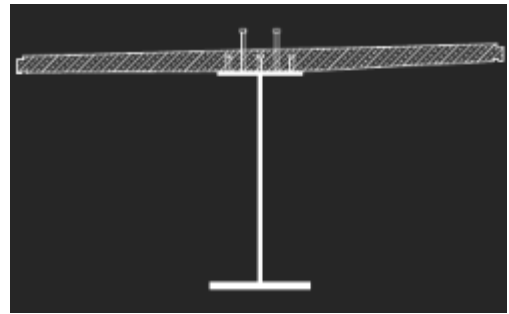
Another alternative for construction is the use of transverse reinforced concrete girder. In this case, all the reinforced concrete work usually needed on the construction site is eliminated.

All the supporting elements in the superstructure can be handled by the main contractor, who is normally only responsible for the solid structure building work. In this way, an efficient modular construction system was development. The VFT construction method evolved from these developments [4].

Fig. 1.4. VFT girder.

2. OBJECTIVES

Nowadays VFT method becomes more and more popular in Poland. Due to the efficient use of steel and concrete in the cross section, girders prefabrication and fast assembly, this technology opens up new possibilities. This paper introduces VFT system as a good alternative for composite bridges and shows differences in design process for both of these solutions. Two concepts of road bridge have been proposed to demonstrate materials savings and advantages of use VFT girders.

3. DESCRIPTION OF THE VFT TECHNOLOGY

3.1. Idea of technology

The essence of **_the VFT system_** is applying prefabricated composite girders with **_10-12cm thickness active concrete flange_**, manufactured in a factory. This flange simultaneously makes up formwork of the deck and actively co-operates with beam to contribute to the dead and useful load carrying capability.
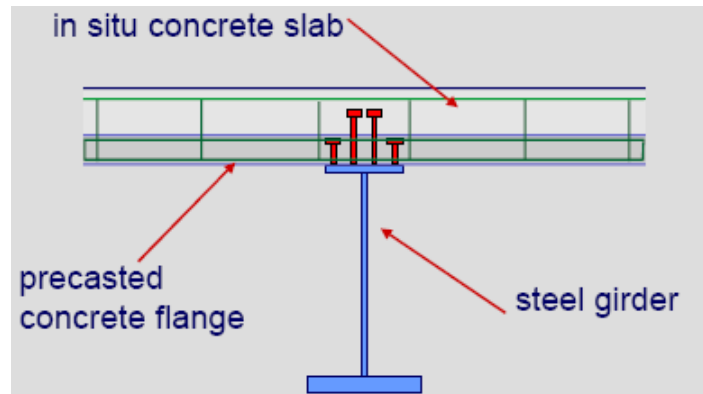

Fig. 3.1. VFT girder.

Additionally, the prefabricated concrete flange stabilises the girder during transport and during the construction phase while the in-situ concrete slab is laid. The limits involved in handling a construction unit, such as weight and rigidity, are extended. This means that larger spans can be bridged with more slender constructions, which are not possible where prestressed concrete girders are used. Because the weight of the individual construction unit is reduced while the same rigidity is maintained, the handling limits are extended [4].
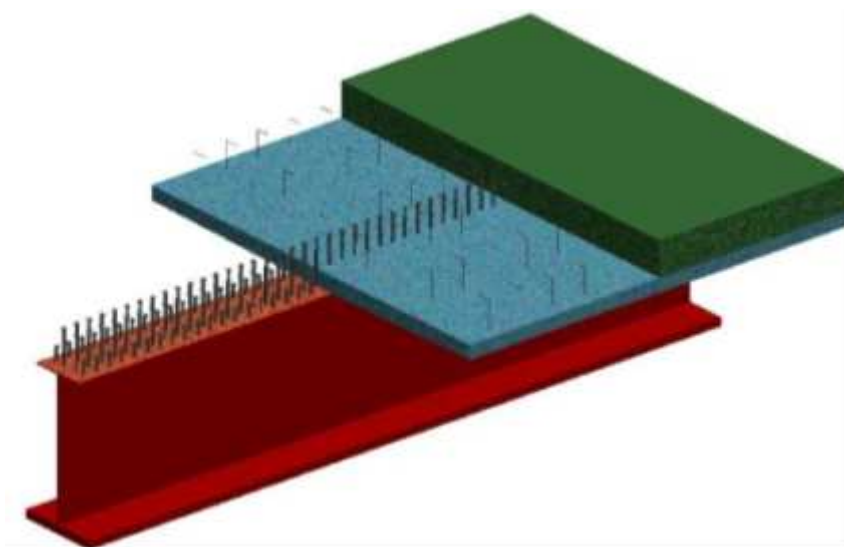

Fig. 3.2. Ideological cross-section.

Prefabricated units are placed next to each other on previously prepared supports and jointed together at assembly time. Then the deck's slab and supported cross-bars are carried out. In this way a monolithic span comes into being although the bigger part of the manufacturing process takes place out of the construction site.

Fig. 3.3. VFT girder showed during "Autostrada-Polska" fair in 2002 year, in Kielce.

The typical way to execute a bridge using VFT technology (applied in Germany) is showed in figures 3.4. and 3.5., on the example of continuous span. There is a clear split into **stage I** (prefabricated unit manufacture) and **stage II** (span assembly). The manufacturing process (figure 3.3.) takes place entirely in a factory, from where prefabricated composite units are transported to the construction site by road transport and built into a span (figure 3.4)[5].
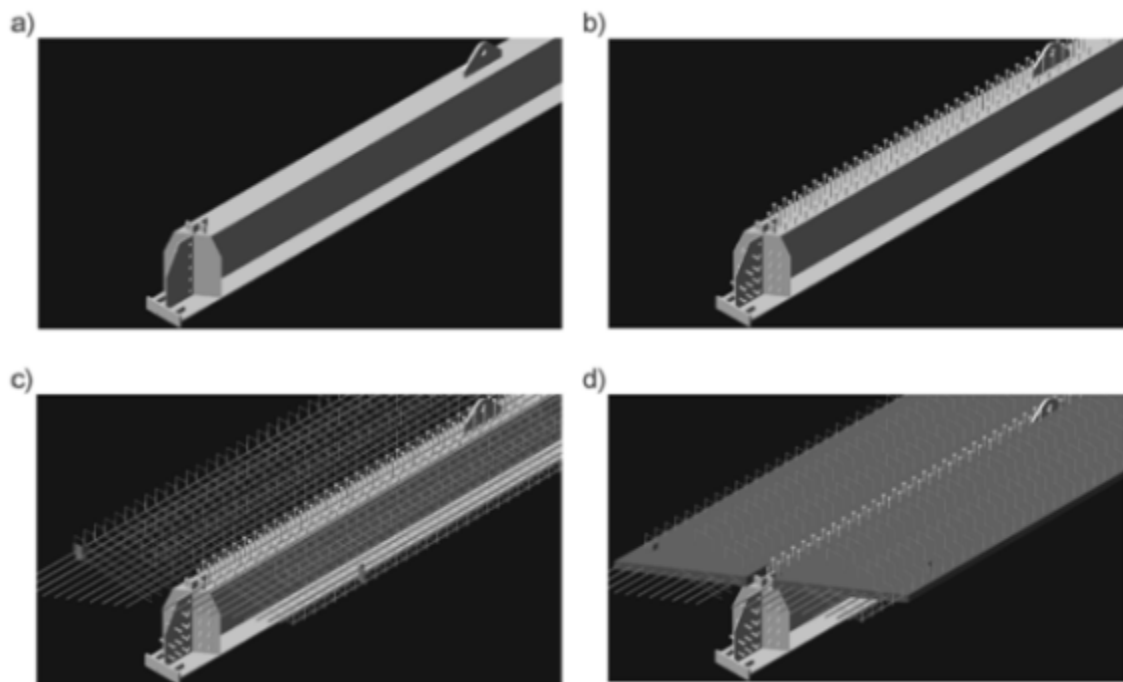

Fig. 3.4. VFT prefabrication phase: a) welded plate girder, b) carrying out of different height studs, c) prefabricated unit reinforcement laying, d) prefabricated flange cemented.
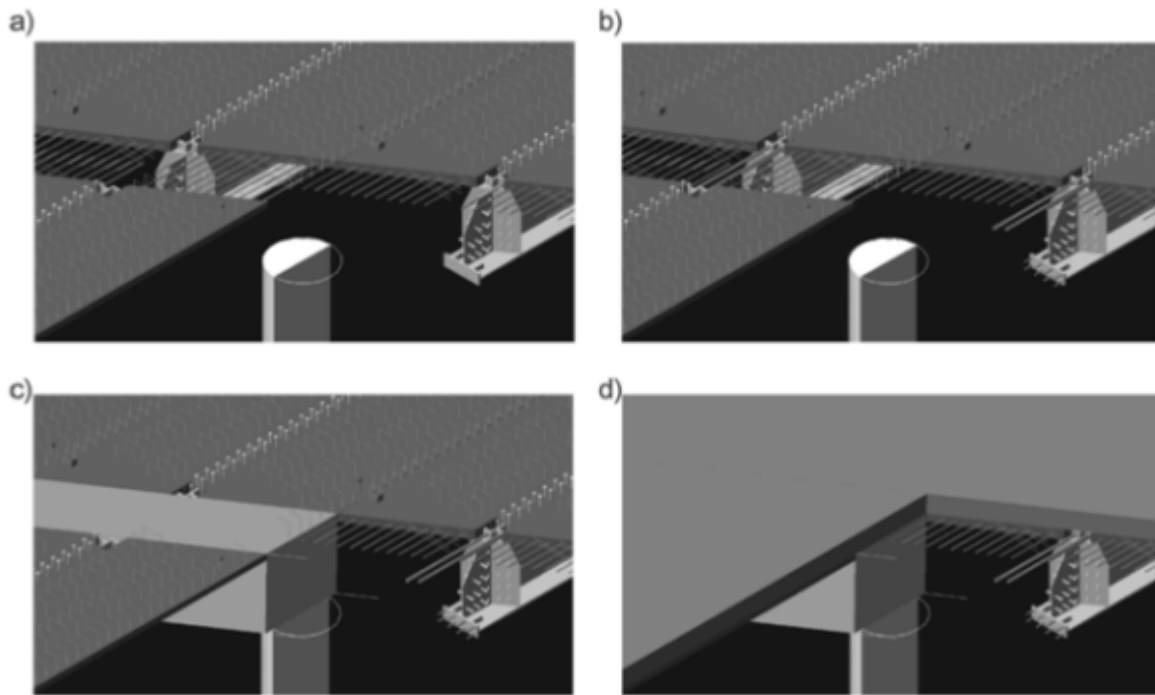
Fig. 3.5. Executing phase of continuous span made by VFT prefabricated units: a) prefabricated units placing on temporary supports, b) to make it continuous, c) cross-bars cementing, d) deck's slab cementing.

3.2. Composite construction in Germany

The composite construction method using reinforced concrete has gained greater importance again since the 1990s, with the authorities taking the initiative for increasingly using steel for the superstructure of road bridges. This can largely attributed to a demand of the general public to show more variety in the field of bridge construction and to come up with better designs in this respect. The fact that composite steel bridges can be much better tested also made them more popular among clients.

3.2.1. Road bridges

Cross sections in concrete are still the standard solution when it comes to road bridges. Composite steel bridges with the same geometry are still not an economical alternative to concrete bridges. Hence, the number of composite and steel bridges has remained unchanged since the 1980s. But the reunification of Germany in 1989 and the ensuing intensification of the building activities were reflected in the higher number of concrete structures.
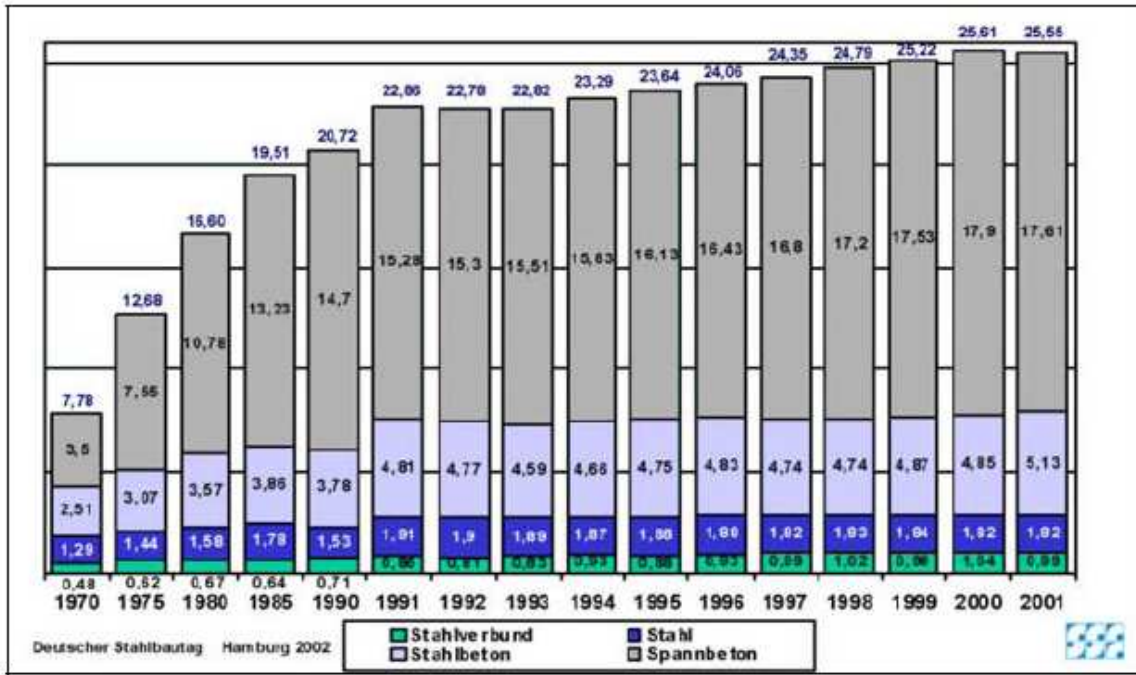
Fig. 3.6. Bridges in Germany, broken down into the different construction method (in mill m²).

- ***The road Bridge at Merseburg – example of VFT bridge in Germany:***

This is a bridge in the course of the federal road B 181 across the river Saale near Merseburg (BW 210/211).

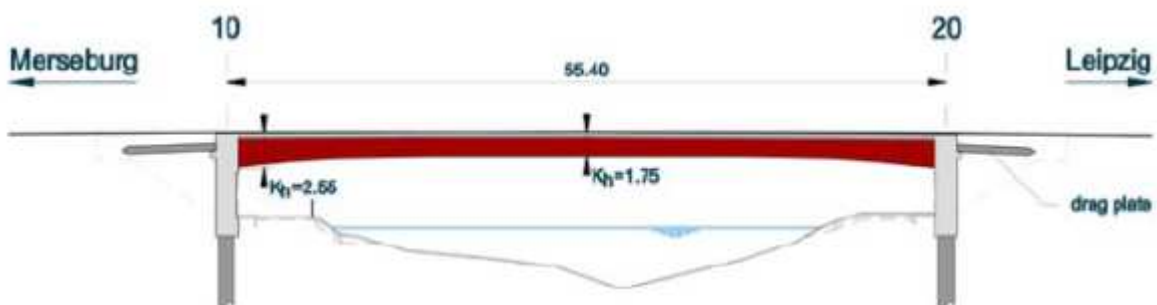Fig. 3.7. Cross section of the bridge across the river Saale in Merseburg.

Fig. 3.8. Longitudinal section of the bridge across the river Saale in Merseburg.

The subject of the invitation to tender was the reconstruction of the existing bridge. As part of the bidding process, a secondary offer was prepared in cooperation with a building firm, by which the construction of a new bridge with a length of 54,5m was proposed. The temporary abutments and the crossway displacement as well as the reconstruction of the superstructure would thus become superfluous. The bearings and temporary structures, and thus the bridge components requiring a high maintenance input, would also become unnecessary. The advantages of the secondary offer, i.e. reliable costs, a short construction time, a defined and longer service life as well as a structure requiring little maintenance, convinced the client. The girders' slenderness makes it possible to put up a structure with the same dimensions in the same place. The prefabricated composite elements have a height of 1,5m in the centre of the span and of 2,3m at the corner of the frame. A 25 cm thick concrete plate is cast in-situ onto the 4 girders which have been laid next to each other (Fig. 3.7 and 3.9). The superstructure is joined monolithically to the abutment (hybrid frame structure, figure 3.10.).

Fig. 3.9. Cross section with 4 VFT girders.　　　　　　Fig. 3.10. Beams support the abutment directly.

The reinforced concrete abutments are based on large bored piles with a diameter of 120cm, which are located directly below the wall disks of the end walls (single-row pile foundation). Low-lying approach slabs are placed behind the abutments, rather than any provisional structures which one would expect at the superstructure of such a length (Fig. 3.8, Fig.3.10). The contract was awarded at the end of April 2002. The 1st building phase, which included the planning, the demolition work and the actual construction work, took about 10 months until the traffic could move across the new bridge. The VFT girders were shipped by road to the building site and lifted with a truck-mounted crane into their position at the end of October, for which purpose the road was blocked for one night.

Fig. 3.11. View of bridge across the river Saale in Merseburg.

3.2.2. Railroad bridges

Unlike other European countries, Germany is the exception when it comes to applying the composite construction method in the field of railroad bridges. Pure steel structures for large spans and the "rolled girders in concrete" method (WIB method) for smaller spans where the steel assumes the main load-bearing function are the standard. The use of composite girders reduces the demand for steel considerably, thus making the building activities more economical. Bridges with large spans have been constructed less and less in steel since pre-stressed concrete has been introduced. A major criterion for the client in this respect is the high rigidity of the supporting framework, which is easily realized by the use of concrete. However the general public has accepted bridges, which are built with a **H/L** slenderness ratio of less than **1/15**, because it is unaware of more slender designs.

- *The railroad Bridge at Schongau – example of VFT bridge in Germany:*

In 1999, the Deutsche Bahn AG (German Railways) invited tender for a composite bridge on the single-track railroad line between Schongau and Peissenberg. The SSF Engineering Office prepared a secondary offer with an extremely short construction time proposing a structure for which the VFT method was to be used in order that crossway displacement became unnecessary.

Fig. 3.12. View of the bridge across the river Lech in Schongau.

The offer was considered to be the most economical one and awarded the contract (Fig. 3.13.). The peripheral geometrical conditions were retained. The span widths of 27 + 30 + 26 m are similar to the existing ones (Fig. 3.14.). The height of the structure varied between 2,0 and 2,8m. A decisive feature was the radius of R = 274m in the ground plan (Fig. 3.15.).

The supports were fixed to the superstructure and are deflection resistant, in order to absorb the high braking forces of the trains. The 83m long, three span bridge was put into operation after a construction time of only 3 months for the main work[6].
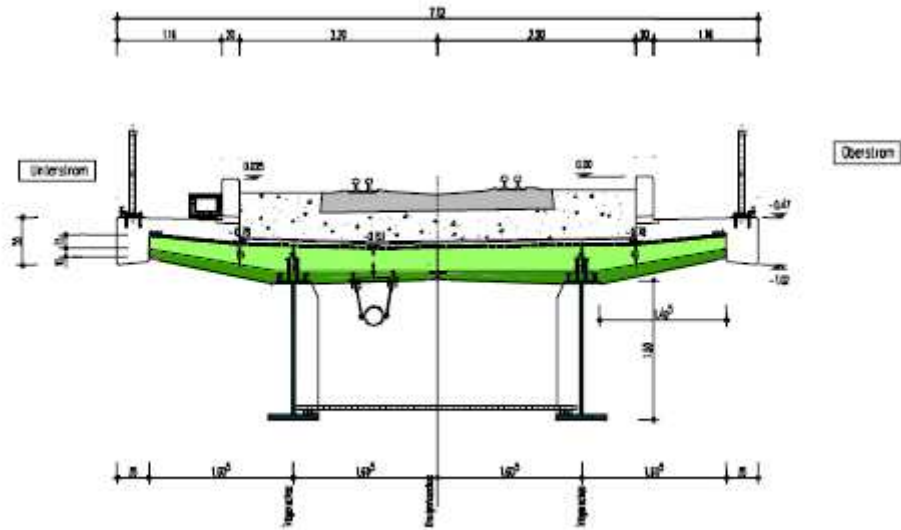

Fig. 3.13. Cross section of the bridge across the river Lech in Schongau.
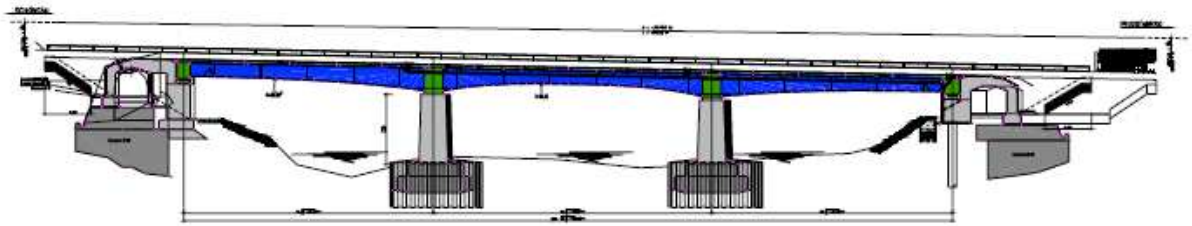

Fig. 3.14. Longitudinal section of the bridge across the river Lech in Schongau.
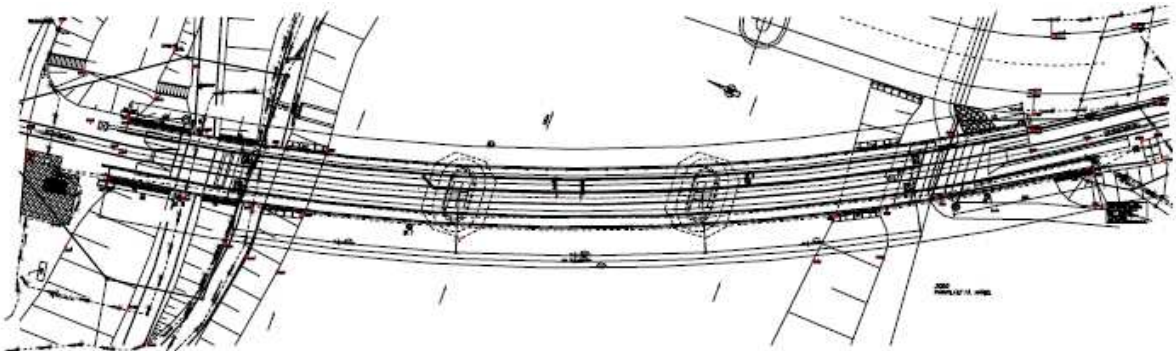

Fig. 3.15. Top view at the bridge across the river Lech in Schongau.

3.3. Differences between VFT in Poland and Germany

Generally, the standard polish method is to transfer part of stage I, just like the transfer of prefabricated flange execution, to the building site. This is because of the conditions of the national road net. In a simple way: it is easier to transfer only the steel girder. Only in the event of one object in Wrocław, where efficient A4 highway access was possible from factory to nearby construction site, could cementation take place in factory and prefabricated composite girders be transported. In the other cases, slab was cemented in position on the building site after putting all girders for one span next to each other in order to get the appropriate geometry of the span. The temporary support of prefabricated units to cementation cross-bars (frame quoin) depends on constructor – for bridges, as will be shown later, they used different solutions, in most cases all beams were supported by rolled steel joist. This solution does not create any problems connected with construction assembly using cranes and in most cases achieved quick span lead time. Test loads confirmed every time that the structure works according to brief foredesign.

3.4. VFT beginnings in Poland

The beginnings of VFT system in Poland occurred after the year 2000, when the implementation of technology during design phase of new bridges wad begun. First girders executed in cooperation with IBDiM were presented in 2002 during the "Autostrada-Polska" fair in Kielce (Fig.3.3.). In that time first constructions like viaducts in Toruń and Warszawa were built . Selected aspects of executing above mentioned bridges were presented during the "Small Bridges: Problems of design, building and maintenance of small and medium span bridges" conference in the year 2004, in Wrocław. A paper inserted in conference materials showed technical, technological and economic aspects of the VFT system, as well the basic assumptions for static and dimensioning analysis during the design phase. In Poland, until the present, bridges have been designed in VFT technology with spans from 15 to 43m and different static schemes, both continuous beam and multi-span frames. These last (multi-span frames) are the first realizations in Poland of integrated bridges with spans composed of composited girders and experiences of carrying out of these objects can be used also during executing of integrated bridges with classical composited girders[5].

4. FIELD OF APPLICATIONS

Techno-economic conditions determine the variety of VFT prefabricated units applications. They are used for single or multi-span bridges with ***spans in range from 15 to 70m***. The main scope of application is ***the executing of viaducts above active road and railway track*** (Figure 4.1.).

Fig. 4.1. VFT girders assembly over active road and railway track.

In relation to another technologies, they are achieving big economic benefits resulting from quick assembly and reduction and simplification of finishing works. The cost to cross to dual motorway with one span is lower than with two spans and intermediate support in the median strip. Angle of intersection with road or railway line axis is also insignificant. Individual design of every prefabricated unit allows readjustment to particular structural-architectonic demands. Obtaining very low construction depth creates the impression that spans are more slender (Figure 4.2.)

Prefabricated VFT® units can be used in the following static schemes:

- in single or multi-span frame, where deck's slab will be rigid connected with supports. Because of that bearings and expansion joints are eliminated;
- in free-supported beam;
- in continuous beam, where every next span will be connected through "in-situ" concrete in casted supported cross-bars;
- in span build by cantilever method, where prefabricated VFT units will be like key blocks;
- in tunnels build by strip-mine method, where prefabricated units will be like elements of the floors[7];

Fig. 4.2. Frame viaduct VFT over the motorway.

UNIVERSITAT POLITÈCNICA DE CATALUNYA

5. GIRDERS PREFABRICATION

Prefabricated VFT® unit is ***a steel girder with concrete flange***, cemented in factory or on the building site. It is simultaneously formwork of deck's slab. The steel part of composite girder is ***welded I-bar***, in which the width of upper beam flange guarantees positioning of connectors. In most cases web does not have additional stiffenings, but they can appear in girders with span from more than 40m and in railway bridges (Figure 5.1.). ***10 to 12cm concrete flange*** of prefabricated unit is connected with steel girder in such way that shearing forces will be transferred. Connectors in composite

Fig. 5.1. Steel girder in manufacturing site.

girder make up ***two different heights of stud shear connector***. Shorter studs guarantee cooperation between steel beam and concrete prefabricated flange. Flange is made from high-resistance, freeze resistant and tight concrete. In prefabricated flange, bottom reinforcement is placed with 40-50mm lagging. Longer studs and also structural stirrups protrude above the prefabricated concrete to ensure composite connection between prefabricated and in-situ concrete.

Fig. 5.2. Steel girder in factory, stud shear connectors and prefabricated slab reinforcement .

Thanks to its active contribution to load carrying capability concrete flange, is gaining big savings in consumption of structural steel (in some cases even up to 30%) [7]. Corrosion protection of steel part is done in factory, where all coating required by the project is applied. Prefabricated unit is delivered on the construction site with equipments and staging.

Width of prefabricated units is readjusted to restrictions resulting from transport conditions from factory to building site.

Figure 5.3. VFT girder transportation

Fig. 5.4. "Ready to transportation" VFT girder in the factory.

6. INDIVIDUAL PRODUCTION AND FAST ASSEMBLY

Apart from the principal of the building contract and planner, there are usually three other parties involved in a VFT construction project:

- ***a steel construction company,***
- ***a prefabricated unit constructor***
- ***the executing company.***

The steel girders are manufactured at a steel construction works licensed for bridge building. This company orders the sheet steel as specified in a structural planning. These are welded into the tension-free factory form, which means with a camber calculated from geometry and the expected deformation. The upper steel flange is fitted with different heights of stud shear connector for the subsequent connection between the prefabricated element flange and the in-situ concrete. After inspection of the girder geometry, full corrosion prevention treatment is carried out at the

Fig. 6.1. Girder assembly by crane.

steel works, protected from the weather and using environmentally friendly methods. For this reason, damage to corrosion prevention coating should be avoided during transportation and assembly.

At the manufacturing site, the steel girder is inserted free of stress in the formwork table. The reinforcement is manufactured in several units and laid on the formwork. The end surface of the flange are protected with forms, and the built-in components of the flange are already integrated in the formwork. Once the prefabricated slabs have been cast, the girders are lifted out of the formwork and stored free of stress on the manufacturing site, in order to prevent unplanned deformation caused by creeping of the fresh concrete. After a defined minimum numbers of lay-days, the VFT girders are fitted with transport reinforcement and taken to the construction site. Stability and vibration problems must be accounted for in advance by planner, in agreement with the transportation company.

When they arrive at the construction site, the girders are supplemented with cap formwork, protective scaffolding and spars. Finally, the completely equipped VFT units are laid on temporary frames with a mobile crane and supported.

Fig. 6.2. Transport of VFT girder.

During this process, the traffic flow underneath the structure only has to be interrupted during the lifting process. Reinforcement braces to prevent the girders tilting are not necessary. Only the adjacent flanges on the prefabricated elements are coupled to one another.

The transverse end and supporting girders of the structure are boarded, reinforced and concreted up to the top edge of the VFT prefabricated element in this condition.

Figure 6.3. Lifting and laying of the VFT prefabricated units.

In the constructions built so far, it has been found useful to set up a "chain" of subcontractors. Here, the contractor of the principal of the building contract is responsible, generally the construction company that builds the superstructure and the substructure for the principal. This company concludes a subcontractor agreement with prefabricated element factory. The latter is responsible for the production of the VFT girder, transportation to the construction site and assembly on site.

Fig. 6.4. VFT unit assembly during the night.

A steel construction company is contracted to manufacture the steel girders. In this way, each party involved is able to contribute to the production process with its specific specialist area. The interfaces between the parties involved must be clearly defined and quality standards monitored[4].
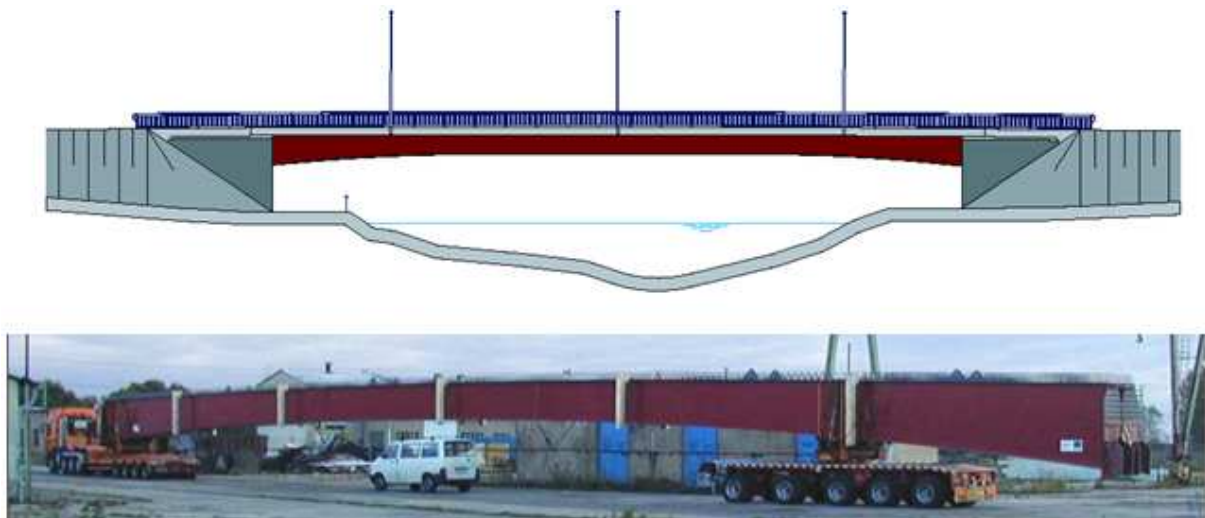

Fig. 6.5. Bridge view and transportation of the VFT girder.

7. SHRINKAGE AND CREEPING

With the shrinkage and creeping factors to be assumed, the influence of the location of the structure during the individual phases of construction are taken into consideration with different basic shrinkage coefficients and basic stress coefficient, as is the change in the effective structure thickness d_{ef} of the concrete cross-sections on addition of the in-situ concrete or pavement.

In contrast to conventional composite bridges, greater attention has to be paid to the shrinkage and creeping calculation for bridges with prefabricated composite girders as two materials with creep tendency are involved which ***shrink and creep at different times***. Furthermore, the static systems and the cross-section which go into state II in the span area change in the individual construction states. The stresses which cause the creeping then change accordingly.

With statically undetermined systems, the intrinsic stresses due to creeping and shrinkage cause not only deformation of the girder and stress distribution of the girder and stress distributions within the cross section but also produce "new" stresses can be calculated using the normal methods employed in stress analysis[4].

8. DURABILITY AND MAINTENECE'S ADVANTAGES

In VFT® system durability is assured by:

- construction solution,
- material and technological solution.

Prefabricated elements are characterized by durability and resistance of destructive corrosion factors. Steel elements are protected by guaranteed ***painting systems with 15-25 years durability*** or ***metal painting with 20-30 years durability***. Prevention of bottom concrete slabs surface and cross-bars is provide increased lagging and using C45/50 concrete, which is characterized by high density and freeze resistance. Side slabs surface is protected by prefabricated bracketed cornice elements of polymerconcrete or special concrete. In construction solutions, fostering construction durability, it's necessary to underline that:

- in the VFT® system, monolithic structure form, which are characterized by great mass and significant rigidity which reduces fatigue type damage,
- compression stresses, caused by wet concrete dead load, close effectively micro-scratch in concrete slabs of prefabricated units, which in connection with lagging (increased to 40-50mm), give great reinforcement protection against corrosion factors penetration,
- carrying out of concrete slabs in two layers, causes concrete shrinkage decrease. Thanks to shrinkage, scratches are not a menace to construction,
- the system excludes necessity of steel structure joining on the construction site; welding and painting works are carried out entirely in the factory,
- VFT® girders surface are free of hard to reach places and they are easy to maintain and conserve.

It's necessary to underline that an increase of durability already guarantees transfer the manufacturing process to steel construction company and prefabricated unit constructor, where without additional amounts of investment, quality of work is comprehensively assured. For instance, carried out in optimal conditions and under full anticorrosion protection, steel overruns by almost threefold the exploitation period of coat [7].

UNIVERSITAT POLITÈCNICA DE CATALUNYA

9. EXAMPLES OF REALIZATION (IN POLAND)

To approximate the field of application of VFT system, below are showed examples of realizations in Poland with characteristic technical data, lead time, data of investor and contractor, photos of extracted bridges or during assembly phase.

- *Szczecin – Struga Avenue:*

The viaduct enables to carry traffic without collision between the cars above Struga Avenue in Szczecin.

Total length: **46,52m**
Theoretical length of spans: **24,00m** + **21,00m**
Total width: **12,00m**
Roadway width: **7,5m** – two traffic line, **3,75m** for each one
Crossing angle: **79•**.
Quantity of VFT girders: **2x4=8**,
Lead time of load carrying structure: **2 months**,
Load time of whole bridge: **7 months**.
Investor: **Urban Department in Szczecin**.
Contractor: **BUDIMEX-DROMEX S.A**.

Figure 9.1. Bridge view (Szczecin – Struga Avenue).

- ***Toruń – Kościuszki Street:***

The viaduct carry through Kościuszki Street above Chrobrego Street and PKP tracks at the angle of 63° and is located in the neighbourhood of East Toruń station.

Total length: ***158,23m***
Bearing system length: ***136,25m***
Theoretical length of spans: ***18,51m* + *18,52m* + *18,51* + *24,53* + *18,45* + *18,44* + *18,56***
Total width of the viaduct: ***29,35m***,
South roadway width: ***7,00m*** – two traffic lane, ***3,50m*** for each one
North roadway width: ***10,40m*** - two traffic lane (***3,50m*** for each one)
                                                           and tram track: ***3,40m***.
South and north bridge deck overhang width:
                                                           4,00m including ***2,89m*** width sidewalk
VFT girders amount: ***7x12=84***.
Lead time of bearing system: ***5 months***.
Lead time of all object: ***8 months***.
Investor: ***MIEJSKI ZARZĄD DRÓG W TORUNIU***.
Contractor: ***BUDIMEX-DROMEX S.A***.

Fig. 9.2. Bridge view (Toruń – Kościuszki).

- ***Kije – DW number 766:***

Road viaduct in Kije along provincial road nr 766 Pińczów – Kielce. National road nr 78 and railway line LHS are located under the construction.

Total length:	***108,99m***
Theoretical length of spans:	***43,00m + 43,00m***
Total width of the viaduct:	***12,20m***
Roadway width:	***7,6m*** – two traffic lane, ***3,50m + 0,30m*** for each one
Pedestrian sidewalk width:	***2,00m***
Working sidewalk width:	***1,00m***
Crossing angle:	***62,20•*** with the road and ***56,30•*** with LHS
Quantity of VFT girders:	***2x5=10***
Lead time of load carrying structure:	***8 months***,
Load time of whole bridge:	***12 months***.
Investor:	***GDDiK, Kielce***
Contractor:	***PRZEDSIĘBIORSTWO ROBÓT INŻYNIERSKICH FART Sp. Z o.o.***
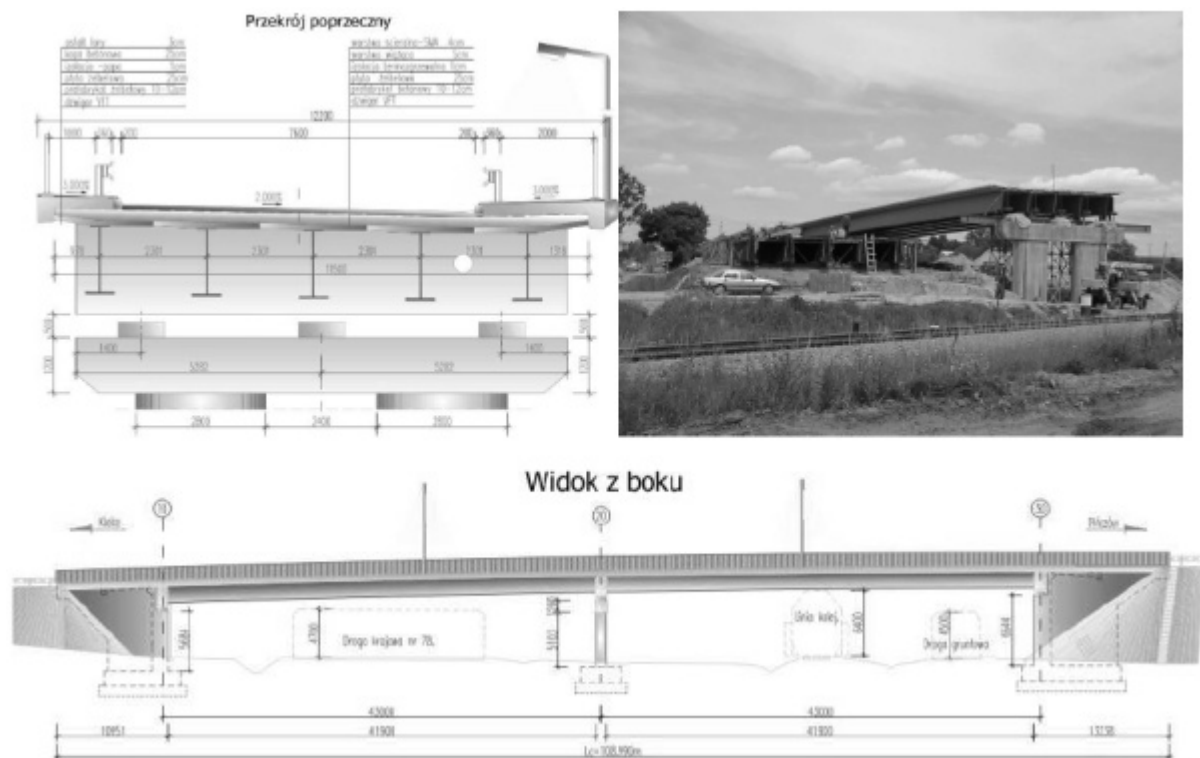
Fig. 9.3. Viaduct in Kije- DW nr 766, cross section, assembly and side view.

- *Elbląg – Akacjowa Street:*

The viaduct enables to carry Akacjowa Street (without collision) above PKP railway track in Elbląg.

Total length:	**81,64m**
Theoretical length of spans:	**25,00m + 30,00m+ 25,00m**
Total width:	**14,20m**
Roadway width:	**7,0m** – two traffic lane, **3,50m** for each one
Crossing angle:	**78•**
Design loads:	**A class**
Quantity if VFT girders:	**3x5=15**
Lead time of load carrying structure:	**3 months**
Load time of whole bridge:	**7 months**
Investor:	**GDDKiA , Olsztyn**
Contractor:	**STRABAG Sp. Z o.o.**

Fig. 9.4. VFT girder assembly (Elbląg– Akacjowa Street).

- *Wrocław – Armii Krajowej Avenue:*

Road viaduct above the PKP railway track in Wrocław, along Armii Krajowej Avenue (two independent constructions under two lines) – reconstruction of existing bridge.

North-West Viaduct:

Bearing system length:	**75,80m**
Theoretical length of spans:	**5 x 15,00m**
Total width:	**14,35m**
Roadway width:	**8,23-10,50m** – two traffic lane, **3,50m** for each one, switch lane (variable width) **1,23-3,50m**
Bridge deck overhang width:	**2,60-4,87m** for pedestrian and **1,25m** for working sidewalk

South-East Viaduct:

Bearing system length:	**75,80m**
Theoretical length of spans:	**5 x 15,00m**
Total width:	**13,40m**
Roadway width:	**7,00m** – two traffic lane, **3,50m** for each one
Bridge deck overhang width:	**5,15m** for pedestrian and
	1,25m for working sidewalk

Design loads:	**A class**
Quantity if VFT girders:	**5x5=25** and **5x6=30**
Lead time of load carrying structure for one lane:	**2 months**
Load time of whole bridge:	**18 months**
Investor:	**ZARZĄD DRÓG I KOMUNIKACJI WE WROCŁAWIU**
Contractor:	**MOTA-ENGIL POLSKA S.A.[5]**

Fig. 9.5. Bridge view during construction phase (Wrocław-Armii Krajowej Avenue).

10. STATISTICAL ECONOMIC ANALYSIS OF EXECUTED OBJECTS

The following graphs (figure 10.1.) show total cost of span carried out in VFT technology as a function of bridge area and share of cost (%) of individual elements of construction. Considered: single-span grid, frame and two-span structure (respectively upper, middle and bottom curve on the graph). Area is defined as a product of light between balustrades and effective span length. Costs are calculated on the basis of national current prices. In order to make use of index numbers easier, calculation does not include expensive elements, conditioned by the localization, like foundation, equipment, project and the like[7].

1 – concrete of active shuttering (prefabricated unit) **8%**
2 – prefabricated unit reinforcement **17%**
  – VFT girder steel
4 – studs **1%**
5 – deck and cross-bars in situ concrete **5%**
6 – deck and cross-bars reinforcement **10%**
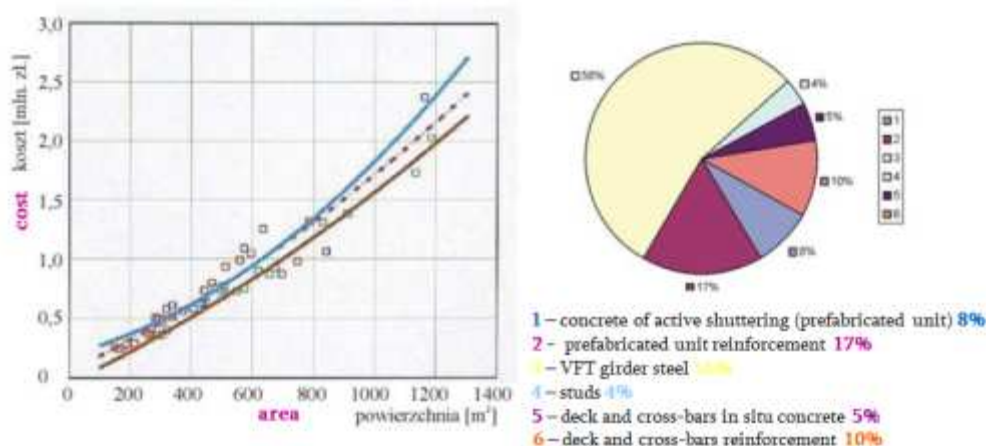
Fig. 10.1. Cost [zł] depending on span area [m^2] and average costs structure of superstructure of VFT span.

The following graphs (figure 10.2.) show dependence between span and construction depth. The left graph show result for grips (single-span – upper curve, two-span – bottom curve), and the right graph show result for frame; upper and middle curve correspond to, respectively, support and span depth for variable depth frame and bottom curve corresponds to constant depth frame[7].
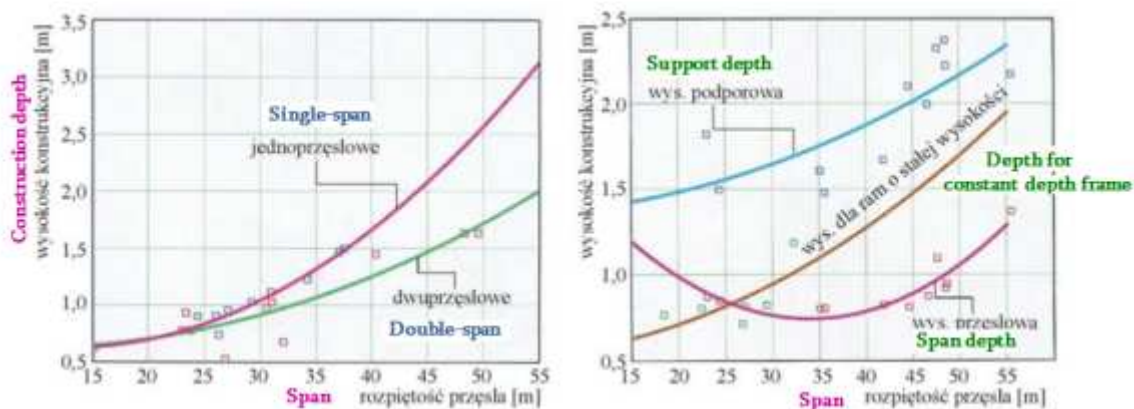
Fig. 10.2. Dependence between span length [cm] and construction depth [mm].

11. FUTHER DEVELOPMENT AND CHANGES

The VFT construction method has established itself in the last years [4] for the cost-effective production of well-designed structures. For flyover, underpasses and bridges, it can be regarded as a proven construction method. This success is attributable i.a. to:

- *low construction costs* thanks to material savings in the structural steel,
- *short construction time* thanks to high degree of prefabrication,
- *sound calculation basis* for the construction company,
- *good testability of the structure substance*,
- *durability and simple subsequent strengthening*.

The VFT method is developing constantly further and finding additional areas of application. To an increasing extent it is preference for flyovers over existing traffic routs with planned centre pillars by replacing two-span bridges with single-cell frames. Monolithic frame system with large slenderness allow the centre support to be eliminated. The critical precondition for the competitive success of the VFT method is the costs for traffic diversion measures, such as traffic guidance measures on the road and operating difficulty costs on the railways are included in the tender along with the construction costs. It would also be expedient to give consideration to the reduction in cost for the user through improvement constructions when evaluating the tenders.

Railway structures thus offer a wide range of potential applications. Here construction work has to be carried out under the pressure of time and space. In inner-urban areas, the construction height plays the major role. The VFT system permits a high slenderness with low deformations rates under traffic loads.

Further fields of applications are opened up to traffic routs over waterways. Here the transport length are limited only by the dimension of the lock chambers. The VFT girders can be optimally linked to the substructures in the hybrid design. A new dimension is opened up for span widths and slendernesses in bridge construction.

For surmounted structural elements such as frameworks or arched bridges, the girders are employed as secondary elements in transverse direction. This again results in economic benefits.

For the production of the girder, the use of rolled girders will grow in importance. Here an external presstresing of the girders is expedient in order to permit an economical exploitation of the symmetrical profiles. Under these conditions, a great future can be predicted for this method of construction [4].

12. ADVANTAGES OF VFT BRIDGES

<u>Advantages of VFT® system:</u>

Use of VFT® girders is particularly economically justified in difficult local conditions.
Around 80 bridges in VFT technology were built in Germany. This system brought measurable benefits for all participants of the investment process, namely:

FOR INVESTORS:

1. It made it possible to order economical construction in particular structure-architectural demands.
2. High degree of prefabrication makes possible careful product control and guarantees right and ecological anticorrosive protection.
3. Thanks to simplicity of cross-sections current control of bridge's condition is facilitated, and maintenance costs are relatively lower.
4. In case of viaducts above highways there is a possibility to give intermediate supports up, which raises traffic safety and eliminates traffic arrestment, route determination and protection of temporary diversion.

FOR BRIDGES COMPANIES:

It ensures minimal executing risk. The solutions in VFT® system are usually offered as an alternative proposal with cost-conscious calculation supported on real BOQ (Bill of Quantity) and known construction cycle, which are not burdened with mistakes in assessment as a result of conditions imposed by orderer (very often impossible to meet). The estimate of these proposals is also more comprehensible. They do not have to be considered individual.

FOR CONSUMERS:

1. Bridges executing without collision is safe for consumers, because there is no device protecting the building site on the road, there are no labour vehicles and bothersome traffic congestions.
2. Low quantity of main girders cause traffic to be stopped only for a short time and practically it do not pose danger.
3. Thanks to architectonic virtues, the new bridges beautify the landscape.

<u>*To recapitulate, the VFT ® system advantages are:*</u>

- Low cost of bridge executing due to material savings;
- Short time of carrying out process resulting from high degree of prefabrication;
- Complete costs calculation;
- Easy control of bridge conditions;
- Minimization of costs connected with traffic organization and protection;
- Durability of the bridge.

The VFT® system is applied in crossing above the existing traffic, especially where it is possible to replace two-span construction with intermediate support for single-span frame and railway engineering, when the investments are carried out in difficult spatial conditions with strict time limitations. With VFT girders you can design span with small construction depth and small deformations, which is important in case of modernization of viaducts over active railway tracks. The VFT girders can be applied in truss and arch constructions as the secondary elements[10].

13. NEW TYPE OF VFT: VFT-WIB

In the beginning of the 1980th the ***Perfobond-strip*** was developed as a continuous connection between steel girders and concrete. A perforated steel strip is vertically welded on the upper flange of a steel girder. A part of the openings in the web are reinforced with horizontal rebars to improve the shear transmission and to avoid the uplift of the concrete slap. Further investigations have shown that this connection, so called ***composite dowels***, is a very reliable construction under dynamic loads. The ultimate limit state is accompanied by large displacements [8].

13.1. Differences between VFT® and VFT-WIB® method, Composite dowels connections – types

The composite dowel connection is implemented in the **VFT-WIB® method**. It is a further development of the VFT® method carried out by SSF (SCHMITT STUMPF FRUEHAUF UND PARTNER). The difference between these two methods is the design of the steel girder. For VFT® construction method the steel girder is a independent structural element with upper and lower flange connected by a steel web. The VFT-WIB® girder is a beam with ***"external reinforcement"*** placed on the tension side.
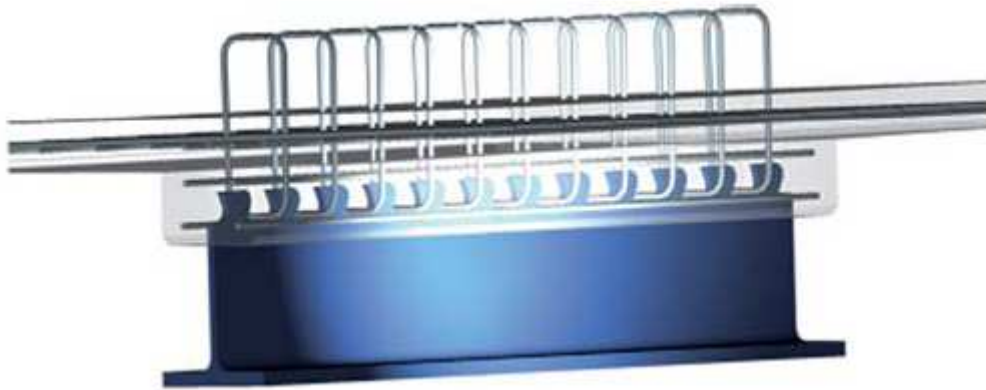
Fig. 13.1. The VFT-WIB® girder.

This "external reinforcement" in the shape of a T is manufactured out of a rolled steel section. In the composite beam the flange of the rolled section is bearing tension, the upper flange compression. The shear connection between the halved steel girder and the concrete is provided by steel dowels manufactured by a special cutting line of the web (Fig.13.3.). This composite dowel can be designed in different shapes (Fig. 13.2.).
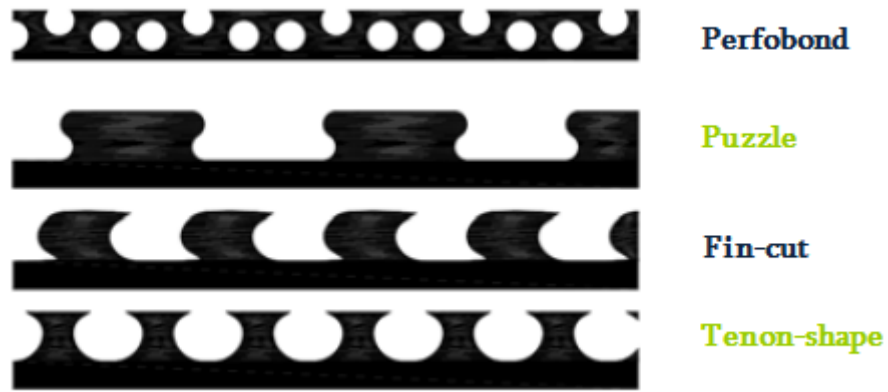
Fig. 13.2. Different cutting lines for composite dowels (Perfobond, Puzzle, Fin-cut, Tenon-shape)

The steel works to manufacture these composite dowels are simple and cost effective. Neither for producing the steel beam nor for placing the connectors welding is necessary. The halved steel girders are completely assembled in the steel mill and coated for corrosion protection. The production costs for steel girders can be reduced on 60% of a welded steel girder with headed studs [8].

Fig.13.3. Cutting line of the web.

13.2. Description of VFT-WIB®

This method is based on ***a rolled steel beam cut longitudinally in two T-sections***. Further ***a concrete top chord*** is added, composed of a prefabricated part and a part which subsequently added on site to achieve the final cross section. This method is a very flexible solution offering varies cross section possibilities according to the design requirements[9], see figures 13.4 and 13.5.
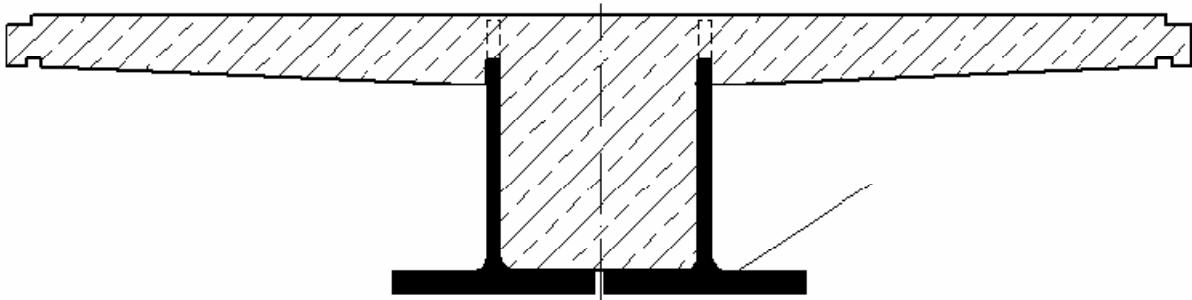
Fig. 13.4. **VFT-mono-WIB** with unlimited construction height because of concrete web, also haunched girders are feasible.
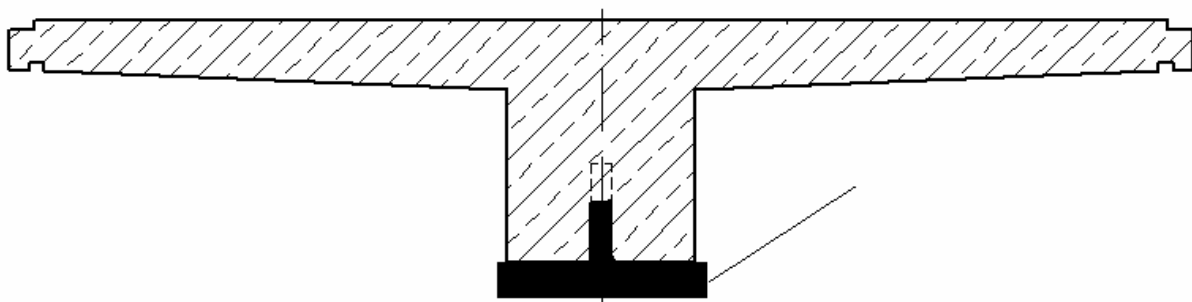
Fig. 13.5. **VFT-duo-WIB** with two halved rolled beams, the construction height is limited by the maximum height of the rolled beam.

The cutting line of the rolled beam has a special shape and creates composite dowels identically to continuous shear connectors mentioned before. In figure 13.6. cut beams already assembled to pairs are shown during appliance of the corrosion protection. In the next step reinforcement bars are places through the cutting shape (figure 13.7.) and concrete top chord is concreted to produce a prefabricated bridge element.

Fig. 13.6. Rolled girders after cutting and coating in the shop

Fig. 13.7. Reinforcement for prefabricated concrete plate

The shape of the cut hereby allows for the shear transmission in the shear joint already in the construction stage similar to VFT®-constructions. Subsequently the prefabricated bridge elements are transported to the site (figure 13.8.), placed on the abutments (figure 13.9.) and, finally, the residual concrete chord is added.

Fig. 13.8. Transport of the VFT-WIB girders from the concrete plant to the construction site

Fig. 13.9. Placing of the VFT-WIB girder with 32,50m length

As a result VFT-WIB construction, with the use of the state of art concerning the concrete dowels technology and integrating the advantages of VFT®-constructions, are meet the following targets for competitive and sustainable construction:

- High safety standard for vehicle impact, especially for bridges with only two girders (shock),
- Reduction of coating surface,
- Shear connection without fatigue problems,
- Elementary steel construction nearly without any welding,
- Sparse maintenance and easy monitoring [9].

Fig. 13.10. Cutting line.

In the following more details of experimental investigations and design concept for VFT-WIB constructions, especially on the steel part of the concrete dowels, are presented.

✖ FAILURE CRITERIA OF CONCRETE DOWELS:

The bearing capacity of a composite dowel is limited by *__steel__* or *__concrete failure__*. In a good design both failures of a concrete dowel are balanced up to the maximum load. *__Steel failure__* is limited in the **ultimate limit state** by

      a) the shear resistance,

      b) yielding due to bending of the dowel

and in the **fatigue limit state** by

      c) fatigue cracks due to dynamic loading, see figure 13.11.
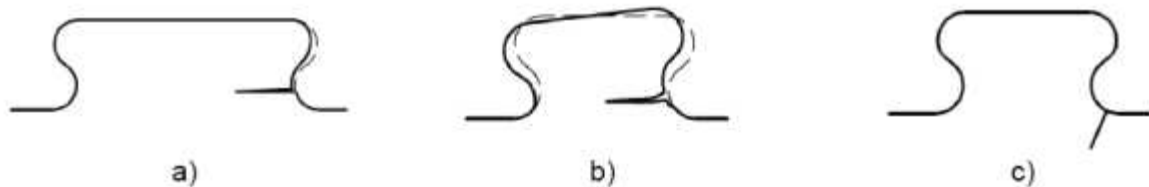
Fig. 13.11. Failure modes for steel.

__Concrete failure__ is characterized by several failure modes. Which mode finally occurs depends on the boundary conditions like geometry, concrete grade, reinforcement design, adding of fibers etc.

✖ OPTIMISATION OF THE CONCRETE DOWEL BY EXPERIMENTAL INVESTIGATIONS:

Static as well as cyclic tests on varies shapes of continuous shear connectors using the concrete dowel approach have been performed in the last years. First, tests have been conducted on the Perfobond strip, characterized by cut-outs in a steel strip used for shear connection, leading to the [DIBT 1991]. Later, tests focusing on composite dowels especially designed for the application in VFT-WIB constructions have been carried out [Schmitt et. al. 2004]. *__The Push-out Standard Tests (POST)__* according to EC4 (figure 13.7.) and beam tests have been performed. In the tests concrete failure as well as steel failure has been observed. It has been concluded, that the ULS resistance of the steel is almost independent from the shape

of the dowel. However fatigue cracks according to figure 13.11. c) have been observed in the POST after *2 million load cycles* [P612 2007]; they have been caused by a very high level of stress amplitude in the tests. The fatigue cracks observed have a limited propagation due to the fact that the steel part is compressed in the POST (equivalent to negative bending moment region); thus a subsequent ULS-test resulted in no significant decrease of the residual strength.

Therefore the ultimate limit state design seems not to be so important for the shear connection in VFT-WIB bridges compared to the fatigue limit state.

Consequently an additional test program has been set up in the scope of [PreCo-Beam*] to investigate in the following:
- Influence of the shape of dowel on the pressure profile coming from concrete to steel dowel to estimate the loading on each dowel;
- Dependency of the ultimate bearing resistance and the fatigue resistance of the steel on the shape of the dowel with regard to derive mechanical models and equations for design;
- Influence of the dowel shape, reinforcing and geometry of the composite element on the concrete failure at ultimate limit state.

One crucial aspect, especially for the fatigue verification of the steel dowels, is the superposition of stresses resulting from shear in the composite joint and global bending of the beam (normal stresses in the web). In case of a concrete dowel located in a tension zone of the web, fatigue cracks would propagate through the web and possibly into the flange which causes not only failure of the shear connection but collapse of the composite beam. Hence **_new POST specimens (NPOT)_** had to be developed to simulate the behaviour of a shear connector located in the tension zone [PreCo-Beam], see figure 13.13, and fatigue tests have been conducted on three different shapes of shear connectors, see table 1.
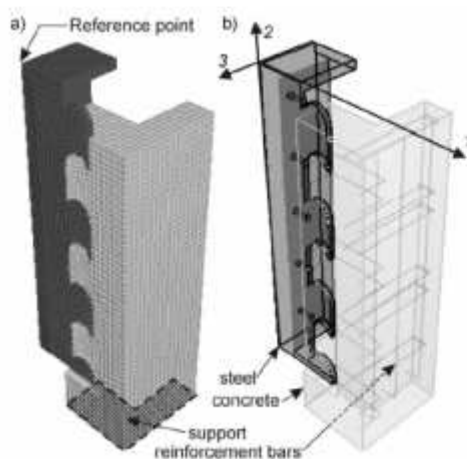
Fig. 13.12. POST
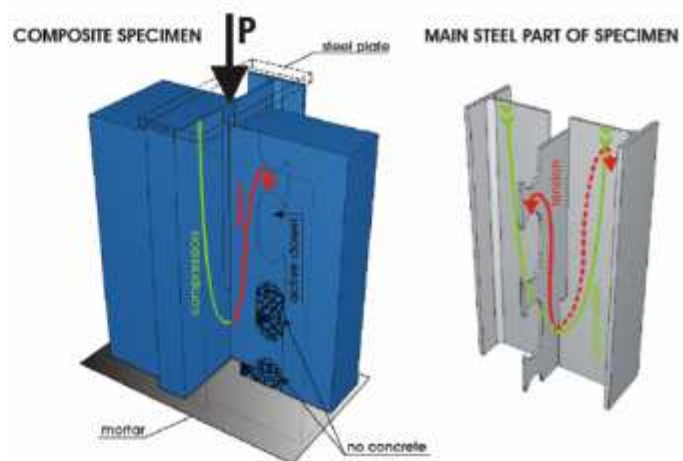
Fig. 13.13. NPOT

As expected one crack in the **_PZ shape_** could be produced with the NPOT fatigue tests according to figure 13.11. c) and, according to the expectations, the crack propagated through the entire web. However, only one of the specimens exhibited a fatigue failure.

Tab.13.1. Comparison of shapes with results from the NPOT fatigue tests [PreCo-Beam].

Shape	PZ	SA	CL

As conclusion of the test series the ***puzzle shape (PZ)*** has been chosen to be the most promising shape considering of fabrication aspects, bearing capacity and fatigue.

✖ ANALYSIS OF LOADING ON THE STEEL DOWEL

In addition to the fatigue test a static NPOT on the ***CL shape*** connector has been carried out with a large number of strain gauges at the steel dowel for analyzing the stresses and for the calibration of FE analyses carried out simultaneously with the tests. The results of the test have been in accordance with the numeric results and the numerical model has been modified for the ***PZ shape*** reference is given to in this paper, see Figure 13.14.

In the first step an analytic model for the local behaviour of a shear connector has been introduced. Here the puzzle geometry has been focused. However it is possible to transfer the approach to any geometry for each inventor of a new shape.

The local approach is based on the load introduction on single tooth. Hereby S represents the centre of the projection area A_p in shearing direction; h_s is the distance from the centre to the base of the shear connector. In figure 13.14 for example, as projection area only the area constricting a concrete block on front of the dowel should be considered.
The force on each steel tooth is composed by the shear force in the composite joint P_τ and the stress distribution due to the global loading depending on the geometry of the composite cross section; Pup for the uplifting forces due to the location of the shear joint in respect to the neutral axis of the cross section and σ_{en} for the notching effect from the nominal stress of the steel section, see figure 13.15.
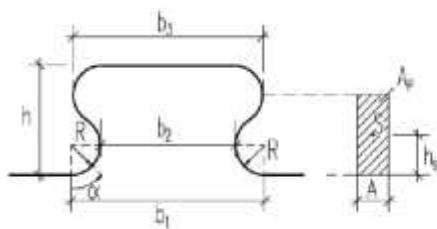
Fig. 13.14. Geometry of puzzle tooth (PZ)   Fig. 13.15. Forces on the steel dowel (PZ shape)
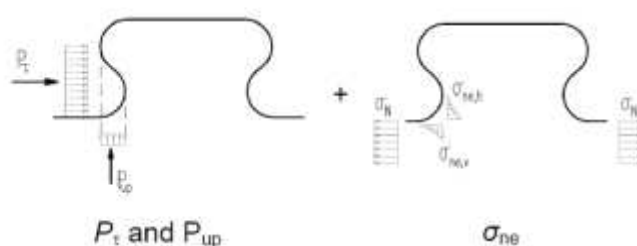
For the determination of P_τ it is conservatively assumed that the load distribution along the height of the dowel is constant and therefore P_τ is located at h_s.

The uplifting force Pup is resulting from the eccentricity ***h'*** of the shear joint to the centre of the composite compression chord, see figure 13.16. The trajectory generates an uplifting force on the steel dowel which would be pushed out of the concrete section if the shape of the steel dowel doesn't contain an undercut. Hence the undercut of the steel dowel

implements two functions; first, it generates the 3D stress state for the kernel of the concrete dowel and second, it locks the shear connection against uplift in vertical direction.
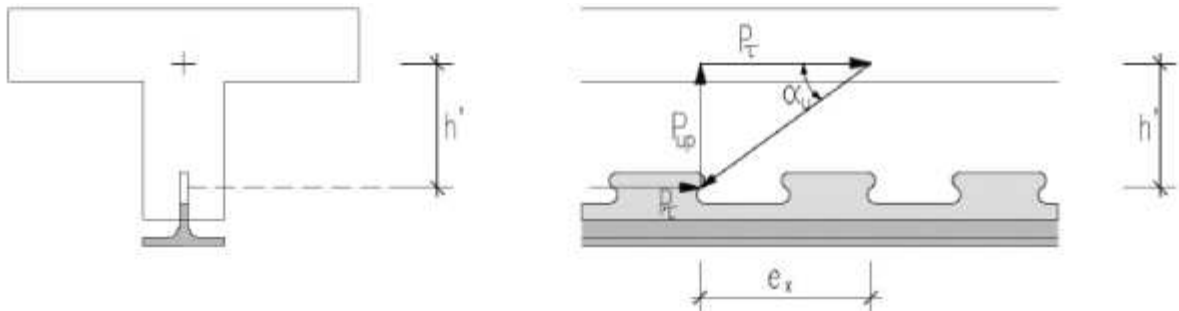
Fig. 13.16. Uplifting force due to eccentricity of the shear joint to the neutral axis at support.
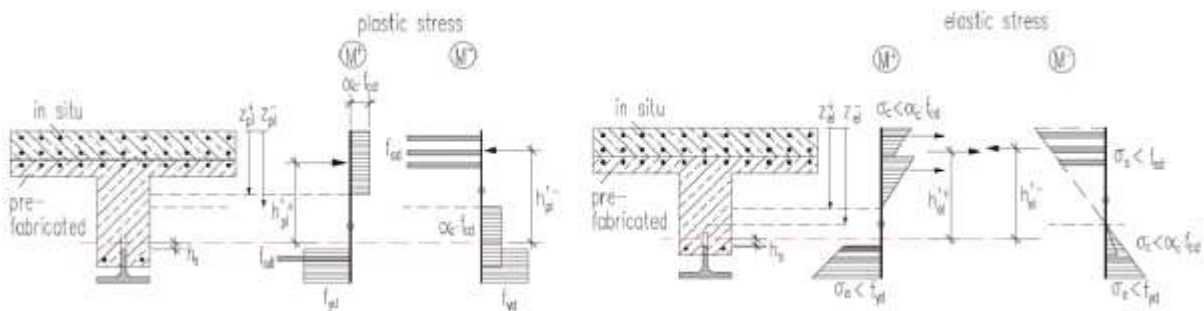
Fig. 13.17. Determination of h'ᵢ for ULS and SLS.

The determination of the uplifting force is based on h'_i depending on the stress distribution of the composite section, see figure 13.17. In the following full shear connection is assumed. It is required to differentiate between the ULS and the SLS respectively the fatigue design. Further the construction stages have to be considered.

Generalised Pup is therefore calculated according to figure 13.16. as:

$$P_{up} = P_\tau \cdot \frac{h'}{e_x} \qquad [kN]$$

<div align="right">Eq.13.1.</div>

with $h' < e_x$ else $P_{up} < P_\tau$.

The σ_{ne} is the notching effect on the normal stresses in the web of the steel girder due to the shape of dowel. The increase in stress hereby depends on the geometry of the dowel.

On the basis of an **_FEA_** (figure 13.18) it has been concluded, that σ_{ne} depends directly on the ratio of the connector length to the radius of the cut out (**b₁/R**), but not on length and radius separately. Moreover, the height **_h_** of the dowel is unimportant for the notching effect.
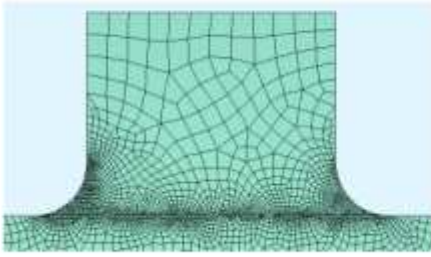
Fig. 13.18. FE model for analysis
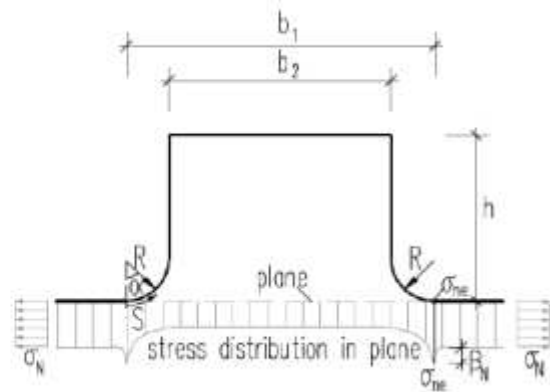
Fig. 13.19. Stress distribution due to notch effects.

On the basis of an extensive parametric study using the FE method the notching stresses have been derived to

$$\sigma_{ne} = \beta_N \cdot \sigma_N \qquad \left[\frac{N}{mm^2}\right] \qquad\qquad \text{Eq.13.2.}$$

with the notch factor

$$\beta_N = \left[1{,}192 + 0{,}1029 \cdot \left(\frac{b_1}{R}\right) - 0{,}0022 \cdot \left(\frac{b_1}{R}\right)^2\right] \cdot f(\alpha) \qquad [-] \qquad \text{Eq.13.3.}$$

where $f(\alpha)$ expresses the decrease of the amplitude along the cut out

$$f(\alpha) = 0{,}9077 + 0{,}0104 \cdot \alpha - 0{,}0005 \cdot \alpha^2 \qquad [-] \qquad\qquad \text{Eq.13.4.}$$

The higher the ratio b_1/R of the tooth, the higher is the notching effect expressed by the factor β_N. Thus, not only the sharpness of the notch itself but also the increase in stiffness depending on the length of the dowel is influencing the notch effect, which is in accordance to the effect of longitudinal stiffeners.

✖ STRESS ANALYSIS ON THE STEEL DOWEL

For the validation of the loading on a steel dowel and the resulting stresses the modified FE analysis to the PZ shape has been consulted. For the local effects due to longitudinal shear, the model presented in [PreCo-Beam] was modified to ***model (M3)*** according to [Lorenc et. al. 2007]. The stresses due to the notching effect of the nominal stresses in the web and the uplift forces have been calculated considering only the steel part in ***model (M2)***. The geometric properties of the dowel have been chosen to b_2 = 125mm, h = 100mm; the web thickness of the steel beam has been t_w = 10.2mm.

In figure 13.20. the influence of the loading on the stresses of a single puzzle tooth has been evaluated along the cut. For this purpose, separate calculations have been conducted for P_τ = 50kN, P_{Up} = 50kN and the global stresses in the web σ_N = 50N/mm^2.

Consequently the influence of each loading parameter on the stress distribution along arc length has been compared with each case **_G,L and U_** (figure 13.20.) and an analytic model has been derived for the ULS and fatigue design of a steel dowel.
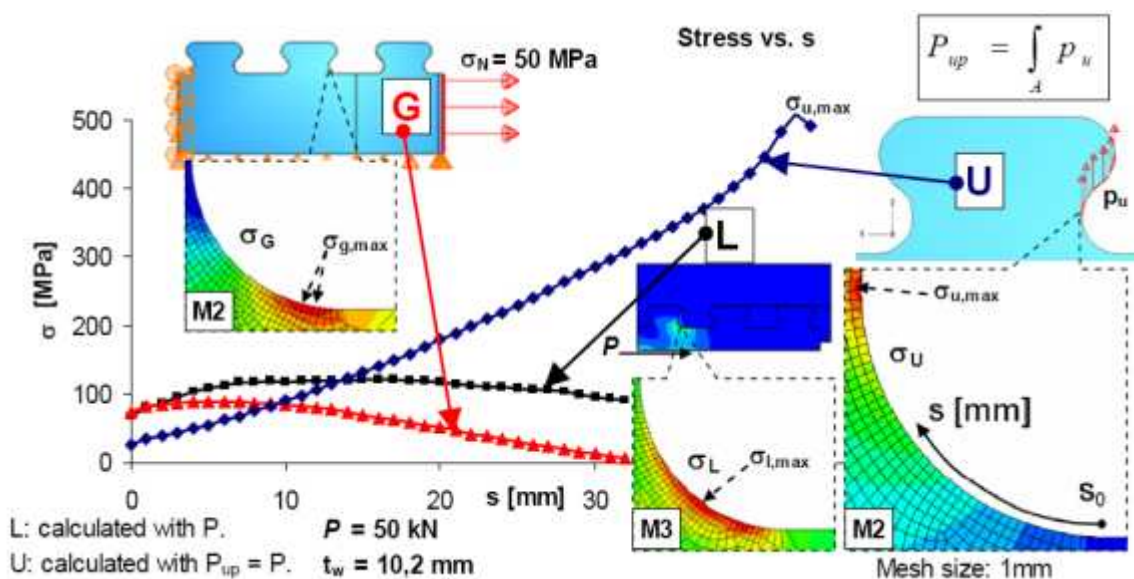
Fig.13.20. Stresses in steel dowel along arc length from specific actions: σ_{ne} ($\sigma_{g,\,G}$), P_τ (L) and P_{up} (U).

⚒ ULTIMATE LIMIT STATE DESIGN OF THE STEEL DOWEL

In [P621 2007] continuous shear connectors have been experimentally investigated. Hereby cracks in the steel strip have been observed whereas the concrete matrix has not been significantly damaged (figure 13.21). In reference to this failure mode a steel failure criterion has been derived.

For its application for VFT-WIB bridges this formula has to be modified to cover the additional uplifting forces from the global geometry of the cross sections, see figure 13.22. However the overall assumption, that the resulting maximum equivalent Von Mises stresses do not exceed the yield strength is kept as basis of design.

Consequently the bearing resistance of a single steel tooth **_P_**_Rd_ is determined in dependency of the loading specified and in accordance with [P621 2007]. Hereby influence of the increase of the nominal stresses of the steel section due to the dowel geometry has been neglected as it is insignificant in the plastic design.

Fig. 13.21. ULS-failure [P621 2007]
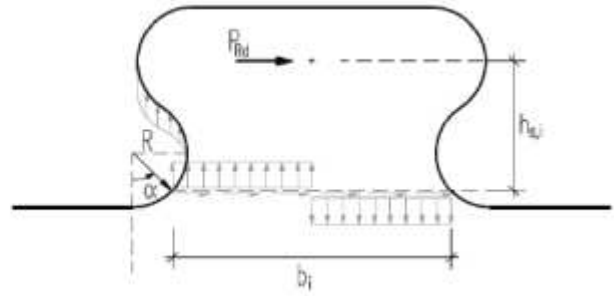
Fig. 13.22. Forces and stresses in a critical section at ULS

Thus, the following design criterion is derived:

$$P_{Rk} = \frac{f_y \cdot t_w \cdot b_i^2}{\sqrt{\left(4 \cdot h_{s,j} + \frac{h'_i \cdot (b_2 + b_3)}{e_x}\right)^2 + 3 \cdot b_i^2}} \qquad [kN] \qquad\qquad \text{Eq.13.5.}$$

with
f_y Yield strength steel $\left[\frac{N}{mm^2}\right]$,

t_w Plate thickness of web [mm],

$h_{s,j}$ Distance of centre of gravity to critical section $= h_s - (1 - cos\alpha) \cdot R$ [mm],

b_i Width at critical section $= b_1 - 2 \cdot sin\alpha \cdot R$ [mm],

h'_i $= h' - (1 - cos\alpha) \cdot R$,

e_x distance between connectors, fig.13.16.

α angle along cutting edge, fig.13.14,

For the puzzle shape the maximum equivalent stresses derived from equation 13.5 has been located to be at $\alpha = 70°$ for the POST which is in accordance to the tests, see figure 13.21.

✖ FATIGUE RESISTANCE OF A GAS CUT EDGE

The fatigue design of the steel part is divided into two parts. One part is dedicated to the fatigue design of the web taking the increase in stress due to the notching effect of the steel tooth into account. The second part treats the estimation of the fatigue stresses along the gas cut edge of the dowel itself, considering the effect of the shear stresses as well as the nominal stresses in the steel section and their verification.

However at first, the fatigue resistance of a gas cut edge has to be specified. According to the Eurocode [EC3-1-9] the fatigue category of a gas cut edge is 140 when subsequent dressing is applied. Hereby all visible signs of edge discontinuities have to be removed. The cut areas are to be machined or ground and all burrs to be removed. Any machinery scratches, for example from grinding operations, can only be parallel to the stresses. If the cut has shallow and regular drag lines with cut quality II according to EN 1090 (for railway bridges cut quality I [DIN FB 103]) the fatigue category is reduced to 125. For both categories repair by weld refill is not allowed. Re-entrant corners are to be improved by grinding appropriate stress concentration factors.

Therefore the roughness and cutting tolerances from the oxy-cutting process have been measured in dependency to the cutting speed. The results are shown in table 2. The deviation is small and all cutting surfaces are class I.

Tab.13.2. Comparison Roughness in dependency of the cutting speed.

Cutting speed *v*	Medium surface roughness Rz	Tolerances of rectangularity and inclination
350 [mm/min]	43 – 63 [µm]	0.10 [mm]
500 [mm/min]	20 – 74 [µm]	0.40 [mm]
650 [mm/min]	40 – 62 [µm]	0.25 [mm]

In addition knowledge on the fatigue resistance is found in the research project [P185]. In this project the influence of the cutting quality on the fatigue design made from fine-grain steels (according of today's EN10025-4) has been investigated. It has been noted, that the initial crack occurs from the blasted surface in ***the heat affected zone (HAZ)*** from cutting. However it has been noticed that short stopping of the flame cutter decreases the fatigue strength to **60%**. This results from the change of the failure initiation to the cut edge. Further it has been observed that hammering (an effect which may occur due to hammering of the continuous shear connector in gaps from which plastified concrete may have disappeared), cutting speed, warming before cutting and material strength have hardly an influence on the fatigue strength.

Therefore crack initiation occurs in the HAZ along the cut. The design value is therefore conservatively derived to $\Delta\sigma C$ = 125 N/mm2. If stopping of the flame cutter can not be avoided it should take place at an irrelevant location in terms fatigue.

✖ FATIGUE DESIGN OF THE STEEL WEB

Due to the notch effect of the steel tooth the stresses of the web along the cut edge are increased. The reduction due to the geometry is comparable to the effect by longitudinal stiffeners, however only the geometrical effect has to be considered as the material notch due to welding is inexistent. Therefore the fatigue verification has to be performed with the fatigue category of gas cut edges $\Delta\sigma_C$ = 125 N/mm2 according to [EC3-1-9] and:

$$\Delta\sigma_{E,2} = \Delta\sigma_{N,w} \cdot \beta_N \qquad \left[\frac{N}{mm^2}\right]$$

Eq.13.6.

with $\quad \Delta\boldsymbol{\sigma_{N,w}}$ relevant longitudinal stresses in the web along the bottom line of the connector,

$\boldsymbol{\beta_N}$ according to equation 13.3.

✖ FATIGUE DESIGN OF THE STEEL CONNECTOR

Fatigue crack initiation and propagation depend on the principle stresses along the cutting edge. To derive an analytic design model for fatigue verification the principle stresses have consequently to be considered, which are supposed perpendicular to the radius (figure 13.23).
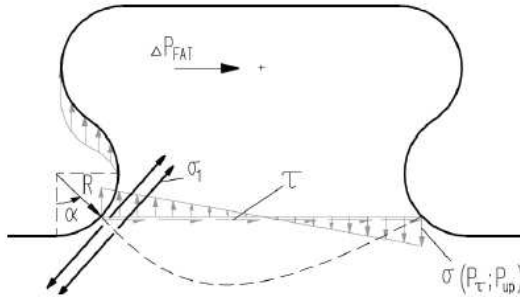
Fig. 13.23. Analytic model for principle stresses
(in dependency of the angular α).
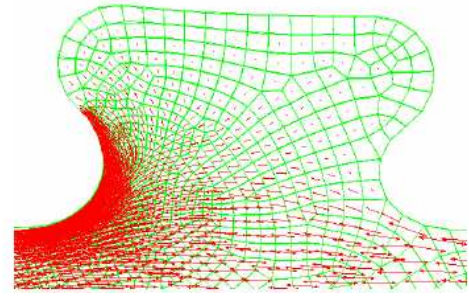
Fig. 13.24. Principal stress trajectories in dowel
(P_{Rd} and $P_{up} \neq 0$ and σ_N influence).

With the loading defined previously and in dependency of α, the following fatigue load resistance has been derived:

$$\Delta P_{FAT} = \left(\Delta\sigma_C - \beta_N \cdot \Delta\sigma_{N,w}\right) \cdot \frac{t_w \cdot b_i^2}{b_r \cdot cos\alpha + \left(6 \cdot h_{si} + \frac{3 \cdot h'_i \cdot (b_2 + b_3)}{2 \cdot e_x}\right) \cdot sin\alpha} \quad [kN] \qquad \text{Eq.13.7.}$$

with $\Delta\sigma_C$ Fatigue strength of gas cut edge $\left[\frac{N}{mm^2}\right]$,

       b_r arc length at critical section $= \dfrac{\pi(90-\alpha)\left(\frac{1}{2}b_1 - sin\alpha \cdot R\right)}{90 \cdot cos\alpha}$ [mm],

       $h_{si}, t_w, h'_i, e_x, \alpha$ see equation 13.5,

       $\Delta\sigma_{N,w}, \beta_N$ see equation 13.6,

For the puzzle geometry investigated the maximum principle stresses along the cut edge have been derive at an angle α = 20°.

✖ SUMMARY

Further the main problems for VFT-WIB construction in design have been identified based on experimental results from the previous years and own test results. Especially the fatigue design of the steel tooths of continuous shear connectors are here to be noticed.

Consequently a design concept for the steel part of continuous shear connectors applied in VFT-WIB constructions has been derived. Main focus has been laid on the analytic approach for hand calculation and its validation by experimental results and FEA.

However it is also possible to calculate the Von Mises and the principle stresses resulting from the local loading by FEA and to derive shape functions for each connector. These factors, Ael,L and Ael,U are embedded in equations 8 for the final design with global loading [PreCo-Beam].

$$\sigma = \frac{1}{I_y} \cdot \left[V \cdot \frac{S_y}{t_w} \cdot \left(\frac{1}{A_{el,L}} + \frac{tan\alpha}{A_{el,U}} \right) + M \cdot z \cdot \beta_{N,w} \right] \qquad \left[\frac{N}{mm^2} \right] \qquad \text{Eq.13.8.}$$

with   V,M   global transversal force and bending moment in beam, respectively,

          z   distance of bottom line of steel dowel to neutral axis,

          α_U uplift angle, see Fig. 13,

          t_w web thickness,

          I_y, S_y second moment of area and moment of area of steel part, respectively[9].

13.3. Examples

- *The road bridge crossing the railroad line in Pöcking:*

The 100 year old bridge in the Community of Pöcking which links the village with Lake Starnberg was reconstructed in 2004. A plan exists to install a lift to the platform which extends under the bridge, in order to allow disabled passengers access to the railway station below. In a move to avoid excessive deformation between the lift and the bridge, the structure was designed with two spans and a central pillar. The bridge, including its recessed abutments, thus has a span of 2 x 16.60 m. The gradient of the road only allows a low construction height of 0.80 m. The bridge crosses the railroad line between Munich and Garmisch that is heavily used by long-distance and local trains. It was therefore necessary to complete the superstructure as quickly as possible.

The cross section of the bridge accommodates 3 VFT-WiB girders, each with a height of 0.55 m and a width of 3.20 m each. In order to simplify the laying process, the prefabricated elements with a length of 32.0 m, extend across both spans (Fig. 13.25). They were lifted into the structure during one night. The frame corners were cast in concrete, together with the 0.25 m thick deck slab, so that a two-cell frame was created (Fig. 13.26).

The rolled steel girders (HE 1000 M) belong to quality class S460E. They were laid at a distance of 3.6 cm from each other and are connected with each other by a steel frame. Both girders are supplemented by a flange and the space between the girders is filled in with concrete (Fig. 13.27). This robust design of the composite girders increases their rigidity so as to absorb traffic loads in a vertical direction and possible impact loads in a horizontal direction. The complete failure of a main girder through an impact can thus be excluded.

The construction method applied in Pöcking proved to be very economical, with the costs amounting to € 1530/m² (app. 1800 $/m²) of bridge area. The invitation to tender was open to secondary offers.
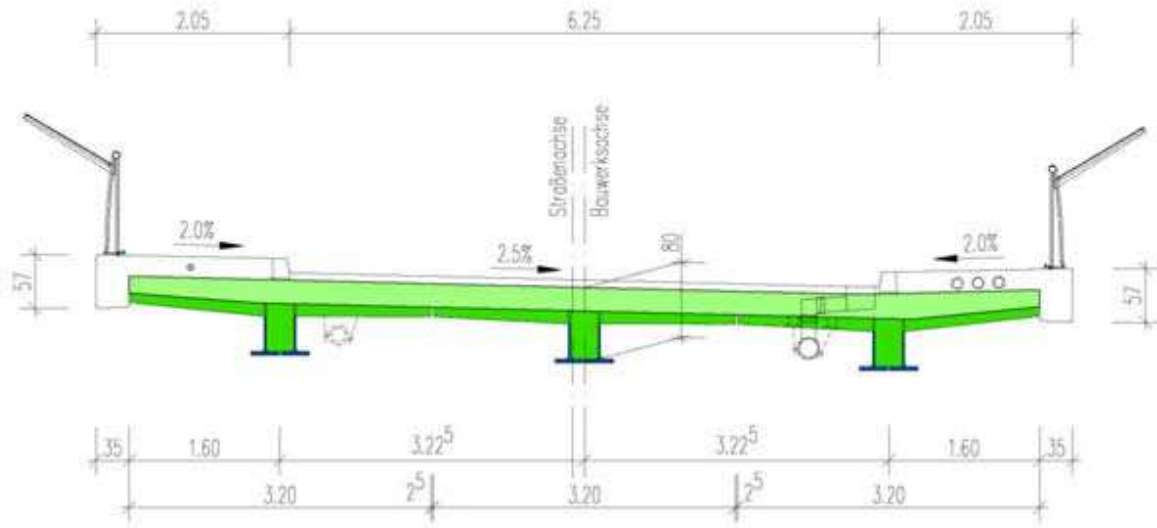
Fig. 13.25. Cross section of the bridge in Pöcking.
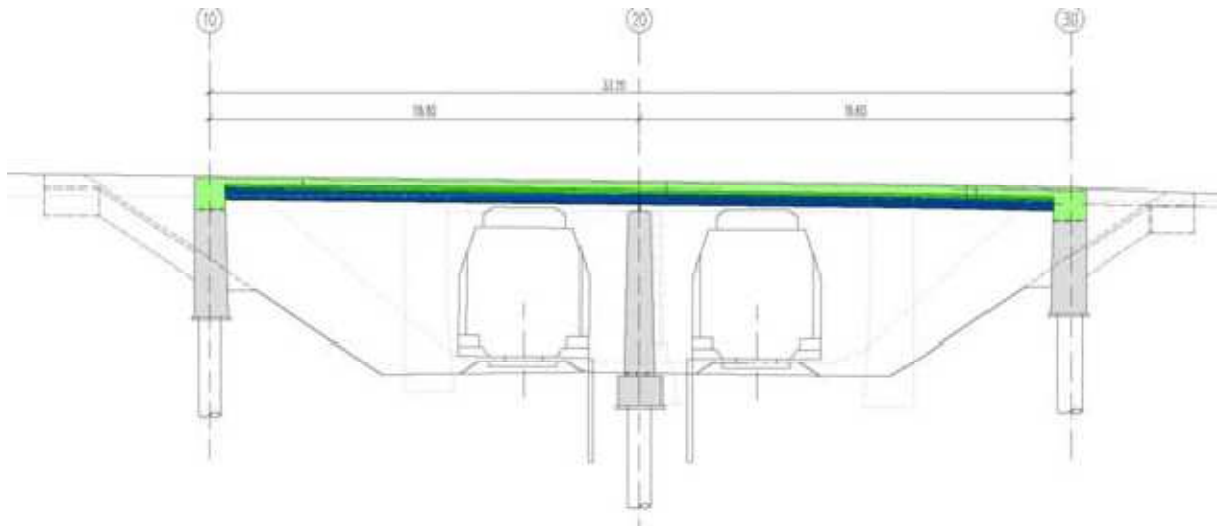
Fig. 13.26. Longitudinal section of the bridge in Pöcking.
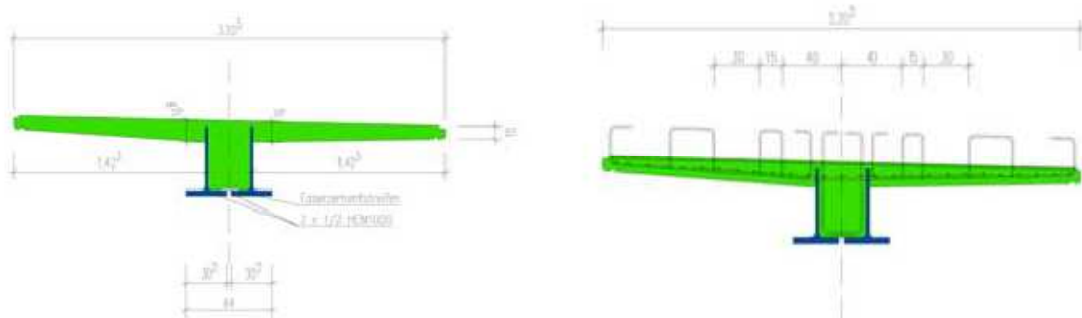
Fig. 13.27. VFT-WIB girder of the bridge in Pöcking.

- ***The road bridge crossing the railroad line in Golling:***

Less steel is needed when the halved rolled girders, with the cuts serving as concrete dowels, are used as external reinforcement. The web of the steel girder with the dowels is integrated in the reinforced concrete web. The shear forces are mainly carried by the concrete web, the steel flange serves as reinforcement. Using this method, haunched girders with a longitudinally variable web-height are easily possible.

This method is being applied in a bridge in Austria over the railway line Salzburg – Wörgl (Fig. 13.28, 13.29). The length of the 4-bay bridge is 80 m. The superstructure is rigidly connected with the columns and the abutments. The shape of the concrete dowels is being modified, the new form looks like a fin. With the new form the concrete dowels (Fig. 13.30, 13.31) reach a higher bearing capacity. Several push-out tests have been carried out at the beginning of the project with good results, which have been confirmed in tests with single-span girders[6].
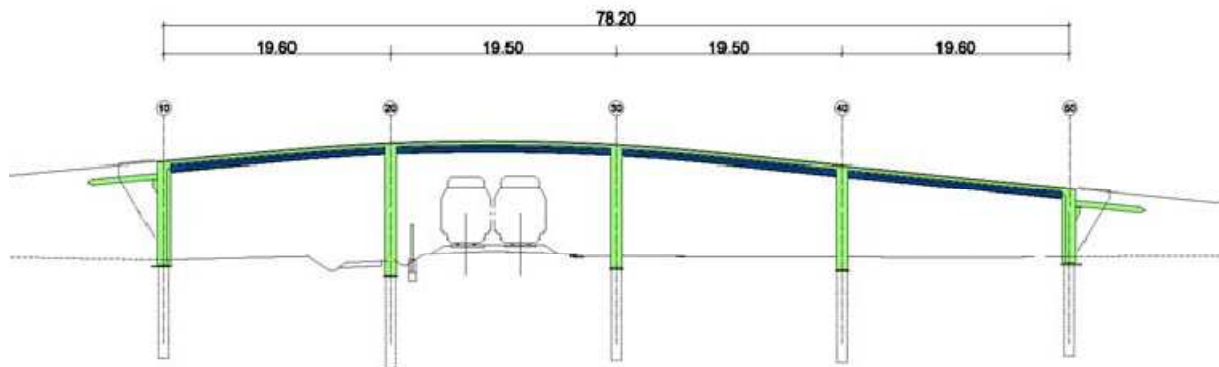
Fig. 13.28. Longitudinal section.
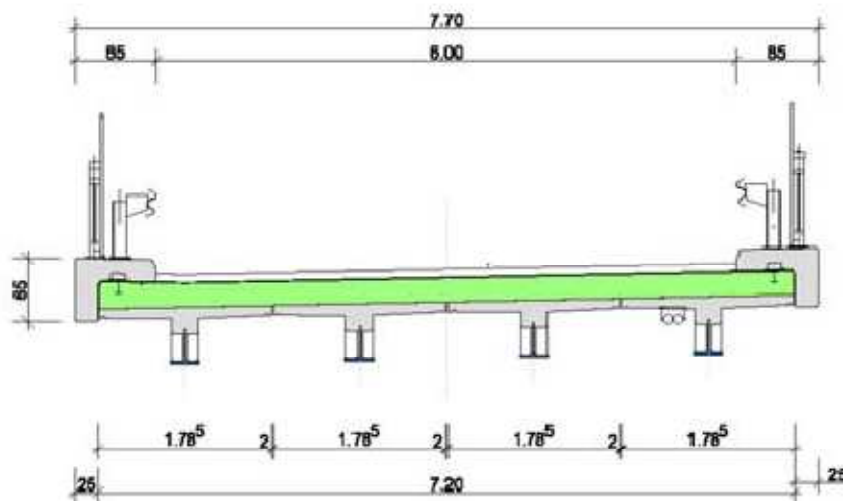
Fig. 13.29. Cross section.
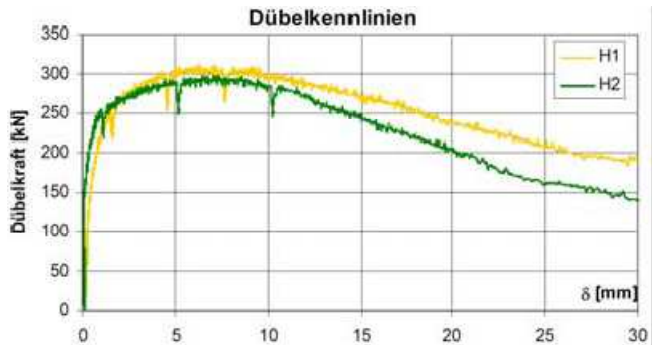
Fig. 13.30. Characteristic load-slip-relations per dowel.
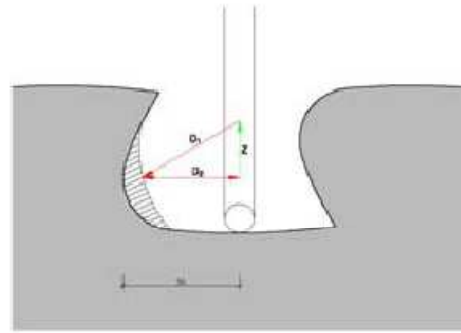
Fig. 13.31. Web – Cut – Line.

14. THE BASICS OF STATIC AND DIMENSIONING ANALYSIS

To show the differences in design process between typical composite bridges and bridges with composite prefabricated girders, two 50,00m length continuous beams (two spans: 25,00m + 25,00m) have been proposed:

- VFT bridge (see point 9.1),
- Composite bridge (see point 9.2).

14.1. Preliminary draft for VFT bridge
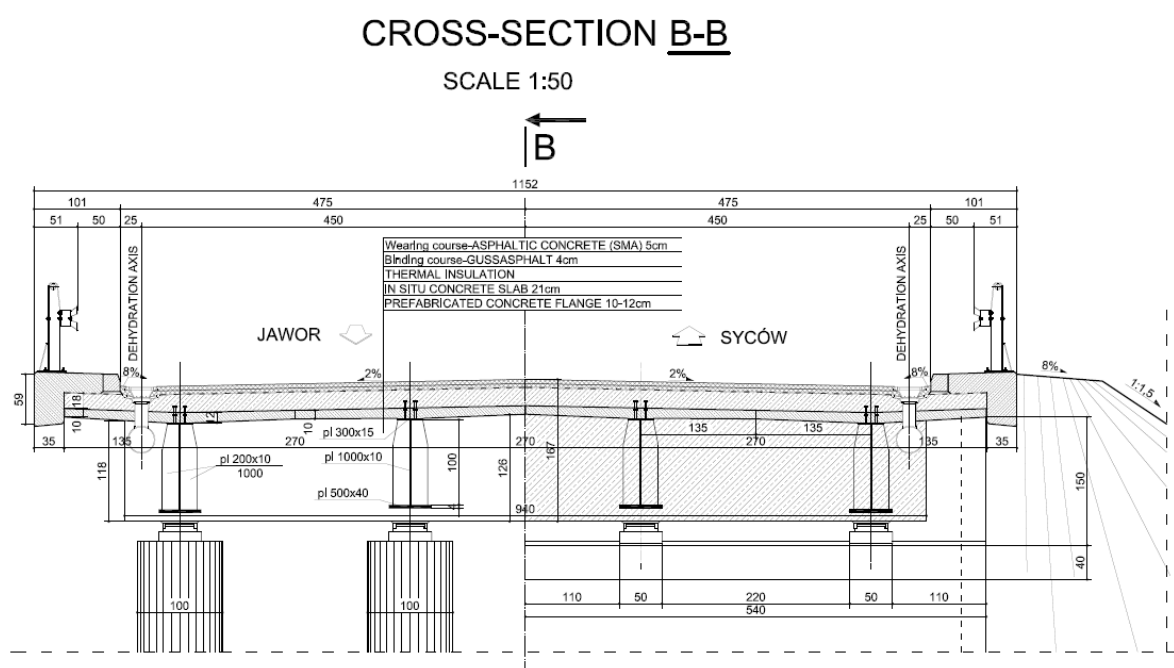
Fig. 14.1. Cross-section consisting of 4 VFT girders.
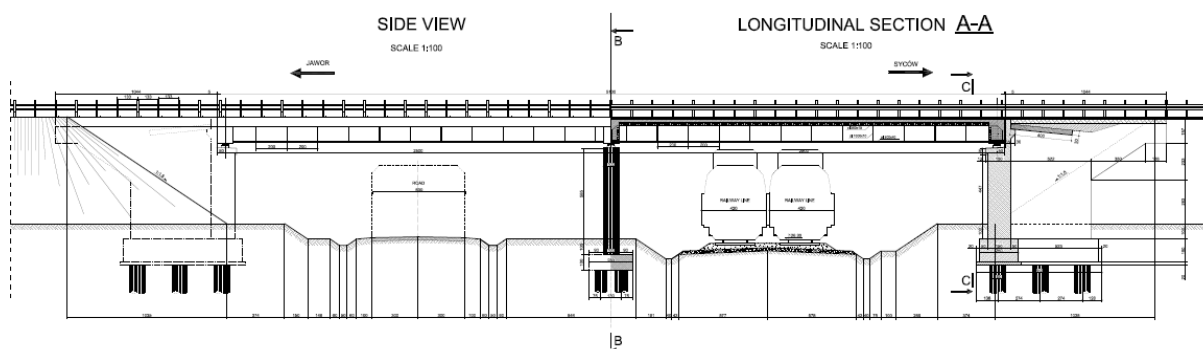
Fig. 14.2. Longitudinal-section of VFT bridge.

14.1.1. Statement of the loads

➔ *Phase 1 :*

- Dead load of steel construction:
- Steel girder:

$$A_s = 0{,}0345m^2 \qquad\qquad l_s = 25m * 4$$

- Rib:

$$A_r = 0{,}00211m^3 \qquad\qquad u_r = 8 * 14$$

$$\gamma_s = 78{,}5\frac{kN}{m^3} + 1{,}4\frac{kN}{m^3} - \text{addition to weight of welded steel construction}$$

Characteristic load:

$$g_s^{ch} = (0{,}0345m^2 \cdot 25m \cdot 4 + 0{,}00211m^3 \cdot 8 \cdot 14) \cdot \frac{\left(78{,}5\frac{kN}{m^3} + 1{,}4\frac{kN}{m^3}\right)}{25{,}0m} = \boldsymbol{11{,}78}\frac{\boldsymbol{kN}}{\boldsymbol{m}}$$

Design load:

$$g_s^d = g_s^{ch} \cdot 1{,}2 = 11{,}78\frac{kN}{m} \cdot 1{,}2 = \boldsymbol{14{,}14}\frac{\boldsymbol{kN}}{\boldsymbol{m}}$$

- Dead load of wet prefabricated concrete flange (for one girder):

$$A_{pf} = 0{,}300m^2 \qquad\qquad \gamma_c = 26\frac{kN}{m^3}$$

Characteristic load:

$$g_{pf}^{ch} = m^2 \cdot 26\frac{kN}{m^3} = \boldsymbol{7{,}80}\frac{\boldsymbol{kN}}{\boldsymbol{m}}$$

Design load:

$$g_{pf}^d = g_{pf}^{ch} \cdot 1{,}2 = 7{,}80\frac{kN}{m} \cdot 1{,}2 = \boldsymbol{9{,}36}\frac{\boldsymbol{kN}}{\boldsymbol{m}}$$

TOTAL LOADS FOR ONE GIRDER:

Characteristic load:

$$g_l^{ch} = \frac{(g_s^{ch})}{4} + g_{pf}^{ch} = \frac{\left(11,78\frac{kN}{m}\right)}{4} + 7,80\frac{kN}{m} = \mathbf{10,745}\frac{\pmb{kN}}{\pmb{m}}$$

Design load:

$$g_l^d = \frac{(g_s^d)}{4} + g_{pf}^a = \frac{\left(14,14\frac{kN}{m}\right)}{4} + 9,36\frac{kN}{m} = \mathbf{12,895}\frac{\pmb{kN}}{\pmb{m}}$$

➔ *Phase 2:*

- Unloading of prefabricated concrete flange:

$$A_{pf} = 0,300m^2 \qquad\qquad \gamma_c = -1\frac{kN}{m^3}$$

Characteristic load:

$$g_{upf}^{ch} = 0,300m^2 \cdot \left(-1\frac{kN}{m^3}\right) = \mathbf{-0,3}\frac{\pmb{kN}}{\pmb{m}}$$

Design load:

$$g_{upf}^d = g_{upf}^{ch} \cdot 1,2 = -0,3\frac{kN}{m} \cdot 1,2 = \mathbf{-0,36}\frac{\pmb{kN}}{\pmb{m}}$$

- Technological load:

$$W_{ds} = 10,82m \qquad\qquad \gamma_t = 1,5\frac{kN}{m^2}$$

Characteristic load:

$$g_t^{ch} = 10,82m \cdot 1,5\frac{kN}{m^2} = \mathbf{16,23}\frac{\pmb{kN}}{\pmb{m}}$$

Design load:

$$g_t^d = g_t^{ch} \cdot 1,3 = 16,23\frac{kN}{m} \cdot 1,5 = \mathbf{21,1}\frac{\pmb{kN}}{\pmb{m}}$$

- Dead load of wet concrete deck slab:

$$A_{ds} = 2,2116m^2 \qquad\qquad \gamma_c = 26\frac{kN}{m^3}$$

$\sim 53 \sim$

Characteristic load:

$$g_{ds}^{ch} = 2,8448 m^2 \cdot 26 \frac{kN}{m^3} = \mathbf{57,50 \frac{kN}{m}}$$

Design load:

$$g_{ds}^{d} = g_{ds}^{ch} \cdot 1,2 = 57,50 \frac{kN}{m} \cdot 1,2 = \mathbf{69,00 \frac{kN}{m}}$$

TOTAL LOADS FOR ONE GIRDER:

Characteristic load:

$$g_{II}^{ch} = g_{upf}^{ch} + \frac{(g_t^{ch} + g_{ds}^{ch})}{4} = -0,3 \frac{kN}{m} + \frac{\left(16,23 \frac{kN}{m} + 57,50 \frac{kN}{m}\right)}{4} = \mathbf{18,124 \frac{kN}{m}}$$

Design load:

$$g_{II}^{d} = g_{upf}^{d} + \frac{(g_t^{d} + g_{ds}^{d})}{4} = -0,36 \frac{kN}{m} \frac{\left(21,1 \frac{kN}{m} + 69,00 \frac{kN}{m}\right)}{4} = \mathbf{22,165 \frac{kN}{m}}$$

➔ *Phase 3:*

- Unloading of deck slab:

$$t_{ds} = 0,21m \qquad \gamma_c = -1 \frac{kN}{m^3}$$

Characteristic load:

$$g_{uds}^{ch} = 0,21m \cdot \left(-1 \frac{kN}{m^3}\right) = \mathbf{-0,21 \frac{kN}{m^2}}$$

Design load:

$$g_{uds}^{d} = g_{ds}^{ch} \cdot 0,9 = -0,21 \frac{kN}{m^2} \cdot 1,2 = \mathbf{-0,189 \frac{kN}{m^2}}$$

- Weight of equipment:

PART 1 (for the "deck overhang ➔ 0,65m width)

- *Bridge deck overhang:*

$A_o = 0,3211 m^2$ $\qquad\qquad$ $u_o = 2$ $\qquad\qquad$ $\gamma_c = 25 \frac{kN}{m^3}$

- Stone curb:

$A_{sc} = 0,0388 m^2$ $\qquad\qquad$ $u_{sc} = 2$ $\qquad\qquad$ $\gamma_{stone} = 27 \frac{kN}{m^3}$

- Crash cushion (I assumed 1,0kN/m for each barrier):

$G_{cc} = 1,0 \frac{kN}{m}$ $\qquad\qquad$ $u_{cc} = 2$

- Insulation:

$t_i = 0,01 m$ $\qquad\qquad$ $\gamma_i = 14 \frac{kN}{m^3}$

Characteristic load:

$$g_{e1}^{ch} = \left(0,3211 m^2 \cdot 2 \cdot 25 \frac{kN}{m^3} + 0,0388 m^2 \cdot 2 \cdot 27 \frac{kN}{m^3} + 1,0 \frac{kN}{m} \cdot 2\right) \cdot \frac{1}{0,65 m} + 0,01 m$$
$$\cdot 14 \frac{kN}{m^3} = \mathbf{31,14 \frac{kN}{m^2}}$$

Design load:

$$g_{e1}^d = g_{e1}^{ch} \cdot 1,5 = 31,14 \frac{kN}{m} \cdot 1,5 = \mathbf{46,71 \frac{kN}{m^2}}$$

PART 2 (for the "pavement" → 9,5m width)

- Pavement:

$t_p = (0,05 m + 0,04 m) = 0,09 m$ $\qquad\qquad$ $\gamma_p = 23 \frac{kN}{m^3}$

- Insulation:

$t_i = 0,01 m$ $\qquad\qquad$ $\gamma_i = 14 \frac{kN}{m^3}$

Characteristic load:

$$g_{e2}^{ch} = 0,09 m \cdot 23 \frac{kN}{m^3} + 0,01 m \cdot 14 \frac{kN}{m^3} = \mathbf{2,21 \frac{kN}{m^2}}$$

Design load:

$$g_{e2}^d = g_{e2}^{ch} \cdot 1,5 = 2,21 \frac{kN}{m^2} \cdot 1,5 = \mathbf{3,315 \frac{kN}{m^2}}$$

- Live loads:

Live loads (B class bridge) according to [PN-85/S-10030] → scheme:
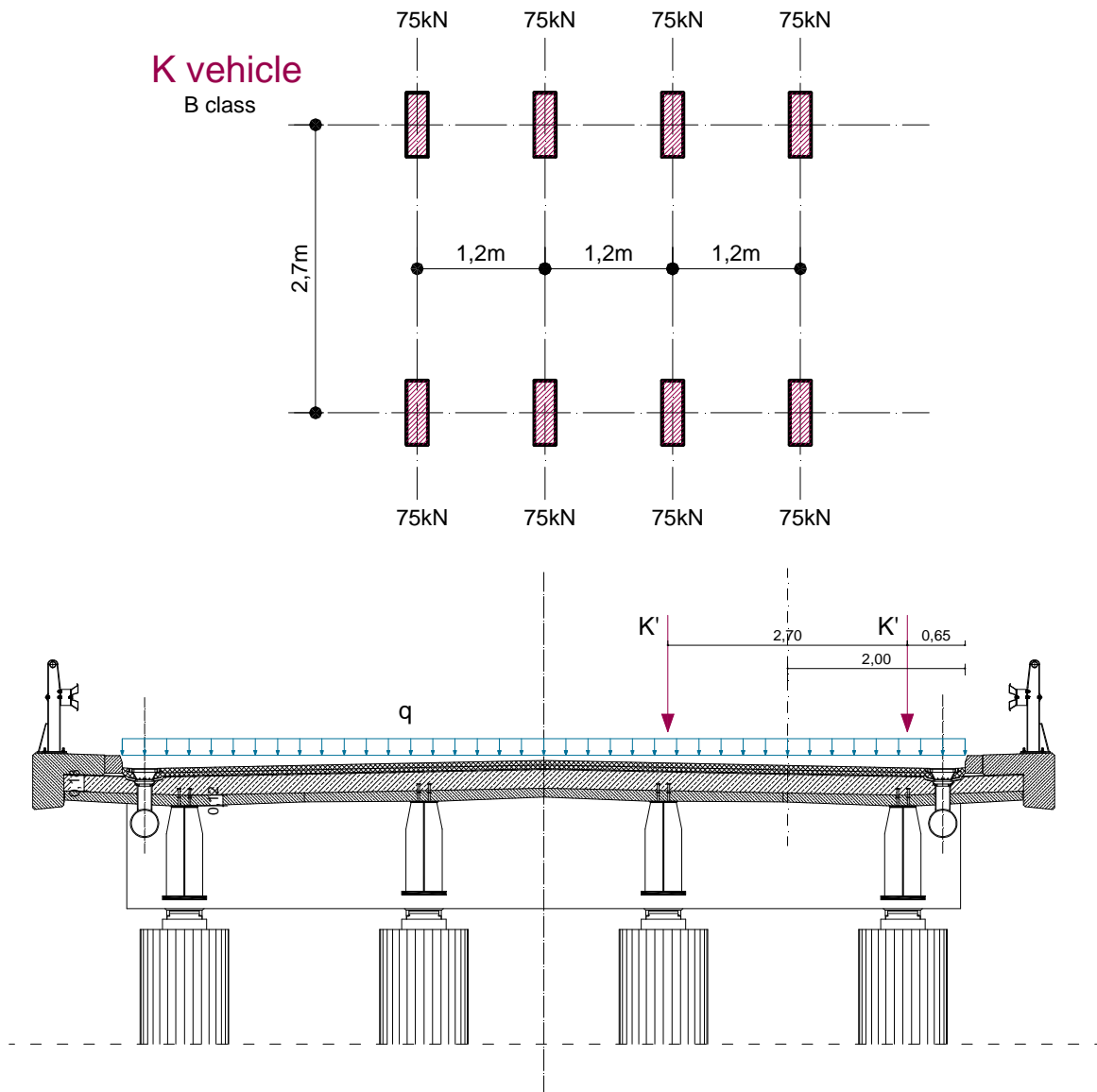
-   Automobiles, B class according to [PN-85/S-10030]:

Characteristic load:

$$q_a^{ch} = 3\frac{kN}{m^2} = \mathbf{3\frac{kN}{m}}$$

Design load:

$$q_a^d = q_a^{ch} \cdot 1{,}5 = 3\frac{kN}{m} \cdot 1{,}5 = \mathbf{4,5\frac{kN}{m}}$$

- K vehicle, B class according to [PN-85/S-10030]:

Dynamical coefficient

$$\varphi = 1{,}35 - 0{,}005 \cdot 25m = 1{,}225 \le 1{,}325$$

Characteristic load:

$$P_K^{ch} = \mathbf{75kN}$$

Design load:

$$P_K^d = P_K^{ch} \cdot 1{,}5 \cdot \varphi = 75kN \cdot 1{,}5 \cdot 1{,}225 = \mathbf{137{,}8125kN}$$

14.1.2. Structural analysis

➔ *Phase 1 :*   *FREE   SUPPORTED   BEAM:*

Influence line of bending moment
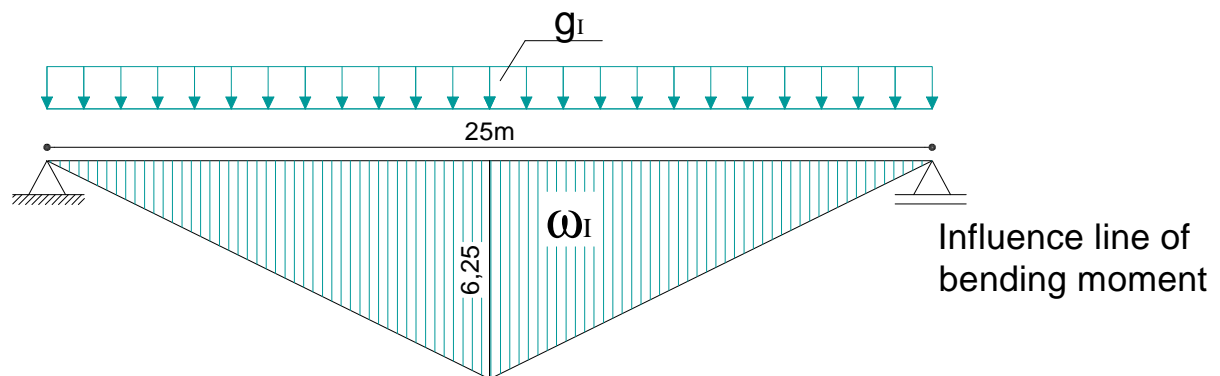
$$\omega_I = 78{,}125m^2$$

$$M_I^{ch} = g_I^{ch} \cdot \omega_I = 10{,}745 \frac{kN}{m} \cdot 78{,}125m^2 = \mathbf{839{,}45kNm}$$

$$M_I^d = g_I^d \cdot \omega_I = 12{,}895 \frac{kN}{m} \cdot 78{,}125m^2 = \mathbf{1007{,}42kNm}$$

➔ **Phase 2 :**   *FREE   SUPPORTED BEAM:*

g_{II}

25m

6,25

ω_{II}

Influence line of bending moment
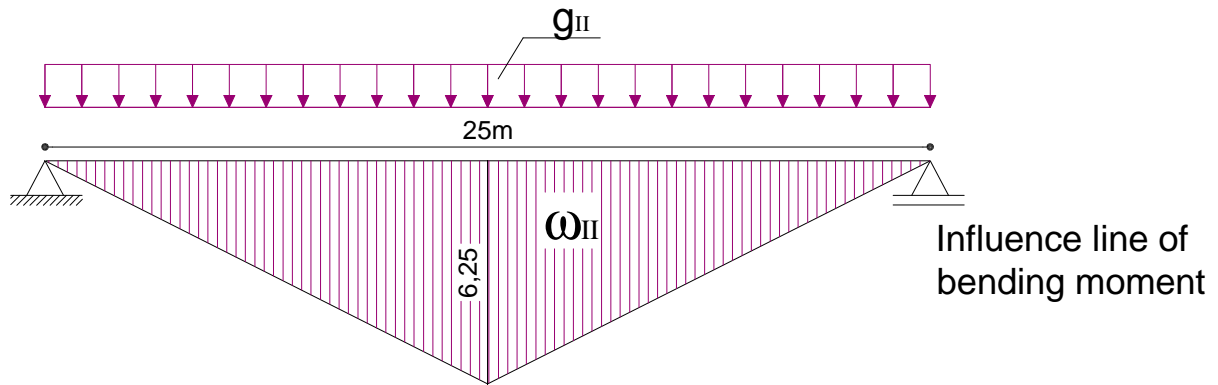
$\omega_{II} = 78{,}125 m^2$

$M_{II}^{ch} = g_{II}^{ch} \cdot \omega_{II} = 18{,}124 \dfrac{kN}{m} \cdot 78{,}125 m^2 = \mathbf{1415{,}94 kNm}$

$M_{II}^{d} = g_{II}^{d} \cdot \omega_{II} = 22{,}165 \dfrac{kN}{m} \cdot 78{,}125 m^2 = \mathbf{1731{,}64 kNm}$

➔ **Phase 3 :**   *CONTINUOUS BEAM:*

LONGITUDINAL ELEMENTS:

✖ **COMPOSITE GIRDER:**

Geometrical characteristic of prefabricated composite girder section:

STEP_1: *(equivalent section "in situ" concrete slab + prefabricated concrete flange)*

Geometrical characteristic of "in situ" slab:

- Concrete slab (B40 according to PN):

  $I_s = \mathbf{0{,}002084 m^4}$

  $A_s = \mathbf{0{,}567 m^2}$

  $E_s = \mathbf{36{,}4 GPa}$

y

2700

210

105 105

0_s

x

~ 58 ~

UNIVERSITAT POLITÈCNICA DE CATALUNYA
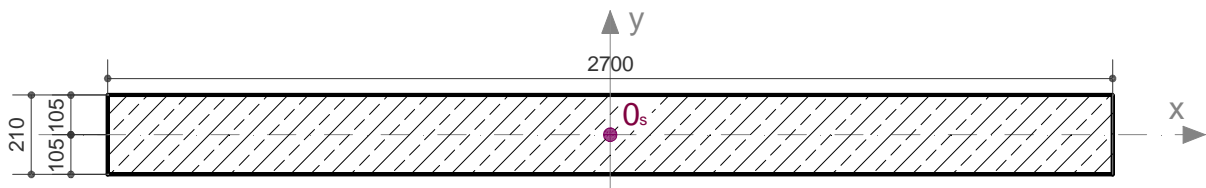
Geometrical characteristic of prefabricated concrete flange:

- Prefabricated concrete flange (B60 according to PN):
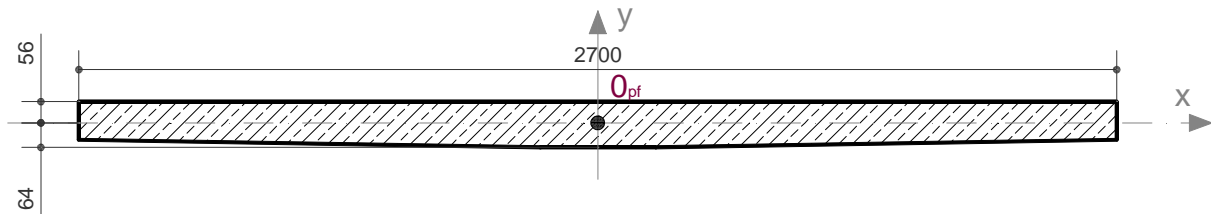
$$I_{pf} = 0,0003145 m^4$$

$$A_{pf} = 0,300 m^2$$

$$E_{pf} = 41 GPa$$

Equivalent section

- Distance between centres of gravity of concrete flange and steel beam
- $a = 0,161m$
- Distance of extreme fibres:
  In situ concrete slab:
- Top fibres: $v_t = 0,105m$
- Bottom fibres: $v_b = 0,105m$
  Prefabricated concrete flange:
- Top fibres: $y_t = 0,056m$
- Bottom fibres: $y_b = 0,064m$

$$n_\varphi = \frac{E_{pf}}{E_s} = \frac{41GPa}{36,4GPa} = 1,13$$

$$A_{s\varphi} = \frac{A_s}{n_\varphi} = \frac{0,567m^2}{1,13} = 0,502m^2$$

$$I_{s\varphi} = \frac{I_s}{n_\varphi} = \frac{0,002084m^4}{1,13} = 0,00184m^4$$

- Distances between centre of gravity of equivalent section and concrete slab / steel beam

$$\frac{a}{a_b} = \frac{A_{pf} + A_{s\varphi}}{A_{s\varphi}} \quad \rightarrow \quad a_b = \frac{A_{s\varphi} \cdot a}{A_{pf} + A_{s\varphi}} = \frac{0,567m^2 \cdot 0,161m}{0,300m^2 + 0,567m^2} = 0,105m$$

$$a_t = a - a_b = 0,161m - 0,105m = 0,056m$$

- Top: $a_t = \mathbf{0,056m}$
- Bottom: $a_b = \mathbf{0,105m}$
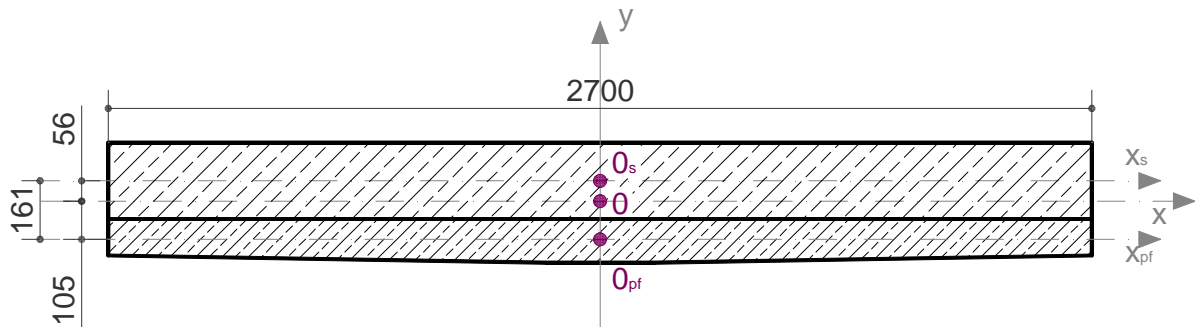
- Area of equivalent section:

$$A_c = A_{pf} + A_{s\varphi} = 0{,}300m^2 + 0{,}502m^2 = \mathbf{0,802m^2}$$

- Moment of inertia of equivalent section:

$$
\begin{aligned}
I_c &= I_{pf} + I_{s\varphi} + A_{pf} \cdot a_b^2 + A_{s\varphi} \cdot a_t^2 \\
&= 0{,}0003145m^4 + 0{,}00184m^4 + 0{,}300m^2 \cdot (0{,}105m)^2 + 0{,}502m^2 \\
&\quad \cdot (0{,}056m)^2 = \mathbf{0,00704m^4}
\end{aligned}
$$

STEP 2: *(equivalent section composite concrete slab and steel beam)*

Geometrical characteristic of composite concrete slab:

- Composite concrete slab:

  $I_c = \mathbf{0,00704m^4}$

  $A_c = \mathbf{0,802m^2}$

  $E_c = \mathbf{41GPa}$

Geometrical characteristic of steel beam:

- Steel beam:

  $I_b = \mathbf{0,005494m^4}$

  $A_b = \mathbf{0,0345m^2}$

  $E_b = \mathbf{205GPa}$

UNIVERSITAT POLITÈCNICA DE CATALUNYA

Equivalent section

- Distance between centres of gravity of concrete flange and steel beam
- $a = \mathbf{0,919m}$
- Distance of extreme fibres:
  Steel beam:
- Top fibres: $v_t = \mathbf{0,750m}$
- Bottom fibres: $v_b = \mathbf{0,305m}$
  Composite concrete slab:
- Top fibres: $y_t = \mathbf{0,161m}$
- Bottom fibres: $y_b = \mathbf{0,169m}$

$$n_\varphi = \frac{E_b}{E_s} = \frac{205GPa}{41GPa} = \mathbf{5}$$

$$A_{c\varphi} = \frac{A_c}{n_\varphi} = \frac{0,802m^2}{5} = \mathbf{0,1604m^2}$$

$$I_{c\varphi} = \frac{I_c}{n_\varphi} = \frac{0,00704m^4}{5} = \mathbf{0,001408m^4}$$

- Distances between centre of gravity of equivalent section and concrete slab / steel beam

$$\frac{a}{a_b} = \frac{A_b + A_{c\varphi}}{A_{c\varphi}} \quad \rightarrow \quad a_b = \frac{A_{c\varphi} \cdot a}{A_b + A_{c\varphi}} = \frac{0,1604m^2 \cdot 0,919m}{0,0345m^2 + 0,1604m^2} = \mathbf{0,756m}$$

$$a_t = a - a_b = 0,919m - 0,756m = \mathbf{0,163m}$$

- Top: $a_t = \mathbf{0,163m}$
- Bottom: $a_b = \mathbf{0,756m}$
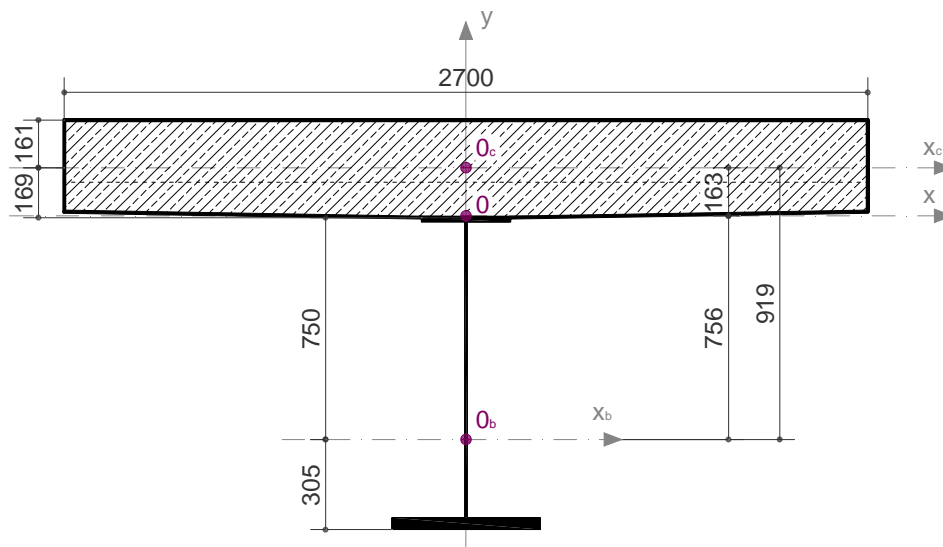
- Area of equivalent section:

$$A = A_b + A_{c\varphi} = 0,0345m^2 + 0,1604m^2 = \mathbf{0,1949m^2}$$

- Moment of inertia of equivalent section:

$$I_x = I_b + I_{c\varphi} + A_b \cdot a_b^2 + A_{c\varphi} \cdot a_t^2$$
$$= 0,005494m^4 + 0,001408m^4 + 0,0345m^2 \cdot (0,756m)^2 + 0,1604m^2$$
$$\cdot (0,163m)^2 = \mathbf{0,03088m^4}$$

- Torsional moment of equivalent section:
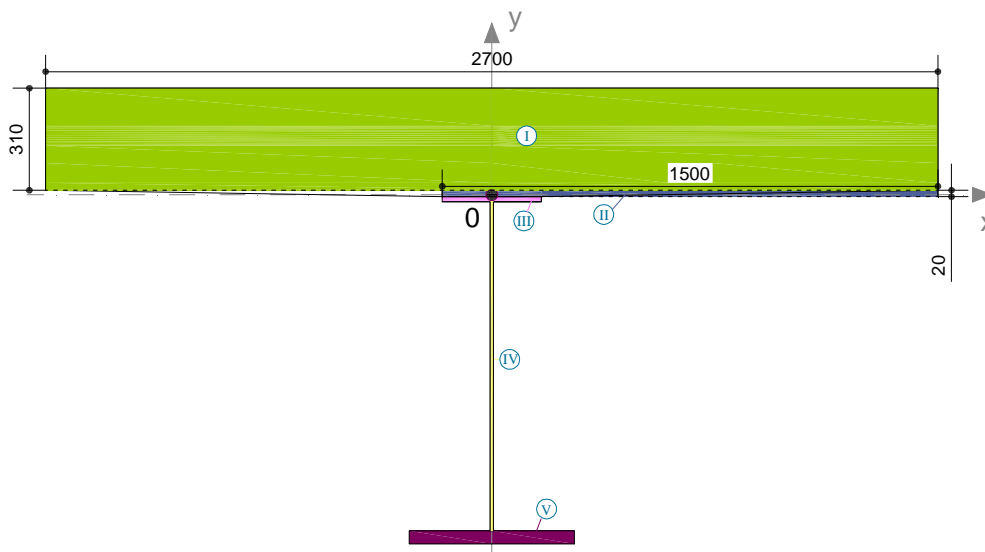
- Torsional moment of concrete slab : Ⓘ

Width: $\quad w = 2500mm$

Thickness: $\quad \delta = 310mm$

$$k_I = \frac{1}{3} \cdot \left[1 - 0,63 \cdot \frac{w}{\delta} \cdot \left(1 - \frac{\delta^4}{12 \cdot w^4} \right) \right] = \mathbf{0,309}$$

$$I_{tI} = k \cdot \delta^3 \cdot w = \mathbf{24872533985mm^4}$$

- Torsional moment of concrete slab : Ⓘⓘ

Width: $\quad w = 1500mm$

Thickness: $\quad \delta = 20mm$

$$k_{II} = \mathbf{0,331}$$

$$I_{tII} = k \cdot \delta^3 \cdot w = \mathbf{3966400mm^4}$$

- Torsional moment of web: IV

Width: $w = 1100\boldsymbol{mm}$

Thickness: $\delta = 10\boldsymbol{mm}$

$k = \mathbf{0,331}$

$$I_{cs} = k \cdot \delta^3 \cdot w = \mathbf{364567mm^4}$$

- Torsional moment of top flange: III

Width: $w = 300\boldsymbol{mm}$

Thickness: $\delta = 15\boldsymbol{mm}$

$k = \mathbf{0,322}$

$$I_{cs} = k \cdot \delta^3 \cdot w = \mathbf{326869mm^4}$$

- Torsional moment of bottom flange: V

Width: $w = 500\boldsymbol{mm}$

Thickness: $\delta = 40\boldsymbol{mm}$

$k = \mathbf{0,316}$

$$I_{cs} = k \cdot \delta^3 \cdot w = \mathbf{10129068mm^4}$$

Torsional moment of equivalent section:

$$
\begin{aligned}
I_t = 0{,}5 \cdot I_I + 0{,}5 \cdot I_{II} + I_{III} + I_{IV} + I_V \\
= 0{,}5 \cdot 24872533985mm^4 + 0{,}5 \cdot 3966400mm^4 + 326869mm^4 \\
+ 364567mm^4 + 10129068mm^4 = \mathbf{12449070696mm^4}
\end{aligned}
$$

TRANSVERSAL ELEMENTS:

GRID

VFT GIRDER
EXTREME SUPPORTED CROSS-BAR
INTERMEDIATE SUPPORTED CROSS-BAR
SLAB ELEMENTS
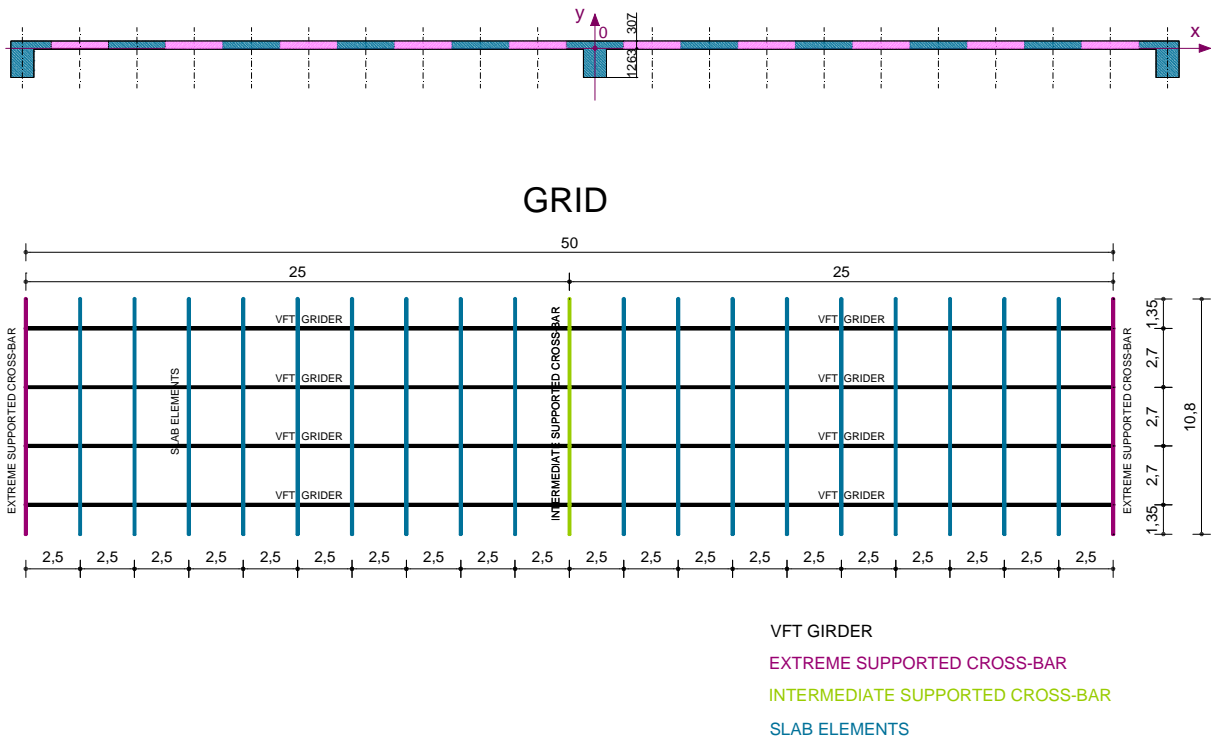
✖ EXTREME SUPPORTED CROSS-BAR:

Geometrical characteristic:

- Moment of inertia:

$$I_{ec} = 0,68618m^4$$

- Area:

$$A_{ec} = 1,8175m^2$$

- Modulus of elasticity:

$$E_{ec} = 36,4GPa$$

- Torsional moment:

I	II
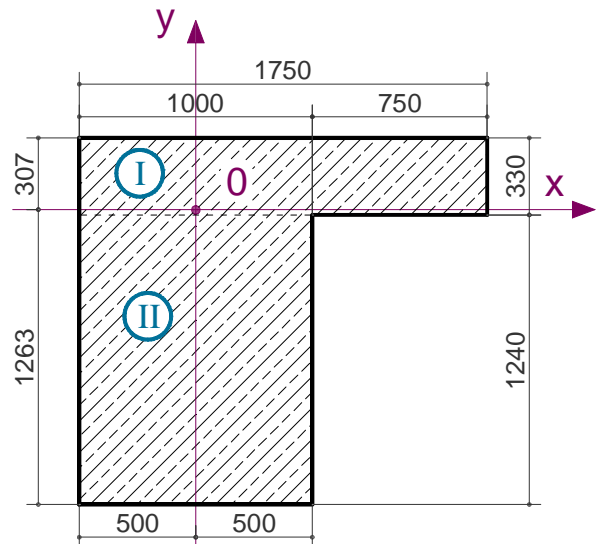
	I	II
WIDTH:	$w_I = 1750mm$	$w_{II} = 1240mm$
THICKNESS:	$\delta_I = 330mm$	$\delta_{II} = 1000mm$

k: $\qquad k_I = 0{,}294 \qquad\qquad\qquad k_{II} = 0{,}170$

$I_{ec_i} = k \cdot \delta^3 \cdot w \qquad I_{ec_I} = \mathbf{18473078320mm^4} \qquad I_{ec_{II}} = \mathbf{210735371294mm^4}$

↓

$I_{ec} = 0{,}5 I_{cs_I} + I_{cs_{II}} = \mathbf{219971910455mm^4}$

✖ INTERMEDIATE SUPPORTED CROSS-BAR:

Geometrical characteristic:

- Moment of inertia:

  $I_{ic} = \mathbf{0{,}68719m^4}$

- Area:

  $A_{ic} = \mathbf{2{,}061m^2}$

- Modulus of elasticity:

  $E_{ic} = \mathbf{36{,}4GPa}$

- Torsional moment:

Ⓘ   Ⓘ Ⓘ
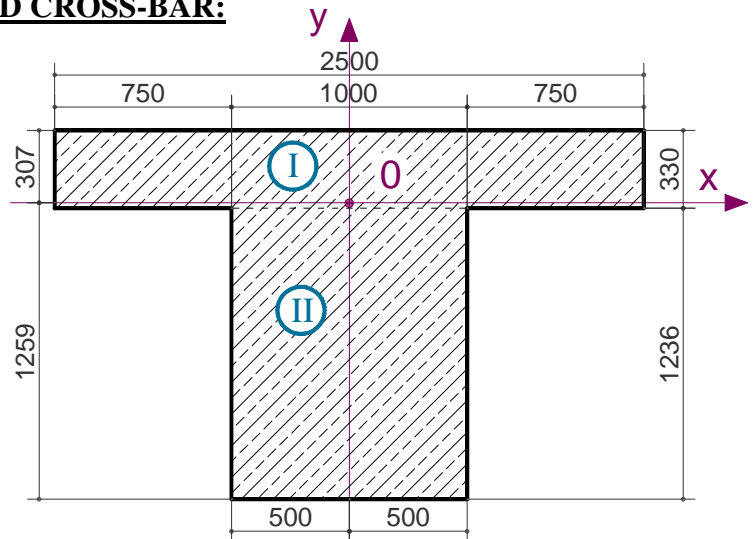
	Ⓘ	Ⓘ Ⓘ
WIDTH:	$w_I = \mathbf{2500mm}$	$w_{II} = 1236\mathbf{mm}$
THICKNESS:	$\delta_I = \mathbf{330mm}$	$\delta_{II} = 1000\mathbf{mm}$
k:	$k_I = 0{,}306$	$k_{II} = 0{,}169$
$I_{ic_i} = k \cdot \delta^3 \cdot w$	$I_{ic_I} = \mathbf{27457128907mm^4}$	$I_{ic_{II}} = \mathbf{209498323369mm^4}$

↓

$I_{ic} = 0{,}5 I_{ic_I} + I_{ic_{II}} = \mathbf{223226887823mm^4}$

✖ SLAB ELEMENTS:

Geometrical characteristic:
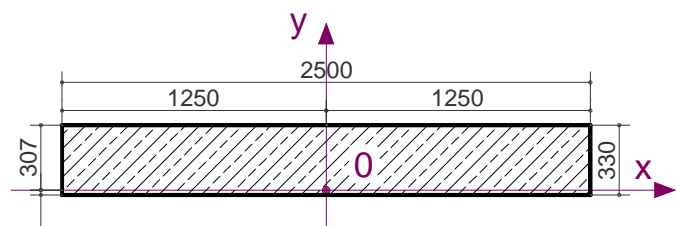
- Moment of inertia:

$$I_{es} = 0,02415m^4$$

- Area:

$$A_{es} = 0,825m^2$$

- Modulus of elasticity:

$$E_{es} = 36,4GPa$$

- Torsional moment:

WIDTH: $\qquad w_I = 2500mm$

THICKNESS: $\qquad \delta_I = 330mm$

k: $\qquad k_I = 0,306$

$I_{es}' = k \cdot \delta^3 \cdot w \qquad I_{es}' = 27457128907mm^4$

↓

$I_{ic} = 0,5I_{ic_I}' = 13728564454mm^4$

Model (e1,s2):
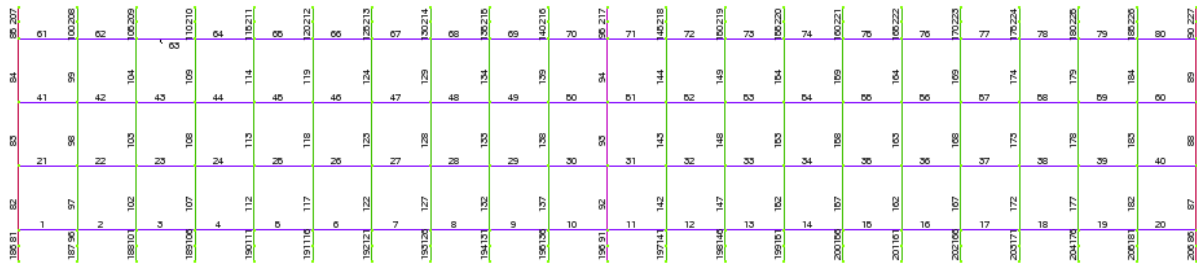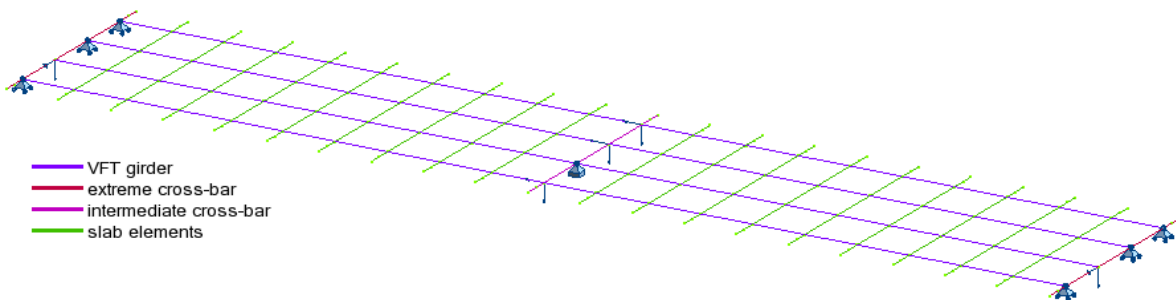
Geometrical characteristic:
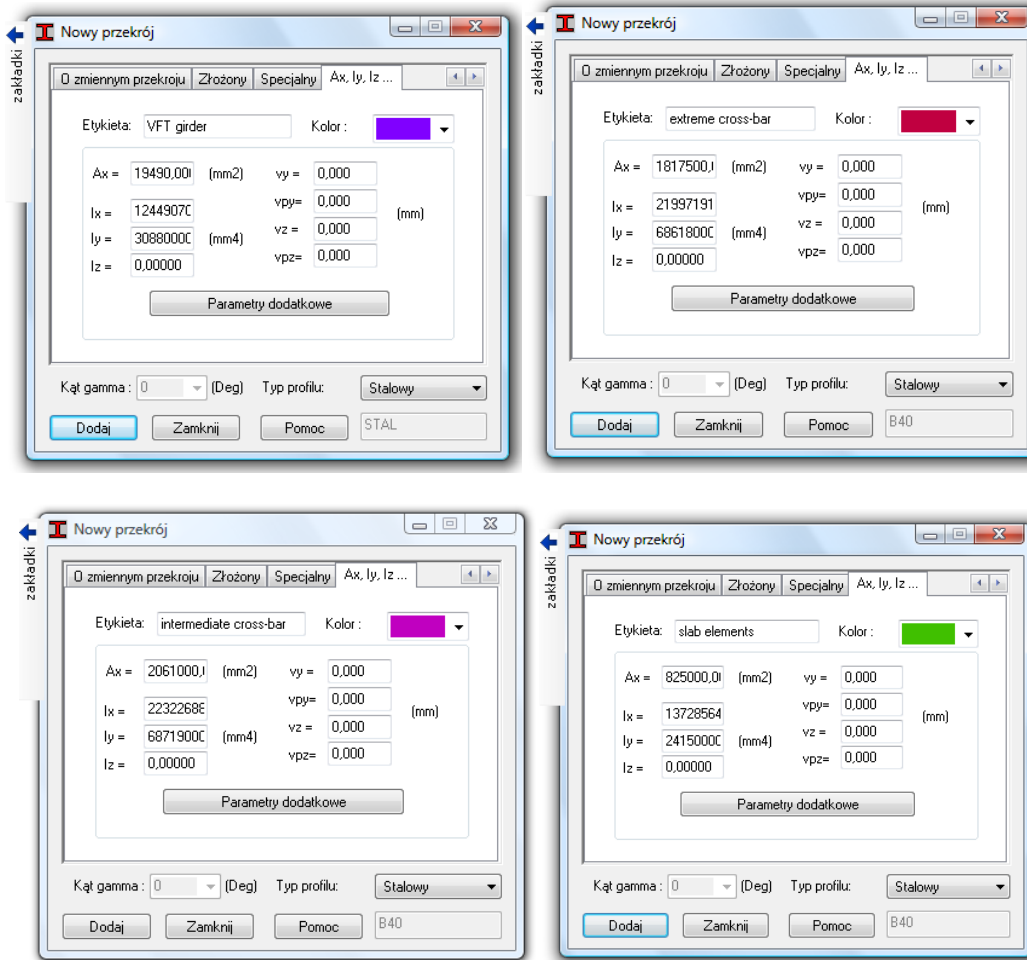
Materials:
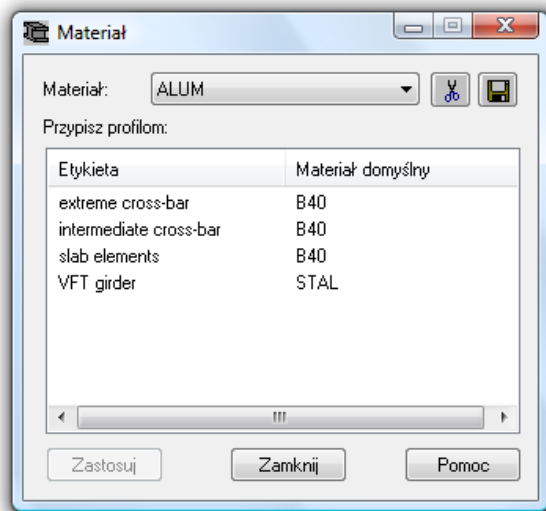
Loads:

- PART 1 (equipment):
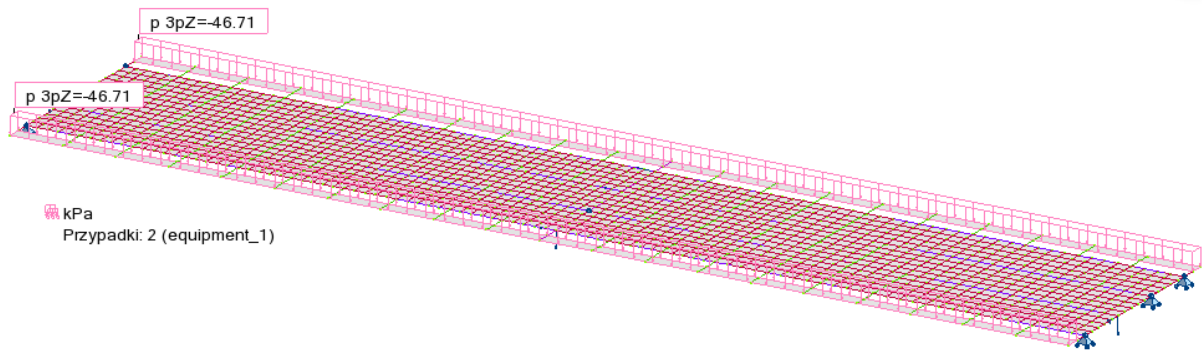
- PART 2 (equipment):
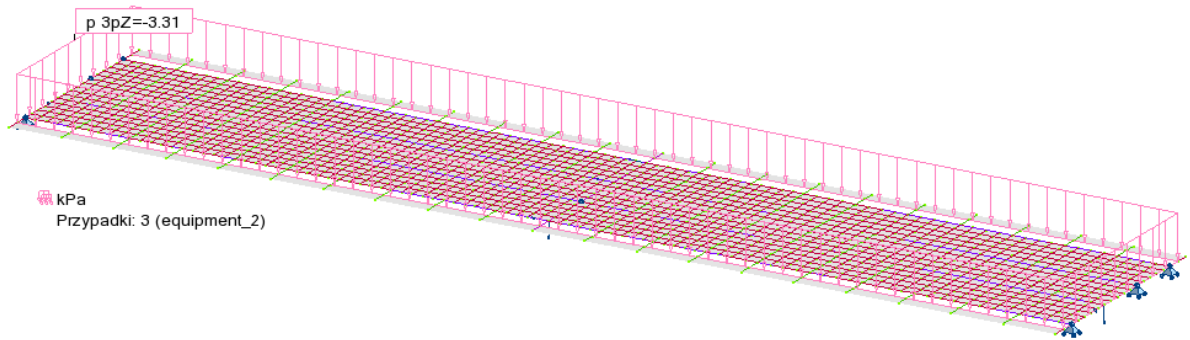
- Live load (Automobiles):

- K vehicle:

FZ=-137.81
FZ=-137.81
FZ=-137.81
FZ=-137.81
FZ=-137.81
FZ=-137.81
FZ=-137.81

kN
Przypadki: 5 (K)

- Unloading of the deck slab:

p 3pZ=0.19

kPa
Przypadki: 7 (Unloading of deck slab)

- Loads combinations:

FZ=-137.81
FZ=-137.81
p 3pZ=0.19
FZ=-137.81
p 3pZ=-46.71
p 3pZ=-4.50
FZ=-137.81
FZ=-137.81
FZ=-137.81
p 3pZ=-46.71
FZ=-137.81
p 3pZ=-3.31

kPa
kN
Przypadki: 6 (KOMB1)
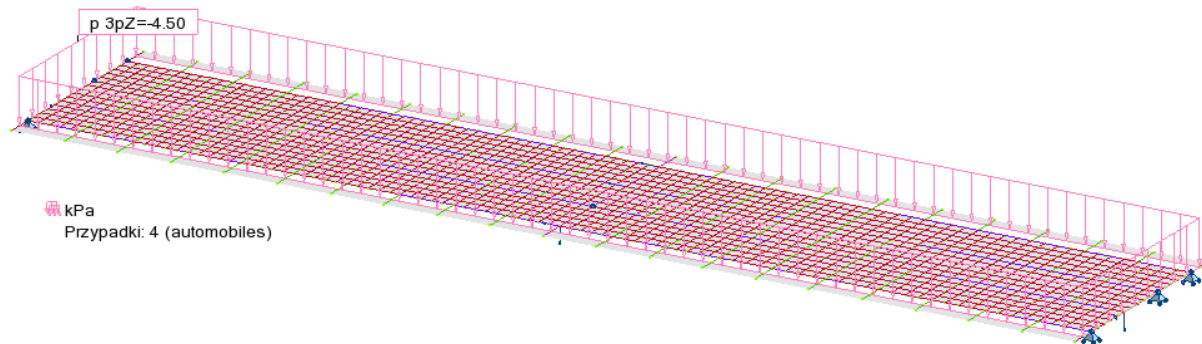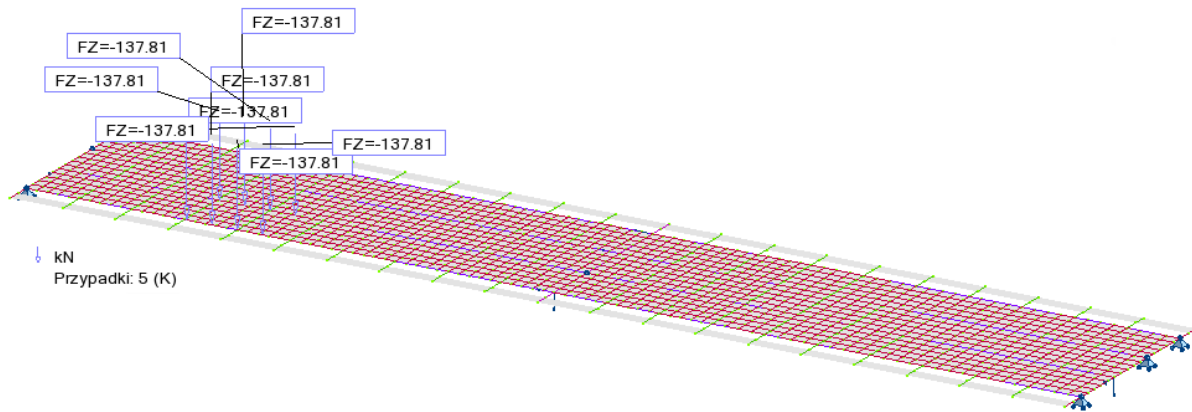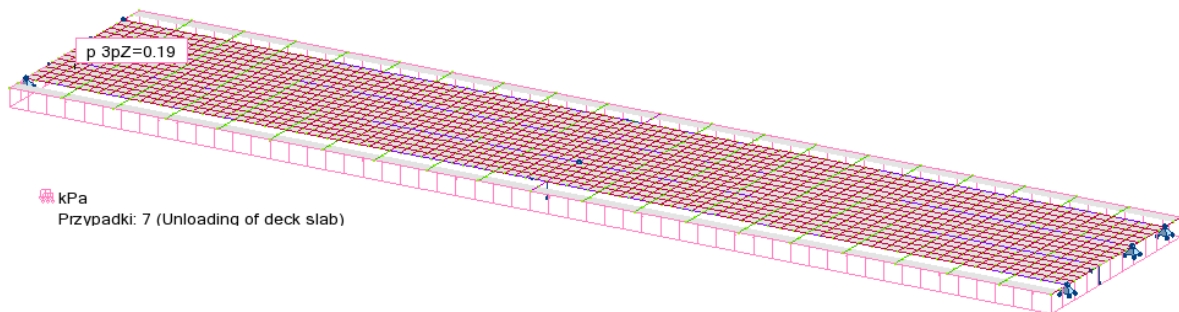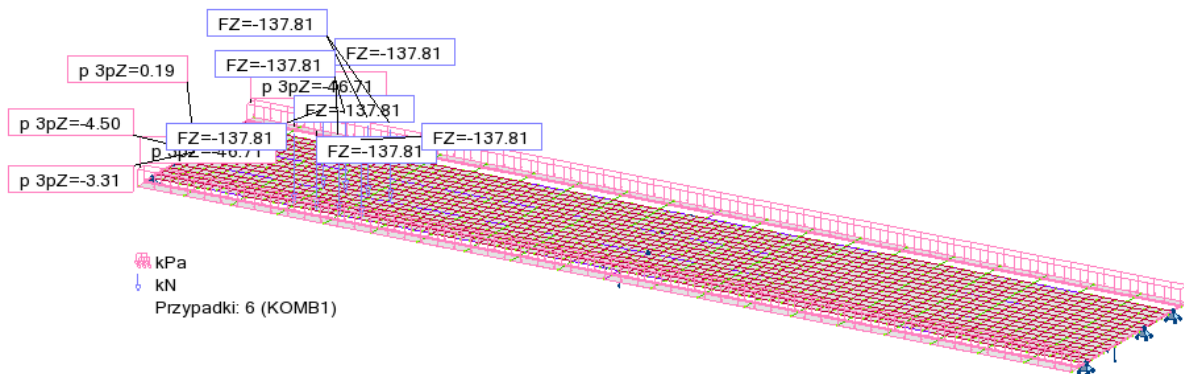
Bending moments:
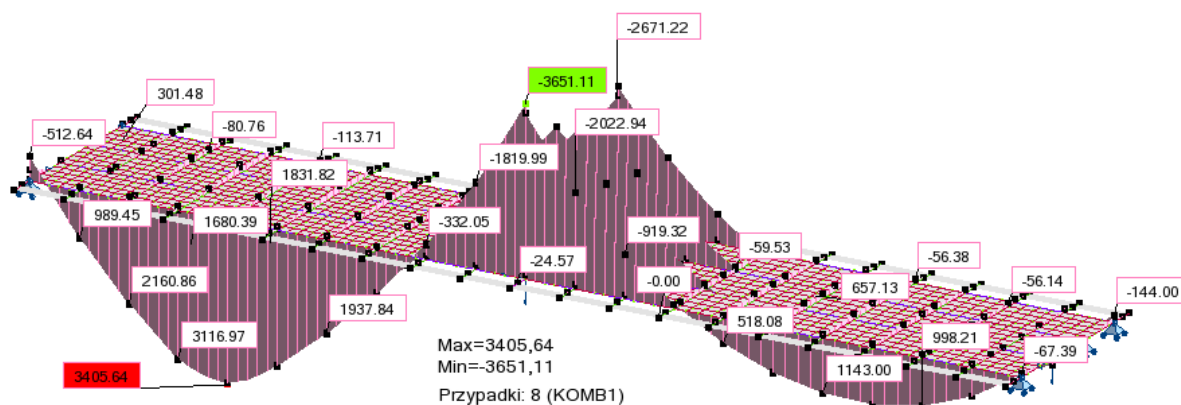
$$M_{max} = 3405{,}64 kNm$$

$$M_{min} = -3651{,}11 kNm$$

14.1.3. Dimensioning

➔ *Phase 1 :*

Geometrical characteristic of the beam (determined by AutoCad programme):

- Moment of inertia:

$$I_b = 0,00549 m^4$$

- Distance of extreme fibres:
- Top fibres: $v_t = 0,750m$
- Bottom fibres: $v_b = 0,305m$
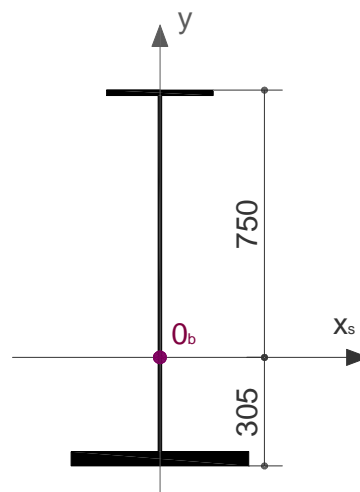
Accepted:

- steel beam made by **S355**.

Characteristic tensile strength: $R_m^{ch} = 355MPa$

Design tensile strength: $R_m^d = \frac{R_m^{ch}}{\gamma_f} = \frac{355MPa}{1,15} = \textbf{308MPa}$

- Concrete class:

Concrete **B40**: $R_{bk} = \textbf{30,0MPa}$ – *characteristic compression strength*

$$R_{b1} = \mathbf{23,1MPa} - \text{design compression strength}$$

Concrete **B60**: $\qquad R_{bk} = \mathbf{45,0MPa} - \text{characteristic compression strength}$

$$R_{b1} = \mathbf{36,4MPa} - \text{design compression strength}$$

<u>*Stresses:*</u>

$$\sigma_{It} = \frac{-M_I^d \cdot v_t}{I_b} = \frac{-1007,42kNm \cdot 0,750m}{0,00549m^4} = -\mathbf{137,62MPa} < R_m^d = \mathbf{308MPa}$$

$$\sigma_{Ib} = \frac{M_I^d \cdot v_b}{I_b} = \frac{-1007,42kNm \cdot 0,305m}{0,00549m^4} = \mathbf{55,97MPa} < R_m^d = \mathbf{308MPa}$$
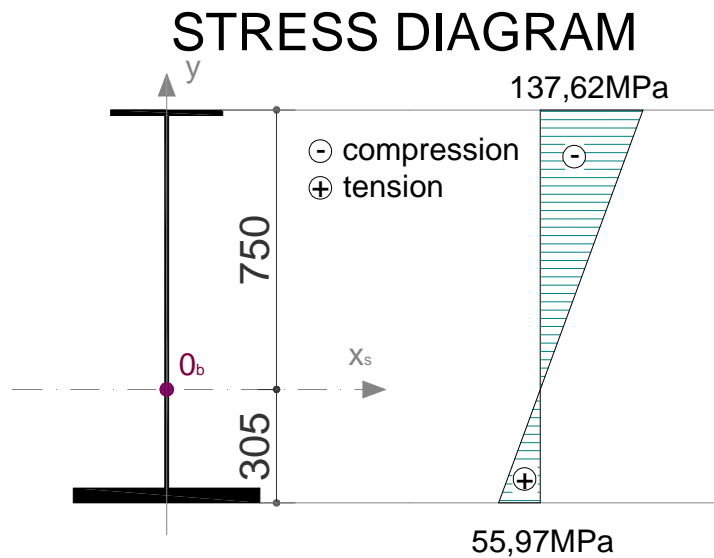
➔ *Phase 2 :*

<u>*Geometrical characteristic of the prefabricated composite girder*</u> :

- Prefabricated concrete flange (B60 according to PN):

$$I_{pf} = \mathbf{0,0003145m^4}$$

$$A_{pf} = \mathbf{0,300m^2}$$

$$E_{pf} = \mathbf{41GPa}$$

- Steel beam:

$$I_b = \mathbf{0,00549m^4}$$

$$A_b = \mathbf{0,0345m^2}$$

$$E_b = \mathbf{205GPa}$$

Equivalent section

- Distance between centres of gravity of concrete flange and steel beam
- $a = 0{,}815\boldsymbol{m}$
- Distance of extreme fibres:
  Steel beam:
- Top fibres: $\qquad v_t = \mathbf{0,750m}$
- Bottom fibres: $\qquad v_b = \mathbf{0,305m}$
  Prefabricated and in-situ concrete flange:
- Top fibres: $\qquad y_t = \mathbf{0,056m}$
- Bottom fibres: $\qquad y_b = \mathbf{0,064m}$

$$n_\varphi = \frac{E_b}{E_s} = \frac{205GPa}{41GPa} = \mathbf{5}$$

$$A_{pf\varphi} = \frac{A_{pf}}{n_\varphi} = \frac{0{,}300m^2}{5} = \mathbf{0,06m^2}$$

$$I_{pf\varphi} = \frac{I_{pf}}{n_\varphi} = \frac{0{,}0003145m^4}{5} = \mathbf{0,0000629m^4}$$

- Distances between centre of gravity of equivalent section and concrete slab / steel beam

$$\frac{a}{a_b} = \frac{A_b + A_{pf\varphi}}{A_{pf\varphi}} \quad \rightarrow \quad a_b = \frac{A_{pf\varphi} \cdot a}{A_b + A_{pf\varphi}} = \frac{0{,}06m^2 \cdot 0{,}815m}{0{,}0345m^2 + 0{,}06m^2} = \mathbf{0,517m}$$

$$a_t = a - a_b = 0{,}815m - 0{,}517m = \mathbf{0,298m}$$

- Top: $\qquad a_t = \mathbf{0,298m}$
- Bottom: $\qquad a_b = \mathbf{0,517m}$
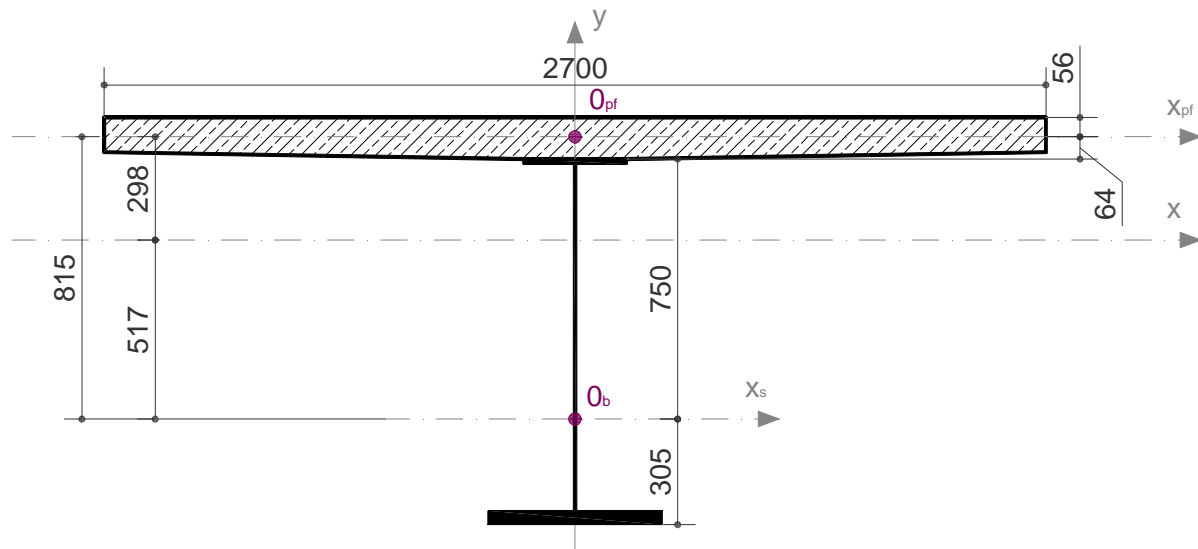
$$I_b = 0,005494m^4 \qquad\qquad a = 0,815m$$

$$I_{pf\varphi} = 0,0000629m^4 \qquad\qquad a_b = 0,517m$$

$$I_{pf} = 0,0003145m^4 \qquad\qquad n_\varphi = 5$$

$$A_b = 0,0345m^2 \qquad\qquad A_{pf} = 0,300m^2$$

Stresses:

<u>$\alpha - \alpha$ section:</u>

$$M^{\alpha-\alpha} = \mathbf{1731,64kNm}$$

$$\begin{bmatrix} \dfrac{I_b + I_{pf\varphi}}{I_{pf\varphi}} & 1 \\[2mm] \dfrac{-a \cdot a_b \cdot A_b}{I_b} & 1 \end{bmatrix} \cdot \begin{bmatrix} M_b \\ a \cdot N_b \end{bmatrix} = \begin{bmatrix} M \\ 0 \end{bmatrix}$$

$$\begin{cases} \dfrac{I_b + I_{pf\varphi}}{I_{pf\varphi}} \cdot M_b + a \cdot N_b - M = 0 \\[4mm] \dfrac{-a \cdot a_b \cdot A_b}{I_b} \cdot M_b + a \cdot N_b = 0 \end{cases} \rightarrow \quad \begin{array}{l} M_b = \mathbf{473,464kNm} \\[2mm] N_b = \mathbf{1537,122kN} \end{array}$$

$$M_{pf} = \frac{I_{pf\varphi}}{I_b} \cdot M_b = \frac{0,0008m^4}{0,00793m^4} \cdot 473,464kNm = \mathbf{5,421kNm}$$

$$N_{pf} = -N_b = \mathbf{-1537,122kN}$$

- In steel beam:

$$\sigma_b^{\alpha-\alpha} = \frac{N_b}{A_b} + \frac{M_b \cdot v_b}{I_b} = \frac{1537,122kN}{0,0345m^2} + \frac{568,642kNm \cdot 0,305m}{0,005494m^4} = \mathbf{76,12MPa} < R_m^d$$
$$= \mathbf{308MP}$$

$$\sigma_t^{\alpha-\alpha} = \frac{N_b}{A_b} - \frac{M_b \cdot v_t}{I_b} = \frac{1537,122kN}{0,0345m^2} - \frac{568,642kNm \cdot 0,750m}{0,005494m^4} = \mathbf{-33,07MPa} < R_m^d$$
$$= \mathbf{308MP}$$

- In prefabricated concrete flange:

$$\sigma_{IIb}^{\alpha-\alpha} = -\frac{N_{pf}}{A_{pf}} + \frac{M_{pf} \cdot y_b}{I_{pf}} = -\frac{-1537,122kN}{0,300m^2} - \frac{57,227kNm \cdot 0,064m}{0,0003145m^4} = \mathbf{1,37MPa} < R_{b1}$$
$$= \mathbf{36,4MPa}$$

$$\sigma_{IIt}^{\alpha-\alpha} = -\frac{N_{pf}}{A_{pf}} - \frac{M_{pf} \cdot y_t}{I_{pf}} = -\frac{-1537,122kN}{0,300m^2} - \frac{57,227kNm \cdot 0,056m}{0,0003145m^4} = \mathbf{5,82MPa} < R_{b1}$$
$$= \mathbf{36,4MPa}$$
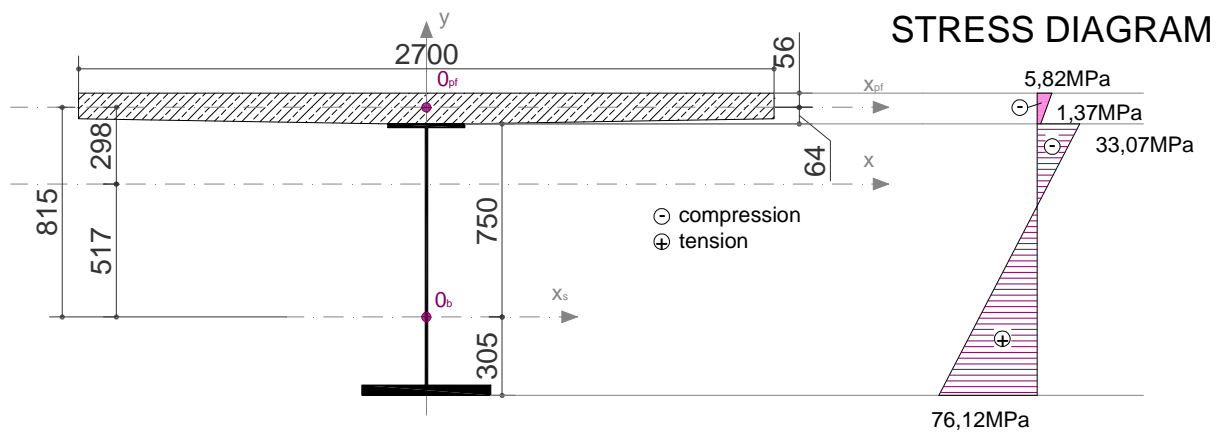
→ *Phase 3 :*

$I_b = 0,00549m^4$ $a = 0,919m$

$I_{c\varphi} = 0,001408m^4$ $a_b = 0,756m$

$I_c = 0,00704m^4$ $n_\varphi = 5$

$A_b = 0,0345m^2$ $A_c = 0,802m^2$

Stresses:

$\alpha - \alpha$ section:

STEP 1:

$M^{\alpha-\alpha} = 3605,64kNm$

$$\begin{bmatrix} \dfrac{I_b + I_{s\varphi}}{I_{s\varphi}} & 1 \\ \dfrac{-a \cdot a_b \cdot A_b}{I_b} & 1 \end{bmatrix} \cdot \begin{bmatrix} M_b \\ a \cdot N_b \end{bmatrix} = \begin{bmatrix} M \\ 0 \end{bmatrix}$$

$$\begin{cases} \dfrac{I_b + I_{c\varphi}}{I_{c\varphi}} \cdot M_b + a \cdot N_b - M = 0 \\ \dfrac{-a \cdot a_b \cdot A_b}{I_b} \cdot M_b + a \cdot N_b = 0 \end{cases} \rightarrow \begin{array}{l} M_b = 605,72kNm \\ N_b = 2877,66kN \end{array}$$

$$M_c = \frac{I_{c\varphi}}{I_b} \cdot M_b = \frac{0,001408m^4}{0,00549m^4} \cdot 605,72kNm = \mathbf{155,347kNm}$$

$$N_c = -N_b = \mathbf{-2877,66kN}$$

- In steel beam:

$$\sigma_{IIIb}^{\alpha-\alpha} = \frac{N_b}{A_b} + \frac{M_b \cdot v_b}{I_b} = \frac{2877,66kN}{0,0345m^2} + \frac{605,72kNm \cdot 0,305m}{0,00549m^4} = \mathbf{174,06MPa}$$

$$\sigma_{IIIt}^{\alpha-\alpha} = \frac{N_b}{A_b} - \frac{M_b \cdot v_t}{I_b} = \frac{2877,66kN}{0,0345m^2} - \frac{605,72kNm \cdot 0,750m}{0,00549m^4} = \mathbf{-0,66MPa}$$

$$\sigma_b^{\alpha-\alpha} = \sigma_{Ib}^{\alpha-\alpha} + \sigma_{IIb}^{\alpha-\alpha} + \sigma_{IIIb}^{\alpha-\alpha} = 55,97MPa + 76,12MPa + 174,06MPa = \mathbf{306,15MPa}$$
$$< R_m^d = \mathbf{308MPa}$$

$$\sigma_t^{\alpha-\alpha} = \sigma_{It}^{\alpha-\alpha} + \sigma_{IIt}^{\alpha-\alpha} + \sigma_{IIIt}^{\alpha-\alpha} = -137,62MPa - 33,07MPa - 0,66MPa$$
$$= \mathbf{-171,35MPa} < R_m^d = \mathbf{308MPa}$$

STEP 2:

$M_c = \mathbf{155,347kNm}$

$N_c = \mathbf{-2877,66kN}$

$$N_{c/pf} = N_c \cdot \frac{A_{pf}}{A_c} = -2877,66kN \cdot \frac{0,300m^2}{0,802m^2} = -\mathbf{1076,43kN}$$

$$N_{c/s} = N_c \cdot \frac{A_s}{n_\varphi \cdot A_c} = -2877,66kN \cdot \frac{0,567m^2}{1,13 \cdot 0,802m^2} = -\mathbf{1800,40kN}$$

Equivalent section

$$n_\varphi = \mathbf{1,13}$$

$$a = \mathbf{0,161mm} \qquad\qquad a_b = \mathbf{0,105m}$$

$$A_{pf} = \mathbf{0,300m^2}$$

$$I_{pf} = \mathbf{0,0003145m^4}$$

$$I_s = \mathbf{0,002084m^4}$$

$$I_{s\varphi} = \mathbf{0,00184m^4}$$

$$\begin{bmatrix} \dfrac{I_{pf} + I_{s\varphi}}{I_{s\varphi}} & 1 \\[2ex] \dfrac{-a \cdot a_b \cdot A_{pf}}{I_{pf}} & 1 \end{bmatrix} \cdot \begin{bmatrix} M_{pf} \\[1ex] a \cdot N_{pf} \end{bmatrix} = \begin{bmatrix} M \\ 0 \end{bmatrix}$$

$$\begin{cases} \dfrac{I_{pf} + I_{s\varphi}}{I_{s\varphi}} \cdot M_b + a \cdot N_b - M = 0 \\[2ex] \dfrac{-a \cdot a_b \cdot A_b}{I_b} \cdot M_b + a \cdot N_b = 0 \end{cases} \rightarrow \quad \begin{array}{l} M_{pf} = \mathbf{6,76kNm} \\[1ex] N_{pf} = \mathbf{677,20kN} \end{array}$$

$$M_s = \frac{I_{s\varphi}}{I_{pf}} \cdot M_{pf} = \mathbf{39,65kNm}$$

$$N_s = -\mathbf{677,20kN}$$

Total N:

$$N_{pf}^t = N_{c/pf} + N_{pf} = -1076,43kN + 677,20kN = -\mathbf{399,23kN}$$

$$N_s^t = N_{c/s} + N_s = -1800,40kN - 677,20kN = -\mathbf{2477,60kN}$$

- In prefabricated concrete flange:

$$\sigma_{IIIb}^{\alpha-\alpha} = -\frac{N_{pf}^t}{A_{pf}} - \frac{M_{pf} \cdot y_b}{I_{pf}} = -\frac{-399,23kN}{0,300m^2} - \frac{6,76kNm \cdot 0,064m}{0,0003145m^4} = -\mathbf{0,045MPa}$$

$$\sigma_{IIIt}^{\alpha-\alpha} = -\frac{N_{pf}^t}{A_{pf}} + \frac{M_{pf} \cdot y_t}{I_{pf}} = -\frac{-399,23kN}{0,300m^2} + \frac{6,76kNm \cdot 0,056m}{0,0003145m^4} = \mathbf{2,53MPa}$$

$$\sigma_b^{\alpha-\alpha} = \sigma_{IIb}^{\alpha-\alpha} + \sigma_{IIIb}^{\alpha-\alpha} = 1,37MPa + (-0,045MPa) = \mathbf{1,33MPa} < R_{b1} = \mathbf{36,4MPa}$$

$$\sigma_t^{\alpha-\alpha} = \sigma_{IIt}^{\alpha-\alpha} + \sigma_{IIIt}^{\alpha-\alpha} = 5,82MPa + 2,53MPa = \mathbf{8,35MPa} < R_{b1} = \mathbf{36,4MPa}$$

- In concrete slab:

$$\sigma_{IIb}^{\alpha-\alpha} = -\frac{N_s^t}{A_s} - \frac{M_s \cdot v_b}{I_s} = -\frac{-2477,60kN}{0,567m^2} - \frac{39,65kNm \cdot 0,105m}{0,002084m^4} = \mathbf{2,37MPa} < R_{b1}$$
$$= \mathbf{23,1MPa}$$

$$\sigma_{IIt}^{\alpha-\alpha} = -\frac{N_s^t}{A_s} + \frac{M_s \cdot v_t}{I_s} = -\frac{-2477,60kN}{0,567m^2} + \frac{39,65kNm \cdot 0,105m}{0,002084m^4} = \mathbf{6,38MPa} < R_{b1}$$
$$= \mathbf{23,1MPa}$$
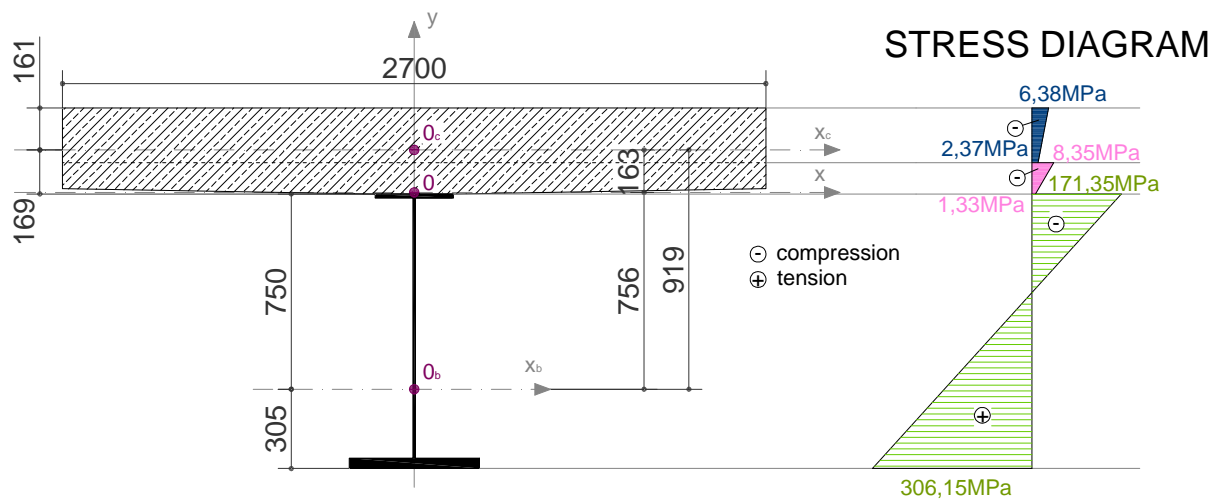
14.2. Preliminary draft for composite bridge

CROSS-SECTION <u>B-B</u> , <u>C-C</u>
SCALE 1:50

<u>B-B</u>   <u>C-C</u>
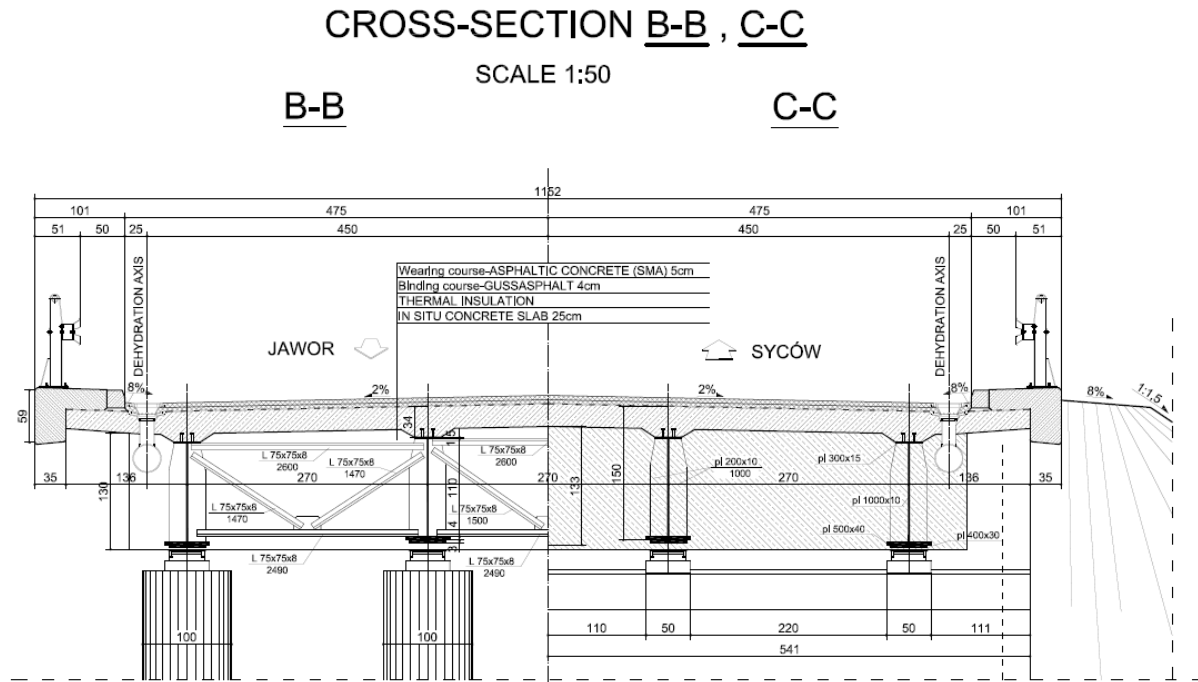
Fig. 14.3. Cross-section consisting of 4 composite girders.

END VIEW   LONGITUDINAL SECTION <u>A-A</u>
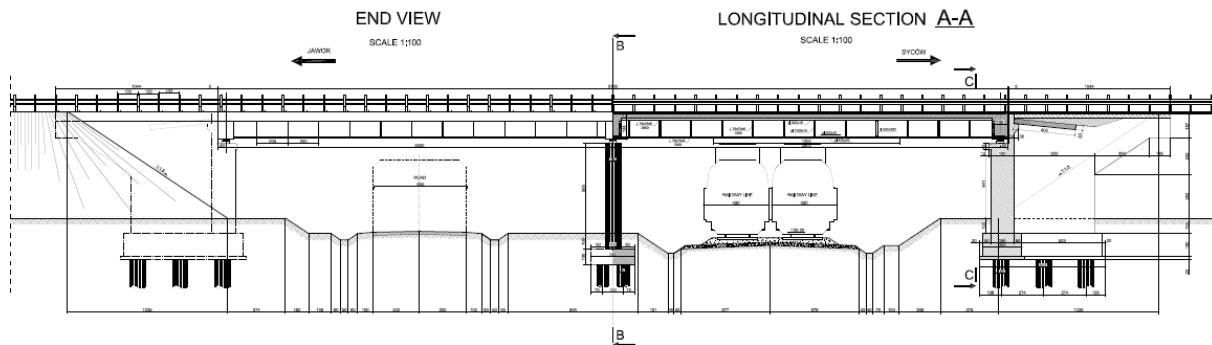
Fig. 14.4. Longitudinal section of composite bridge.

14.2.1. Statement of the loads
➔ *Phase 1:*
- Dead load of steel construction:
- *Steel girder:*

$$A_s = 0,0355m^2 \qquad\qquad l_s = 25m * 4$$

- *Cover plate on bottom flange:*

$A_p = 0,0123m^2$ $\qquad\qquad\qquad l_p = 12m * 4$

- *Ribs:*

$A_r = 0,00211m^3$ $\qquad\qquad\qquad u_r = 8 * 14$

- *Slating strut:*

$A_{ss} = 0,00169m^3$ $\qquad\qquad\qquad u_{ss} = 6 * 12$

- *Horizontal strut:*

$A_{hs} = 0,00293m^3$ $\qquad\qquad\qquad u_{hs} = 6 * 12$

- *Gusset plate:*

$A_{gp} = 0,00044m^3$ $\qquad\qquad\qquad u_{gp} = 3 * 12$

$\gamma_s = 78,5\frac{kN}{m^3} + 1,4\frac{kN}{m^3}$ – addition to weight of welded steel construction

Characteristic load:

$$g_s^{ch} = (0,0355m^2 \cdot 25m \cdot 4 + 0,0123m^2 \cdot 12m \cdot 4 + 0,00211m^3 \cdot 8 \cdot 14 + 0,00169m^3 \cdot 6$$
$$\cdot 12 + 0,00293m^3 \cdot 6 \cdot 12 + 0,00044m^3 \cdot 3 \cdot 12) \cdot \frac{\left(78,5\frac{kN}{m^3} + 1,4\frac{kN}{m^3}\right)}{25,0m}$$
$$= \boldsymbol{15,10\frac{kN}{m}}$$

Design load:

$$g_s^d = g_s^{ch} \cdot 1,2 = 15,10\frac{kN}{m} \cdot 1,2 = \boldsymbol{18,12\frac{kN}{m}}$$

- Dead load of wet concrete deck slab:

$A_{ds} = 2,8448m^2$ $\qquad\qquad\qquad \gamma_c = 26\frac{kN}{m^3}$

Characteristic load:

$$g_{ds}^{ch} = 2,8448m^2 \cdot 26\frac{kN}{m^3} = \boldsymbol{73,96\frac{kN}{m}}$$

Design load:

$$g_{ds}^d = g_{ds}^{ch} \cdot 1,2 = 73,96 \frac{kN}{m} \cdot 1,2 = \mathbf{88,76 \frac{kN}{m}}$$

- Formwork load:

$$W_{ds} = 10,82m \qquad\qquad \gamma_c = 0,5 \frac{kN}{m^2}$$

Characteristic load:

$$g_f^{ch} = 10,82m \cdot 0,5 \frac{kN}{m^2} = \mathbf{5,41 \frac{kN}{m}}$$

Design load:

$$g_f^d = g_f^{ch} \cdot 1,5 = 5,41 \frac{kN}{m} \cdot 1,5 = \mathbf{8,12 \frac{kN}{m}}$$

- Technological load:

$$W_{ds} = 10,82m \qquad\qquad \gamma_t = 1,5 \frac{kN}{m^2}$$

Characteristic load:

$$g_t^{ch} = 10,82m \cdot 0,5 \frac{kN}{m^2} = \mathbf{16,23 \frac{kN}{m}}$$

Design load:

$$g_t^d = g_t^{ch} \cdot 1,3 = 16,23 \frac{kN}{m} \cdot 1,5 = \mathbf{21,1 \frac{kN}{m}}$$

TOTAL LOADS FOR ONE GIRDER:

Characteristic load:

$$g_I^{ch} = \frac{\left(g_s^{ch} + g_{ds}^{ch} + g_f^{ch} + g_t^{ch}\right)}{4} = \frac{\left(15,10\frac{kN}{m} + 73,96\frac{kN}{m} + 5,41\frac{kN}{m} + 16,23\frac{kN}{m}\right)}{4}$$
$$= \mathbf{27,68 \frac{kN}{m}}$$

Design load:

$$g_I^d = \frac{(g_s^a + g_{ds}^a + g_f^a + g_t^a)}{4} = \frac{\left(18{,}12\frac{kN}{m} + 88{,}76\frac{kN}{m} + 8{,}12\frac{kN}{m} + 21{,}1\frac{kN}{m}\right)}{4} = \mathbf{34,02}\frac{\boldsymbol{kN}}{\boldsymbol{m}}$$

Characteristic load:

$$g_{I\_II}^{ch} = \frac{(g_s^{ch} + g_{ds}^{ch} + g_f^{ch})}{4} = \frac{\left(15{,}10\frac{kN}{m} + 73{,}96\frac{kN}{m} + 5{,}41\frac{kN}{m}\right)}{4} = \mathbf{23,62}\frac{\boldsymbol{kN}}{\boldsymbol{m}}$$

Design load:

$$g_{I\_II}^d = \frac{(g_s^a + g_{ds}^a + g_f^a)}{4} = \frac{\left(18{,}12\frac{kN}{m} + 88{,}76\frac{kN}{m} + 8{,}12\frac{kN}{m}\right)}{4} = \mathbf{28,75}\frac{\boldsymbol{kN}}{\boldsymbol{m}}$$

➔ ***Phase 2:***
- Removal of forms:

Characteristic load:

$$g_{rf}^{ch} = \frac{-g_f^{ch}}{w_{ds}} = -\mathbf{0,5}\frac{\boldsymbol{kN}}{\boldsymbol{m^2}}$$

Design load:

$$g_{rf}^d = g_{rf}^{ch} \cdot 0{,}9 = -0{,}5\frac{kN}{m} \cdot 0{,}9 = -\mathbf{0,45}\frac{\boldsymbol{kN}}{\boldsymbol{m^2}}$$

- Unloading of deck slab:

$$t_{ds} = 0{,}25m \qquad \gamma_c = -1\frac{kN}{m^3}$$

Characteristic load:

$$g_{uds}^{ch} = 0{,}25m \cdot \left(-1\frac{kN}{m^3}\right) = -\mathbf{0,25}\frac{\boldsymbol{kN}}{\boldsymbol{m^2}}$$

Design load:

$$g_{uds}^d = g_{ds}^{ch} \cdot 0{,}9 = -0{,}25\frac{kN}{m^2} \cdot 0{,}9 = -\mathbf{0,225}\frac{\boldsymbol{kN}}{\boldsymbol{m^2}}$$

- Weight of equipment:

- Bridge deck overhang:

$$A_o = 0,3211m^2 \qquad\qquad u_o = 2 \qquad\qquad \gamma_c = 25\frac{kN}{m^3}$$

- Stone curb:

$$A_{sc} = 0,0388m^2 \qquad\qquad u_{sc} = 2 \qquad\qquad \gamma_{stone} = 27\frac{kN}{m^3}$$

- Crash cushion (I assumed 1,0kN/m for each barrier) :

$$G_{cc} = 1,0\frac{kN}{m} \qquad\qquad u_{cc} = 2$$

- Insulation:

$$t_i = 0,01m \qquad\qquad \gamma_i = 14\frac{kN}{m^3}$$

Characteristic load:

$$g_{e1}^{ch} = \left(0,3211m^2 \cdot 2 \cdot 25\frac{kN}{m^3} + 0,0388m^2 \cdot 2 \cdot 27\frac{kN}{m^3} + 1,0\frac{kN}{m} \cdot 2\right) \cdot \frac{1}{0,65m} + 0,01m$$
$$\cdot 14\frac{kN}{m^3} = \mathbf{31,14\frac{kN}{m^2}}$$

Design load:

$$g_{e1}^d = g_{e1}^{ch} \cdot 1,5 = 31,14\frac{kN}{m} \cdot 1,5 = \mathbf{46,71\frac{kN}{m^2}}$$

- Pavement:

$$t_p = (0,05m + 0,04m) = 0,09m \qquad\qquad \gamma_p = 23\frac{kN}{m^3}$$

- Insulation:

$$t_i = 0,01m \qquad\qquad \gamma_i = 14\frac{kN}{m^3}$$

Characteristic load:

$$g_{e2}^{ch} = 0,09m \cdot 23\frac{kN}{m^3} + 0,01m \cdot 14\frac{kN}{m^3} = \mathbf{2,21\frac{kN}{m^2}}$$

Design load:

$$g_{e2}^{d} = g_{e2}^{ch} \cdot 1,5 = 2,21\frac{kN}{m^2} \cdot 1,5 = \mathbf{3,315\frac{kN}{m^2}}$$

- Live loads:
- Automobiles, B class according to [PN-85/S-10030]:

Characteristic load:

$$q_{a}^{ch} = 3\frac{kN}{m^2} = \mathbf{3\frac{kN}{m}}$$

Design load:

$$q_{a}^{d} = q_{a}^{ch} \cdot 1,5 = 3\frac{kN}{m} \cdot 1,5 = \mathbf{4,5\frac{kN}{m}}$$

- K vehicle, B class according to [PN-85/S-10030] (per one wheel):

Dynamical coefficient

$$\varphi = 1,35 - 0,005 \cdot 25m = 1,225 \leq 1,325$$

Characteristic load:

$$P_{K}^{ch} = \mathbf{75kN}$$

Design load:

$$P_{K}^{d} = P_{K}^{ch} \cdot 1,5 \cdot \varphi = 75kN \cdot 1,5 \cdot 1,225 = \mathbf{137,8125kN}$$

14.2.2. Structural analysis
➔ ***Phase 1:***   *FREE SUPPORTED BEAM:*

g_I

25m

6,25

ω_I

Influence line of bending moment
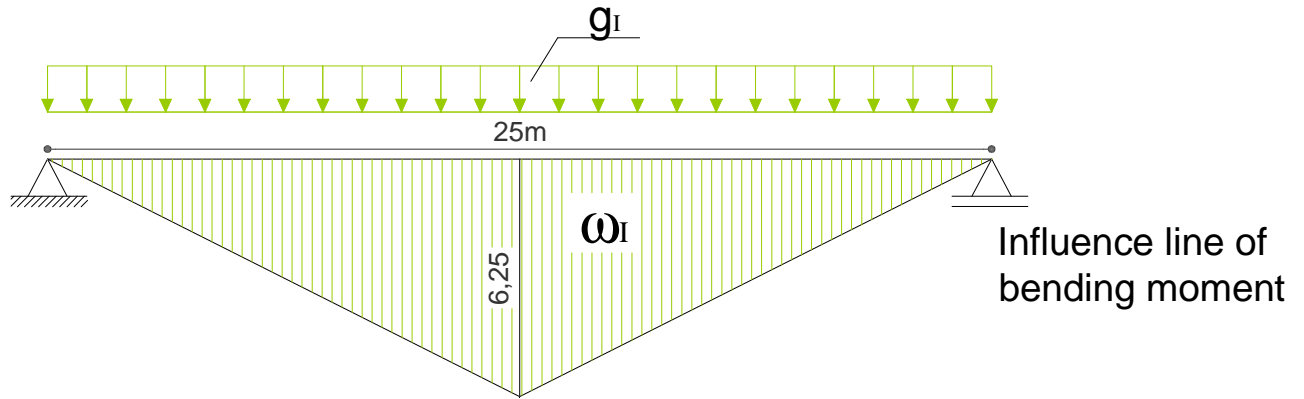
$\omega_I = 78,125m^2$

$$M_I^{ch} = g_I^{ch} \cdot \omega_I = 27,68 \frac{kN}{m} \cdot 78,125m^2 = \mathbf{2162,24 kNm}$$

$$M_I^{d} = g_I^{d} \cdot \omega_I = 34,02 \frac{kN}{m} \cdot 78,125m^2 = \mathbf{2658,08 kNm}$$

g_{I_II}

25m

6,25

ω_{I_II}

Influence line of bending moment
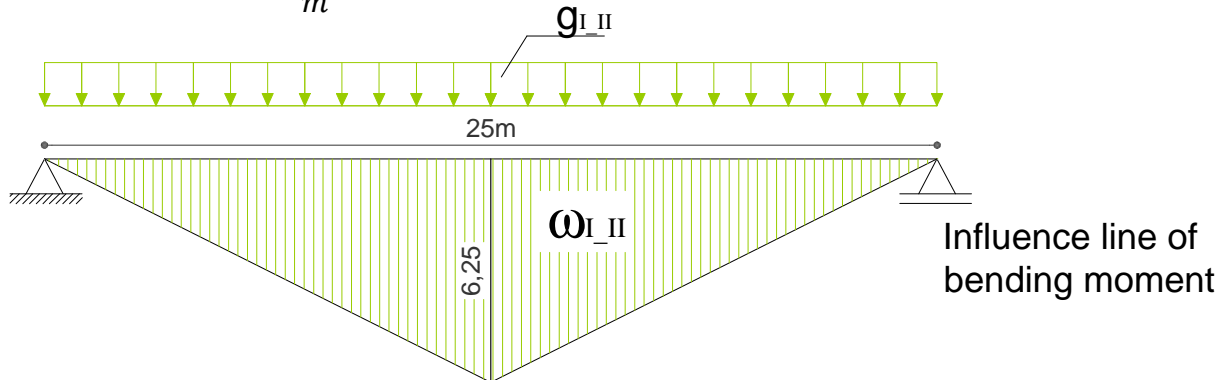
$\omega_{I\_II} = 78,125m^2$

$$M_{I\_II}^{ch} = g_{I\_II}^{ch} \cdot \omega_{I\_II} = 23,62 \frac{kN}{m} \cdot 78,125m^2 = \mathbf{1845,24 kNm}$$

$$M_{I\_II}^{d} = g_{I\_II}^{d} \cdot \omega_{I\_II} = 28,75 \frac{kN}{m} \cdot 78,125m^2 = \mathbf{2245,99 kNm}$$

➔ *Phase 2:*   *CONTINUOUS BEAM:*

LONGITUDINAL ELEMENTS:

✖ **COMPOSITE GIRDER:**

Collaboration width b_p:

Minimum of:

- $0,15 \cdot L_t$ $L_t = 25m$

$0,15 \cdot 25m = \mathbf{3,75m}$

- $0.5 \cdot beams\ spacing$ $\qquad s_t = 2.7m$

$0.5 \cdot 2.7m = \mathbf{1,35m}$

- $6t + b_{s0} - intermediate\ field$ $\quad b_{s0} = 0.25m$ $\qquad t = 0.25m$

$6 \cdot 0.25m + 0.25m = \mathbf{1,75m}$

- $4t + b_{s0} - extreme\ field$ $\qquad b_{s0} = 0.25m$ $\qquad t = 0.25m$

$4 \cdot 0.25m + 0.25m = \mathbf{1,25m}$

$b_p = min\{3.75m; 1.35; 1.75m; 1.25m\} = \mathbf{1,25m}$
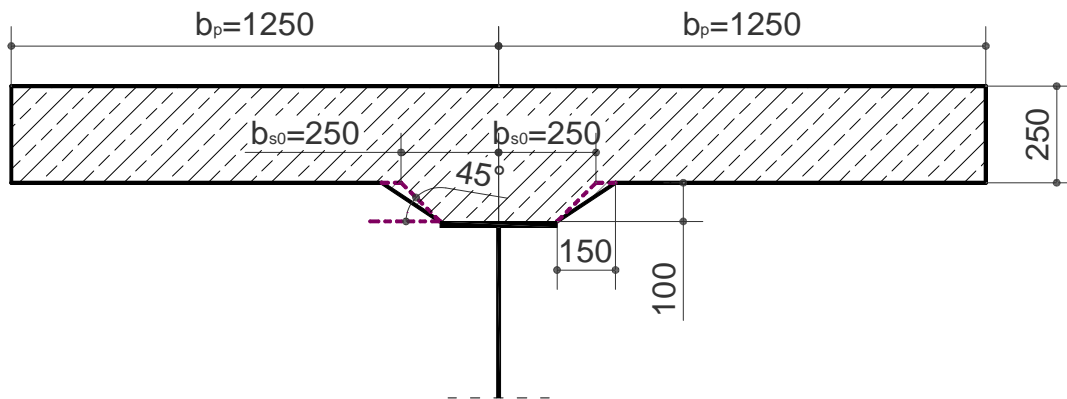
Geometrical characteristic of composite beam section:

- Concrete slab:

    $I_s = \mathbf{0,004497m^4}$

    $A_s = \mathbf{0,67m^2}$

    $E_s = \mathbf{36,4GPa}$

- Steel beam:

    $I_b = \mathbf{0,00793m^4}$

    $A_b = \mathbf{0,0478m^2}$

    $E_b = \mathbf{205GPa}$

Equivalent section

- Distance between centres of gravity of concrete flange and steel beam
- $a = \mathbf{1,120m}$

- Distance of extreme fibres:
  <u>Steel beam:</u>
- Top fibres: $v_t = \mathbf{0,907m}$
- Bottom fibres: $v_b = \mathbf{0,278m}$
  <u>Concrete slab:</u>
- Top fibres: $y_t = \mathbf{0,136m}$
- Bottom fibres: $y_b = \mathbf{0,214m}$

$$n_\varphi = \frac{E_b}{E_s} = \frac{205GPa}{36,4GPa} = \mathbf{5,63}$$

$$A_{s\varphi} = \frac{A_s}{n_\varphi} = \frac{0,67m^2}{5,63} = \mathbf{0,12m^2}$$

$$I_{s\varphi} = \frac{I_s}{n_\varphi} = \frac{0,004497m^4}{5,63} = \mathbf{0,0008m^4}$$

- Distances between centre of gravity of equivalent section and concrete slab / steel beam

$$\frac{a}{a_b} = \frac{A_b + A_{s\varphi}}{A_{s\varphi}} \quad \rightarrow \quad a_b = \frac{A_{s\varphi} \cdot a}{A_b + A_{s\varphi}} = \frac{0,12m^2 \cdot 1,12m}{0,0478m^2 + 0,12m^2} = \mathbf{0,8m}$$

$$a_t = a - a_b = 1,120m - 0,8m = \mathbf{0,32m}$$

- Top: $a_t = \mathbf{0,32m}$
- Bottom: $a_b = \mathbf{0,80m}$
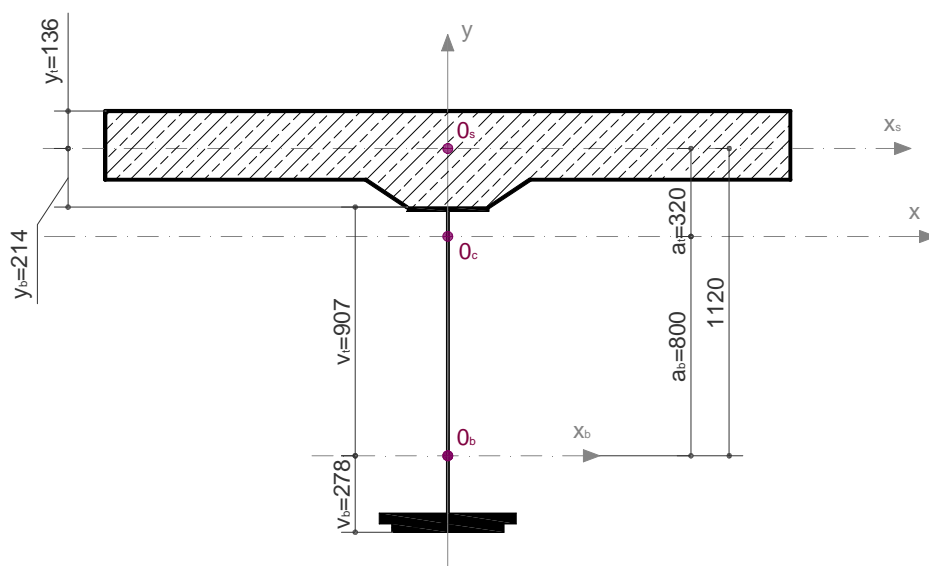
- Area of equivalent section:

$$A = A_b + A_{s\varphi} = 0{,}0478m^2 + 0{,}12m^2 = \mathbf{0,1678m^2}$$

- Moment of inertia of equivalent section:

$$I_x = I_b + I_{s\varphi} + A_b \cdot a_b^2 + A_{s\varphi} \cdot a_t^2$$
$$= 0{,}00793m^4 + 0{,}0008m^4 + 0{,}0478m^2 \cdot (0{,}8m)^2 + 0{,}12m^2 \cdot (0{,}32m)^2$$
$$= \mathbf{0,0515m^4}$$

- Torsional moment of equivalent section:
- Torsional moment of concrete slab (1):

Width: $w = 2500mm$

Thickness: $\delta = 250mm$

$$k = \frac{1}{3} \cdot \left[1 - 0{,}63 \cdot \frac{w}{\delta} \cdot \left(1 - \frac{\delta^4}{12 \cdot w^4}\right)\right] = \mathbf{0,312}$$

$$I_{cs1} = k \cdot \delta^3 \cdot w = \mathbf{12200527669mm^4}$$

- Torsional moment of concrete slab (2):

Width: $w = 450mm$

Thickness: $\delta = 100mm$

$$k = \mathbf{0,287}$$

$$I_{cs2} = k \cdot \delta^3 \cdot w = \mathbf{129004268mm^4}$$

→ *Torsional moment of concrete slab:*

$$I_{sc} = 0{,}5 \cdot I_{cs1} + 0{,}5 \cdot I_{cs2} = 0{,}5 \cdot 12200527669mm^4 + 0{,}5 \cdot 129004268mm^4$$
$$= \mathbf{12329531937mm^4}$$

- Torsional moment of web:

Width: $w = 1100mm$

Thickness: $\delta = 10mm$

$$k = \mathbf{0,331}$$

$$I_{cs} = k \cdot \delta^3 \cdot w = \mathbf{364567 mm^4}$$

- Torsional moment of top flange:

Width: $\quad w = 300\boldsymbol{mm}$

Thickness: $\quad \delta = 15\boldsymbol{mm}$

$$k = \mathbf{0,322}$$

$$I_{cs} = k \cdot \delta^3 \cdot w = \mathbf{326869 mm^4}$$

- Torsional moment of bottom flange:

Width: $\quad w = 500\boldsymbol{mm}$

Thickness: $\quad \delta = 40\boldsymbol{mm}$

$$k = \mathbf{0,316}$$

$$I_{cs} = k \cdot \delta^3 \cdot w = \mathbf{10129069 mm^4}$$

- Torsional moment of cover plate:

Width: $\quad w = 410\boldsymbol{mm}$

Thickness: $\quad \delta = 30\boldsymbol{mm}$

$$k = 0,318$$

$$I_{cs} = k \cdot \delta^3 \cdot w = \mathbf{3519900 mm^4}$$

Torsional moment of equivalent section:

$$
\begin{aligned}
I_t = I_{cs} + I_w + I_{tf} + I_{bf} + I_{cp} \\
= 12329531937 mm^4 + 364567 mm^4 + 326869 mm^4 + 10129069 mm^4 \\
+ 3519900 mm^4 = \mathbf{6179106373 mm^4}
\end{aligned}
$$

TRANSVERSAL ELEMENTS:

GRID

COMPOSITE GIRDER
EXTREME SUPPORTED CROSS-BAR
INTERMEDIATE SUPPORTED CROSS-BAR
SLAB ELEMENTS
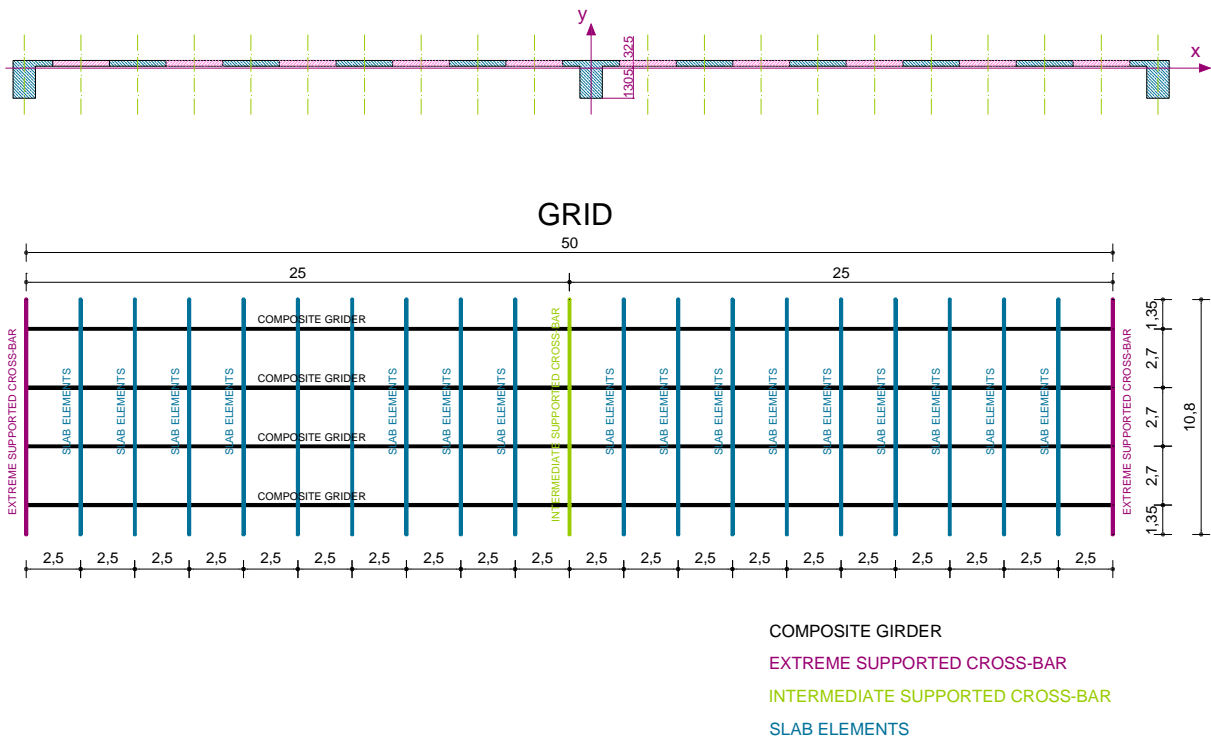
✖ EXTREME SUPPORTED CROSS-BAR:

Geometrical characteristic:

- Moment of inertia:

  $I_{ec} = 0,7619m^4$

- Area:

  $A_{ec} = 1,8175m^2$

- Modulus of elasticity:

  $E_{ec} = 36,4GPa$

- Torsional moment:
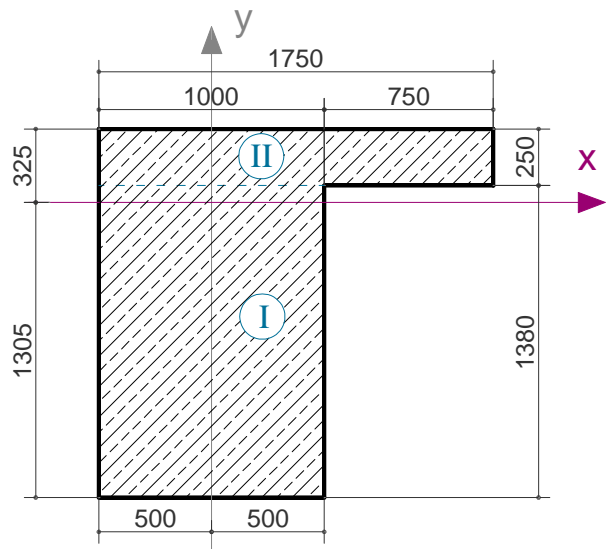
	I	II
WIDTH:	$w_I = 1750mm$	$w_{II} = 1305mm$
THICKNESS:	$\delta_I = 250mm$	$\delta_{II} = 1000mm$
k:	$k_I = 0,303$	$k_{II} = 0,177$

$$I_{ec_i} = k \cdot \delta^3 \cdot w \qquad I_{ec_I} = \mathbf{8294299304 mm^4} \qquad I_{ec_{II}} = \mathbf{231033870736 mm^4}$$

↓

$$I_{ec} = 0{,}5 I_{cs_I} + I_{cs_{II}} = \mathbf{235181020388 mm^4}$$

✖ <u>**INTERMEDIATE SUPPORTED CROSS-BAR:**</u>

Geometrical characteristic:

* Moment of inertia:

  $$I_{ic} = \mathbf{0,76955 m^4}$$

* Area:

  $$A_{ic} = \mathbf{2,005 m^2}$$

* Modulus of elasticity:

  $$E_{ic} = \mathbf{36,4 GPa}$$

* Torsional moment:
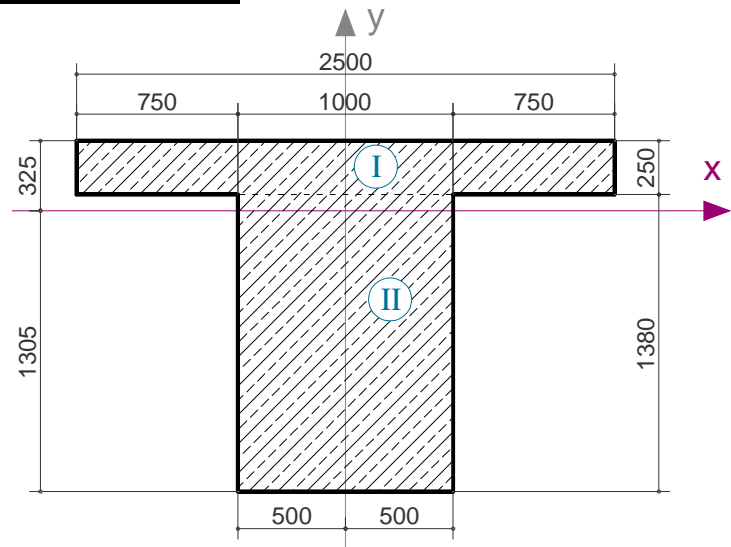
	Ⓘ	Ⓘ	Ⓘ
WIDTH:	$w_I = \mathbf{2500 mm}$		$w_{II} = 1305 \mathbf{mm}$
THICKNESS:	$\delta_I = \mathbf{250 mm}$		$\delta_{II} = 1000 \mathbf{mm}$
k:	$k_I = 0{,}312$		$k_{II} = 0{,}185$
$I_{ic_i} = k \cdot \delta^3 \cdot w$	$I_{ic_I} = \mathbf{12200527669 mm^4}$		$I_{ic_{II}} = \mathbf{254825270929 mm^4}$

↓

$$I_{ic} = 0{,}5 I_{ic_I} + I_{ic_{II}} = \mathbf{260925534763 mm^4}$$

✖ <u>**SLAB ELEMENTS:**</u>

Geometrical characteristic:

* Moment of inertia:

  $$I_{es} = \mathbf{0,028198 m^4}$$
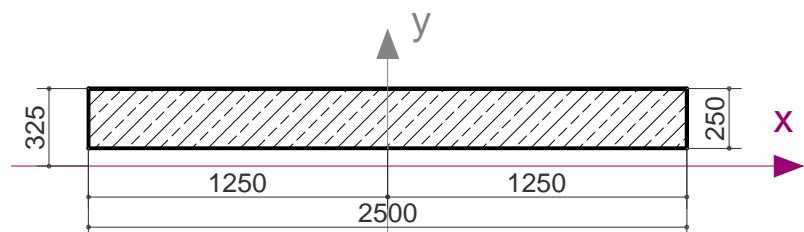
- Area:

$$A_{es} = \mathbf{0,625m^2}$$

- Modulus of elasticity:

$$E_{es} = \mathbf{36,4GPa}$$

- Torsional moment:

WIDTH: $\qquad w_I = \mathbf{2500mm}$

THICKNESS: $\qquad \delta_I = \mathbf{250mm}$

k: $\qquad k_I = 0,312$

$$I_{es}' = k \cdot \delta^3 \cdot w \qquad I_{es}' = \mathbf{12200527669mm^4}$$

↓

$$I_{ic} = 0,5 I_{ic_I}' = \mathbf{6100263835mm^4}$$

Model (e1,s2):
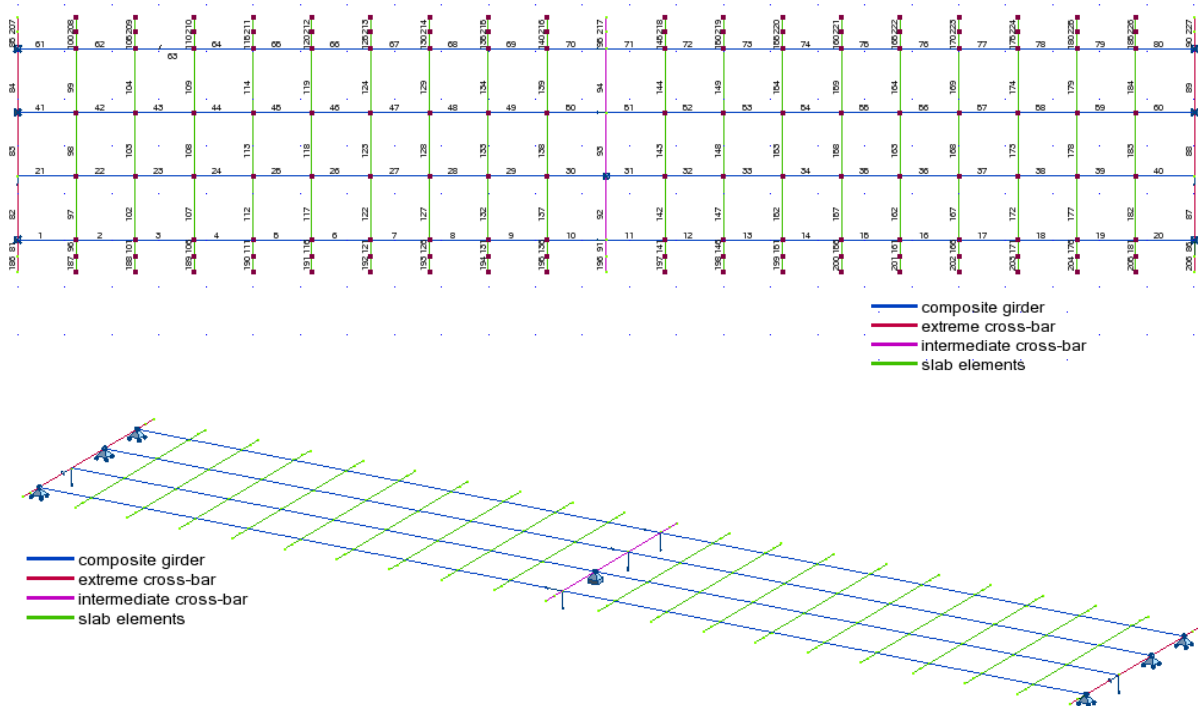
Geometrical characteristic:
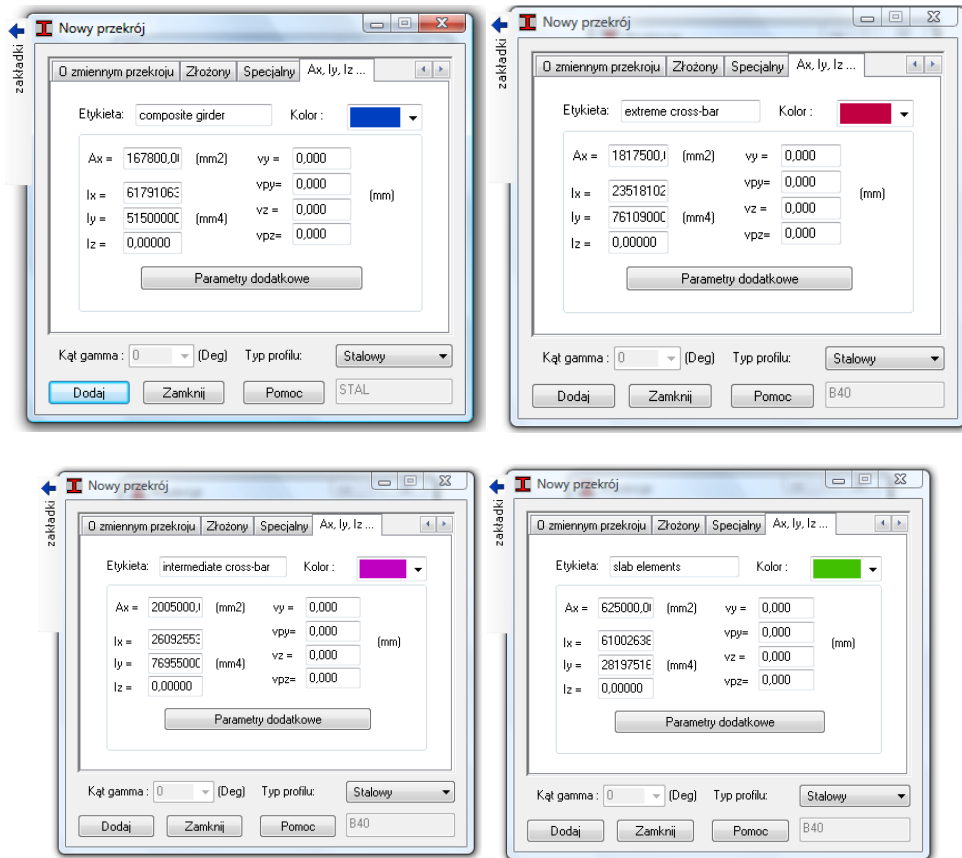
Materials:
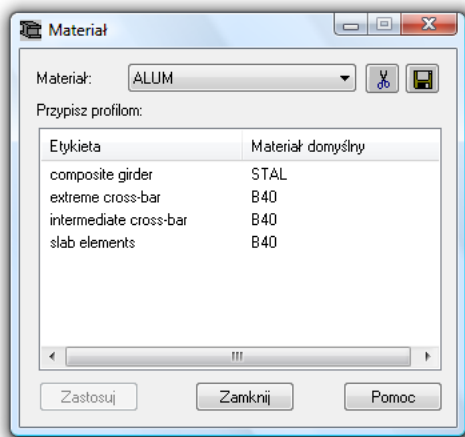
Determination of maximum section (dead load):

- extreme girder:
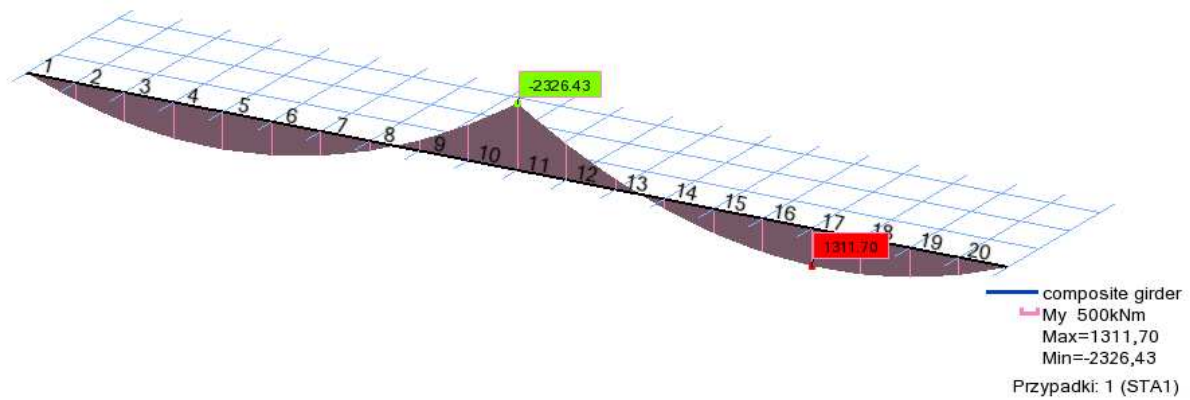
$M_{max} = 1311,70 kNm$

$M_{min} = -2326,43 kNm$

- internal girder:
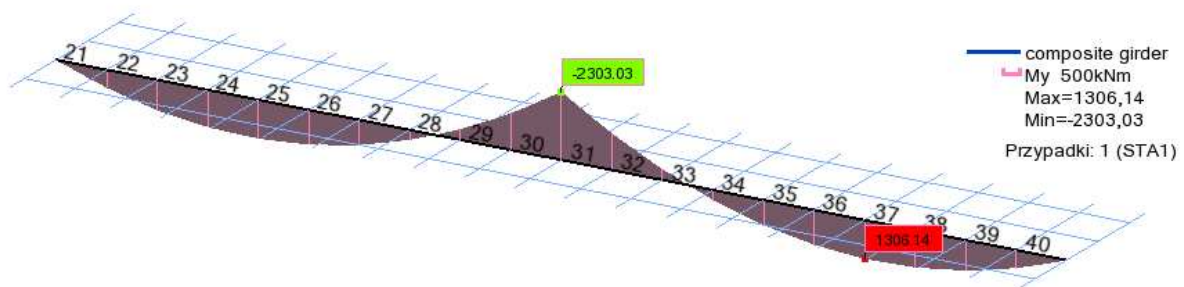
$M_{max} = 1306,14 kNm$

$M_{min} = -2303,03 kNm$

*NOTE: Maximum bending moment in section $\gamma - \gamma = 0,4l = 10m$ from the extreme support, minimum bending moment in section $\beta - \beta$ over the intermediate support.

Loads:

- PART 1 (equipment):

p 3pZ=-46.71

p 3pZ=-46.71

kPa
Przypadki: 2 (equipment_1)

- PART 2 (equipment):

p 3pZ=-3.31

kPa
Przypadki: 3 (equipment_2)

- Automobiles:

p 3pZ=-4.50

kPa
Przypadki: 4 (automobiles)

- K:

FZ=-137.81
FZ=-137.81
FZ=-137.81
FZ=-137.81
FZ=-137.81
FZ=-137.81
FZ=-137.81
FZ=-137.81

kN
Przypadki: 5 (K)

UNIVERSITAT POLITÈCNICA
DE CATALUNYA
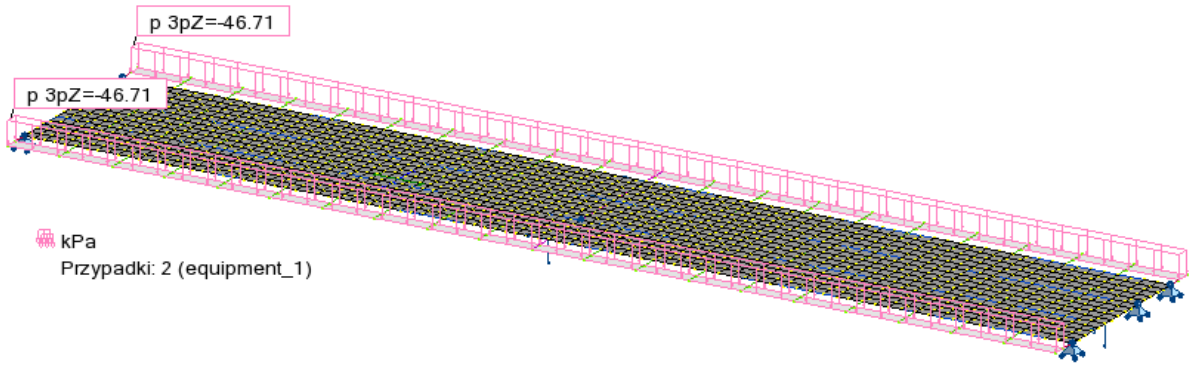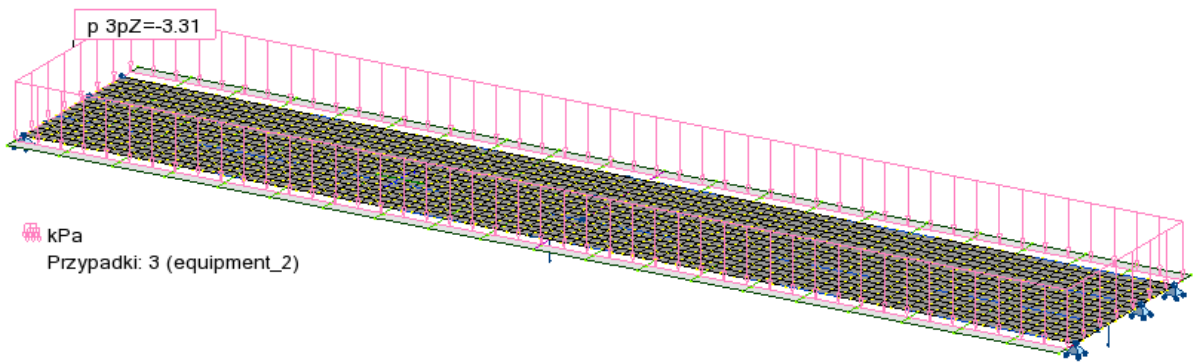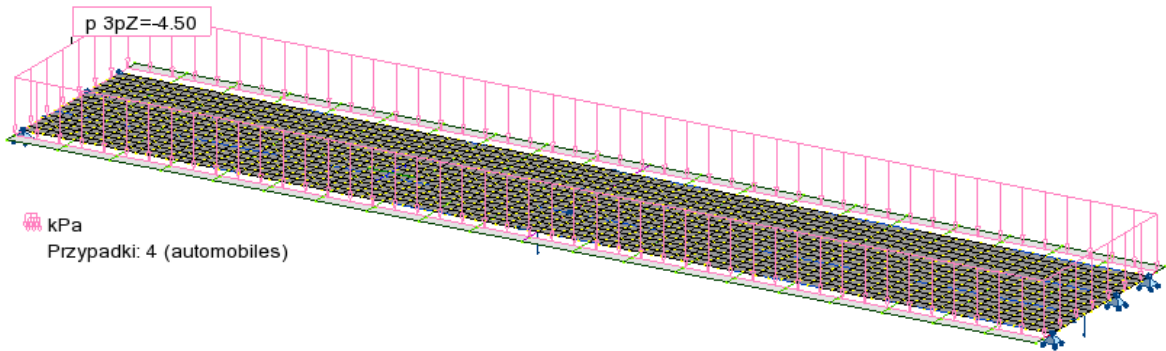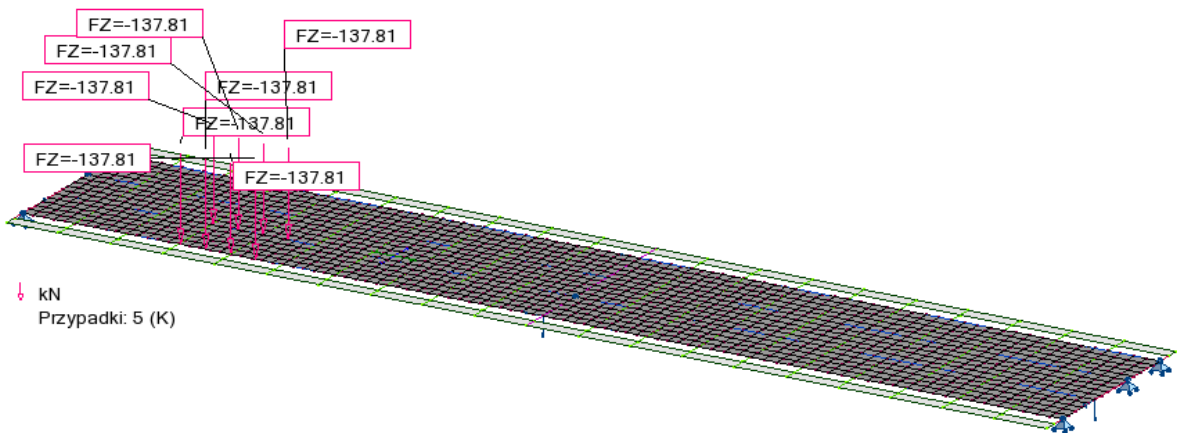
- Removing of the formwork:

p 3pZ=0.45

kPa
Przypadki: 6 (remove of formworks)

- Unloading of the deck slab:

p 3pZ=0.23

kPa
Przypadki: 7 (Unloading of deck slab)

- Loads combinations:

FZ=-137.81
FZ=-137.81
FZ=-137.81
FZ=-137.81
p 3pZ=0.23
p 3pZ=-4.50
p 3pZ=46.71
FZ=-137.81
FZ=-137.81
FZ=-137.81
p 3pZ=46.71
p 3pZ=-3.31
p 3pZ=0.45

kPa
kN
Przypadki: 8 (KOMB1)
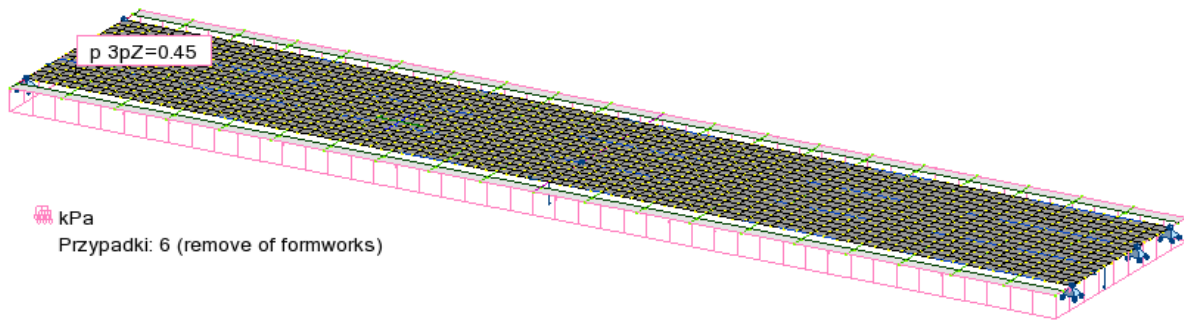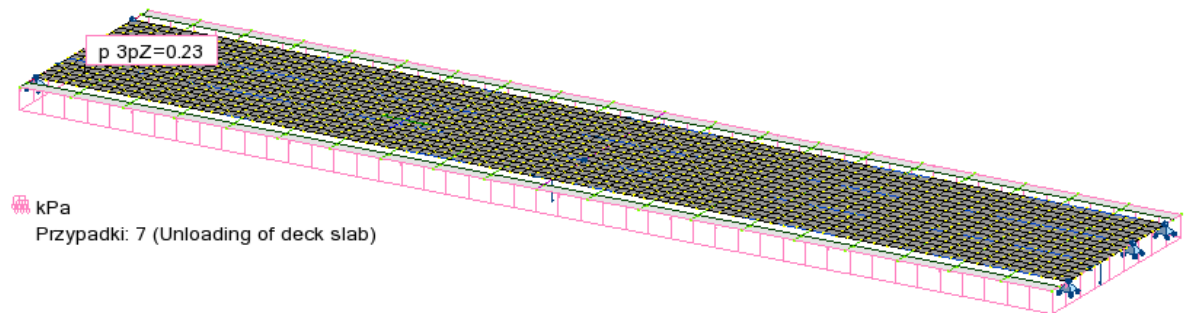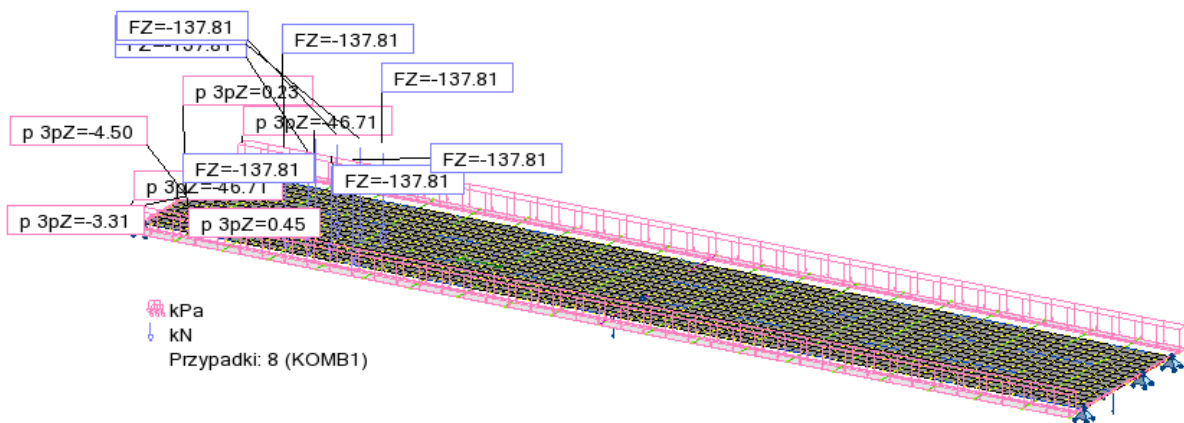
Bending moments:
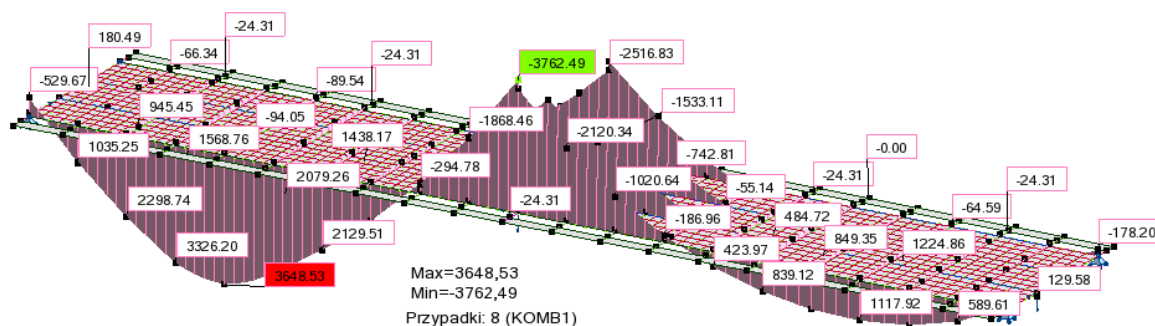
$M_{max} = 3648,53 kNm$

$M_{min} = -3762,49 kNm$

$M_{\frac{1}{2}l} = 3645,53 kNm$
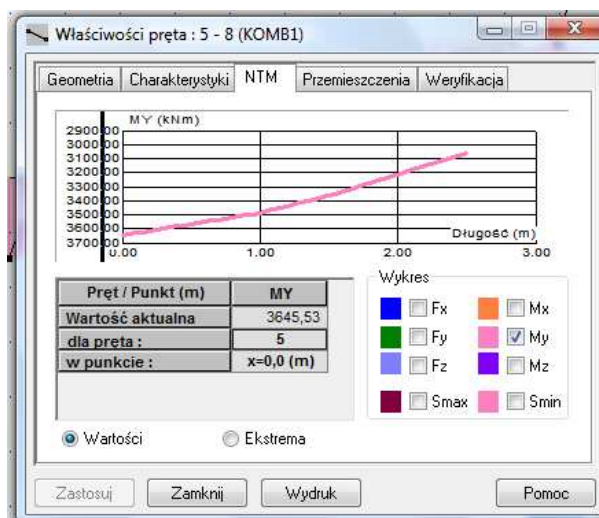
14.2.3. Dimensioning
➔ *Phase 1:*

Geometrical characteristic of the beam (determined by AutoCad programme):

- Moment of inertia:

$I_b = 0,00793 m^4$

- Distance of extreme fibres:
- Top fibres: $v_t = 0,907 m$
- Bottom fibres: $v_b = 0,278 m$

Accepted: steel beam made by **S355**.

Characteristic tensile strength: $R_m^{ch} = 355 MPa$

Design tensile strength: $R_m^d = \frac{R_m^{ch}}{\gamma_f} = \frac{355 MPa}{1,15} = \mathbf{308 MPa}$
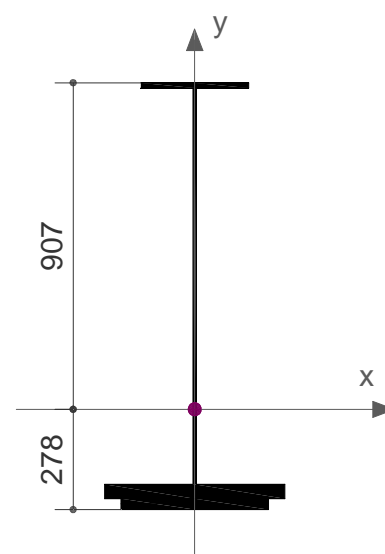
Stresses:

$\alpha - \alpha$ section:

$$\sigma_{It}^{\alpha-\alpha} = \frac{-M_I^d \cdot v_t}{I_b} = \frac{-2658,08kNm \cdot 0,907m}{0,00793m^4} = \mathbf{-303,99MPa} < R_m^d = \mathbf{308MPa}$$

$$\sigma_{Ib}^{\alpha-\alpha} = \frac{M_I^d \cdot v_b}{I_b} = \frac{-2658,08kNm \cdot 0,278m}{0,00793m^4} = \mathbf{93,17MPa} < R_m^d = \mathbf{308MPa}$$

$$\sigma_{I\_IIt}^{\alpha-\alpha} = \frac{-M_{I\_II}^d \cdot v_t}{I_b} = \frac{-2245,99kNm \cdot 0,907m}{0,00793m^4} = \mathbf{-256,86MPa} < R_m^d = \mathbf{308MPa}$$

$$\sigma_{I\_IIb}^{\alpha-\alpha} = \frac{M_{I\_II}^d \cdot v_b}{I_b} = \frac{-2245,99kNm \cdot 0,278m}{0,00793m^4} = \mathbf{78,73MPa} < R_m^d = \mathbf{308MPa}$$

STRESS DIAGRAM
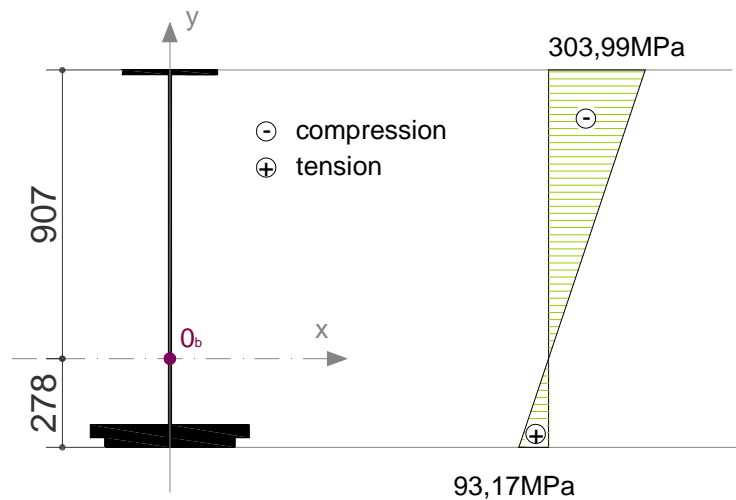
$\gamma - \gamma$ section:

$$\omega_{I\_II} = 62,5m^2$$

$$M_{I\_II}^d = g_{I\_II}^d \cdot \omega_{I\_II} = 28,75\frac{kN}{m} \cdot 62,5m^2 = \mathbf{1796,875kNm}$$

$$\sigma_{I\_IIt}^{\gamma-\gamma} = \frac{-M_{I\_II}^d \cdot v_t}{I_b} = \frac{-1796,875kNm \cdot 0,907m}{0,00793m^4} = \mathbf{-204,744MPa} < R_m^d = \mathbf{308MPa}$$

$$\sigma_{I\_IIb}^{\gamma-\gamma} = \frac{M_{I\_II}^d \cdot v_b}{I_b} = \frac{-1796,875kNm \cdot 0,278m}{0,00793m^4} = \mathbf{62,99MPa} < R_m^d = \mathbf{308MPa}$$

➔ **Phase 2:**

$I_b = 0,00793m^4$ $\qquad\qquad\qquad a = 1,120m$

$I_{s\varphi} = 0,0008m^4$ $\qquad\qquad\qquad a_b = 0,800m$

$I_s = 0,004497m^4$ $\qquad\qquad\qquad n_\varphi = 5,63$

$A_b = 0,0478m^2$ $\qquad\qquad\qquad A_s = 0,0478m^2$

Stresses:

$\alpha - \alpha$ *section:*

$M^{\alpha-\alpha} = 3645,53kNm$

$$\begin{bmatrix} \dfrac{I_b + I_{s\varphi}}{I_{s\varphi}} & 1 \\[2mm] \dfrac{-a \cdot a_b \cdot A_b}{I_b} & 1 \end{bmatrix} \cdot \begin{bmatrix} M_b \\ a \cdot N_b \end{bmatrix} = \begin{bmatrix} M \\ 0 \end{bmatrix} \rightarrow \quad \begin{array}{l} M_b = \mathbf{568,642kNm} \\ N_b = \mathbf{2742,10kN} \end{array}$$

$$M_s = \frac{I_{s\varphi}}{I_b} \cdot M_b = \frac{0,0008m^4}{0,00793m^4} \cdot 568,642kNm = \mathbf{57,277kNm}$$

$$N_s = -N_b + N_\varepsilon = \mathbf{-2742,10kN}$$

- In steel beam:

$$\sigma_b^{\alpha-\alpha} = \frac{N_b}{A_b} + \frac{M_b \cdot v_b}{I_b} = \frac{2742,10kN}{0,0478m^2} + \frac{568,642kNm \cdot 0,278m}{0,00793m^4} = \mathbf{77,30MPa}$$

$$\sigma_t^{\alpha-\alpha} = \frac{N_b}{A_b} - \frac{M_b \cdot v_t}{I_b} = \frac{2742,10kN}{0,0478m^2} - \frac{568,642kNm \cdot 0,907m}{0,00793m^4} = \mathbf{-7,67MPa}$$

$$\sigma_{IIb}^{\alpha-\alpha} = \sigma_b^{\alpha-\alpha} + \sigma_{II\_Ib}^{\alpha-\alpha} = 77,30MPa + 78,73MPa = \mathbf{156,03MPa} < R_m^d = \mathbf{308MPa}$$

$$\sigma_{IIt}^{\alpha-\alpha} = \sigma_t^{\alpha-\alpha} + \sigma_{II\_It}^{\alpha-\alpha} = -7,67MPa - 256,86MPa = \mathbf{-264,53MPa} < R_m^d = \mathbf{308MPa}$$

- In concrete slab:

$$\sigma_{IIb}^{\alpha-\alpha} = -\frac{N_s}{A_s} + \frac{M_b \cdot y_b}{I_s} = -\frac{-2742,10kN}{0,67m^2} - \frac{57,227kNm \cdot 0,214m}{0,004497m^4} = \mathbf{1,40MPa}$$

$$\sigma_{IIt}^{\alpha-\alpha} = -\frac{N_s}{A_s} - \frac{M_b \cdot y_t}{I_s} = -\frac{-2742,10kN}{0,67m^2} + \frac{57,227kNm \cdot 0,136m}{0,004497m^4} = \mathbf{5,82MPa}$$
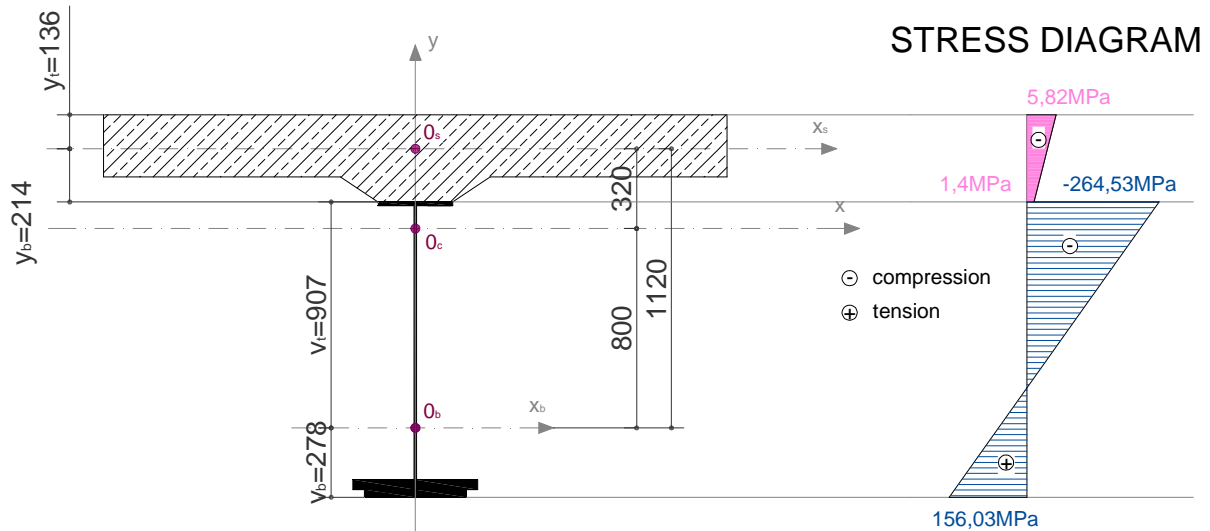
γ − γ section:

$$M^{\gamma-\gamma} = \mathbf{3648,53kNm}$$

$$\begin{bmatrix} \dfrac{I_b + I_{s\varphi}}{I_{s\varphi}} & 1 \\ \dfrac{-a \cdot a_b \cdot A_b}{I_b} & 1 \end{bmatrix} \cdot \begin{bmatrix} M_b \\ a \cdot N_b \end{bmatrix} = \begin{bmatrix} M \\ 0 \end{bmatrix} \rightarrow \quad \begin{matrix} M_b = \mathbf{568,642kNm} \\ N_b = \mathbf{2744,356kN} \end{matrix}$$

$$M_s = \frac{I_{s\varphi}}{I_b} \cdot M_b = \frac{0,0008m^4}{0,00793m^4} \cdot 568,642kNm = \mathbf{57,324kNm}$$

$$N_s = -N_b + N_\varepsilon = \mathbf{-2744,356kN}$$

- In steel beam:

$$\sigma_b^{\gamma-\gamma} = \frac{N_b}{A_b} + \frac{M_b \cdot v_b}{I_b} = \frac{2744,356kN}{0,0478m^2} + \frac{568,642kNm \cdot 0,278m}{0,00793m^4} = \mathbf{77,35MPa}$$

$$\sigma_t^{\gamma-\gamma} = \frac{N_b}{A_b} - \frac{M_b \cdot v_t}{I_b} = \frac{2744,356kN}{0,0478m^2} - \frac{568,642kNm \cdot 0,907m}{0,00793m^4} = \mathbf{-7,63MPa}$$

$$\sigma_{IIb}^{\gamma-\gamma} = \sigma_b^{\gamma-\gamma} + \sigma_{II\_Ib}^{\gamma-\gamma\alpha} = 77{,}35 MPa + 62{,}99 MPa = \boldsymbol{140{,}34 MPa} < R_m^d = \boldsymbol{308 MPa}$$

$$\sigma_{IIt}^{\gamma-\gamma} = \sigma_t^{\gamma-\gamma} + \sigma_{II\_It}^{\gamma-\gamma} = -7{,}63 - 204{,}744 MPa = \boldsymbol{-212{,}374 MPa} < R_m^d = \boldsymbol{308 MPa}$$

- In concrete slab:

$$\sigma_{IIb}^{\gamma-\gamma} = -\frac{N_s}{A_s} + \frac{M_b \cdot y_b}{I_s} = -\frac{-2744{,}356 kN}{0{,}67 m^2} + \frac{57{,}324 kNm \cdot 0{,}214 m}{0{,}004497 m^4} = \boldsymbol{6{,}82 MPa}$$

$$\sigma_{IIt}^{\gamma-\gamma} = -\frac{N_s}{A_s} - \frac{M_b \cdot y_t}{I_s} = -\frac{-2744{,}356 kN}{0{,}67 m^2} - \frac{57{,}324 kNm \cdot 0{,}136 m}{0{,}004497 m^4} = \boldsymbol{2{,}36 MPa}$$

15. CONCLUSION

This paper explains benefits of VFT method in bridge engineering. Calculation results confirm economic aspect of use this technology. Compared two road bridges with the same spans, width and load classes. Simplify analysis shows that for VFT bridge lower construction depth is demand (cross-section consist of four **1055mm** depth steel I beam → material effort: **99,4%**) than for alternative composite bridge (cross-section consist of four **1185mm** depth steel I beam → material effort: **98,7%**). The difference in construction depth gives advantage of material savings what nowadays is one of the most important reason during the tender process. Reading this document it is easy to see that VFT method provides many advantages. The main benefits are:

- Short time of carrying out (high degree of prefabrication),
- Simple assembly and low quantity of main girders cause traffic to be stopped only for a short time,
- Careful product control, right and ecological anticorrosive protection due to high degree of prefabrication,
- Obtaining very low construction depth creates the impression that spans are more slender.

Describing this technology it is necessary to mention about disadvantages. One of them is the fact that this kind of structure (also typical composite construction) is more complicated from the designer's point of view, because the majority problem for both steel and concrete construction appears during the design phase. Simple examples of calculation, introduced in this project, pass over shrinkage and creep effect but, in standard design way, these influences are very important. Besides, in country with bad or insufficient good conditions of the national road net, it is necessary to transfer of prefabricated flange execution to the building site (it is easier to transfer only the steel girder). For this reason some additional actions are being appeared (for instance: organization of place for prefabrication unit constructor).

Nevertheless the VFT technology is becoming more and more popular. The new types are constantly developed, in example VFT-WIB structure, which is characterized by (apart from the typical advantages of VFT construction):

- Shear connection without fatigue problems,
- Elementary steel construction nearly without any welding.

Summarizing: VFT technology is certainly strong competition for other solutions (concrete bridges, steel bridges and even composite bridges) due to the efficient use of steel and concrete in the cross section and aforementioned short time of bridge executing.

16. REFERENCES

[1] http://en.wikipedia.org/wiki/Composite_construction

[2] Lorenc W., *Konstrukcje zespolone stalowo – betonowe,* university notes 2009.

[3] Kołakowski T., Kosecki W., Marecki A. VFT® - *Prefabrykowane dźwigary zespolone z betonowym deskowaniem aktywnym* (Prefabricated composite girders with active concrete formwork). Inżynieria i Budownictwo nr 3/2003, page 144-148, http://www.europrojekt.pl/aktualnosci/artykuly/iib_3_03_vft_prefab_dzwigary.pdf (25.06.2009).

[4] Schmitt V., Seidl G., Wolf H. *VFT Construction Method*. Strait crossings 2001: proceedings of the Fourth Symposium on Strait Crossings, Bergen, Norway, 2-5 September 2001, page 201-208.

[5] Kołakowski T., Kosecki W., Lorenc W. *Polskie doświadczenia z realizacji obiektów w technologii VFT®* (Polish experiences in executing of VFT bridges), http://www.europrojekt.pl/aktualnosci/artykuly/iib_3_03_vft_prefab_dzwigary.pdf (25.06.2009).

[6] Schmitt V., Weizenegger. *New construction. Innovative building method for bridges with small and medium spans - VFT® and VFT-VIB®.*

[7] Kołakowski T., Marecki A., Lorenc W., Kubica E. *VFT® - Prefabrykowane dźwigary zespolone z aktywnym deskowaniem betonowym* (Prefabricated composite girders with active concrete formwork). 11 VFT Mosty Małe (Small Bridges) Wrocław_2004, http://www.europrojekt.pl/aktualnosci/konferencje/wroclaw/vft_k_mosty_male.pdf (25.06.2009).

[8] Seidl G., Schmitt V., Lorenc W. *Shear Transmission of Fibre Reinforced Concrete Dowels.*

[9] Hechler O., Lorenc W., Seidl G., Viefhues E. *Continuous shear connectors in bridge construction.*

[10] Kołakowski T., Kosecki W., Marecki A. *Technologia VFT®* (VFT® technology). 10' 2003 (nr 374), http://www.europrojekt.pl/aktualnosci/artykuly/materialy_budowlane_10_03_technologia_vft .pd (25.06.2009).

17. SOURCES OF FIGURES AND EQUATION

Figures:

Figure 1.1.   Author

Figure 1.2.   Author

Figure 1.3.   Schmitt Stumpf Frühauf Und Partner, engineering consultancy. VFT®
construction.

Figure 1.4.   VFT® - Starker Verbund im Brückenbau

Figure 3.1.   Hanswille G., Sedlacek G., Steel and composite bridges in Germany. State of
the Art.

Figure 3.2.   Lorenc Wojciech

Figure 3.3.   Kołakowski T., Kosecki W., Lorenc W. Polskie doświadczenia z realizacji
obiektów w technologii VFT®.

Figure 3.4.   Kołakowski T., Kosecki W., Lorenc W. Polskie doświadczenia z realizacji
obiektów w technologii VFT®.

Figure 3.5.   Kołakowski T., Kosecki W., Lorenc W. Polskie doświadczenia z realizacji
obiektów w technologii VFT®.

Figure 3.6.   Schmitt V., Weizenegger. New construction. Innovative building method
for bridges with small and medium spans - VFT® and VFT-VIB®.

Figure 3.7.   Schmitt V., Weizenegger. New construction. Innovative building method
for bridges with small and medium spans - VFT® and VFT-VIB®.

Figure 3.8.   Schmitt V., Weizenegger. New construction. Innovative building method
for bridges with small and medium spans - VFT® and VFT-VIB®.

Figure 3.9.   BW 0210 / 0211 Saalebrücke Merseburg in VFT-Bauweise. Überführung der
B 181 über die Saale bei km 23 + 990,000. Kurze Bilddokumentation zur
Trägermontage vom 26./27. Oktober 2002.

Figure 3.10.   BW 0210 / 0211 Saalebrücke Merseburg in VFT-Bauweise. Überführung der
B 181 über die Saale bei km 23 + 990,000. Kurze Bilddokumentation zur
Trägermontage vom 26./27. Oktober 2002.

Figure 3.11.   BW 0210 / 0211 Saalebrücke Merseburg in VFT-Bauweise. Überführung der
B 181 über die Saale bei km 23 + 990,000. Kurze Bilddokumentation zur
Trägermontage vom 26./27. Oktober 2002.

Figure 3.12.   Lorenc Wojciech

Equations:

UNIVERSITAT POLITÈCNICA
DE CATALUNYA

18. APPENDIX

Drawing 1.1. Conception 1: Side view and longitudinal-section of VFT bridge. (Author)

Drawing 1.2. Conception 1: Cross-section of VFT bridge. (Author)

Drawing 2.1. Conception 2: Side view and longitudinal-section of composite bridge. (Author)

Drawing 2.2. Conception 1: Cross-section of composite bridge. (Author)

SIDE VIEW

SCALE 1:100

LONGITUDINAL SECTION A-A

SCALE 1:100

JAWOR

SYCÓW

B

C

ROAD
600

2500

200 200

50

1044

133 133 133

5

5100

200 200

2500

585

100

RAILWAY LINE
420

RAILWAY LINE
420

126,30

pł 300x15

pł 1000x10

pł 500x40

400

30

5

1044

157

233

283

522

350

136

447

150

12

100

20

50 150 50
250

523

20

150

20

812

138 274 274 128

C

100

90 100 90

100

90 280

100

75 130 75

1035

374

150

146 60 50 60 100

300

300

100 60 50 60

844

191

40 43

577

578

43 40 75 100

266

374

1035

B

CROSS-SECTION B-B , C-C

SCALE 1:50

B-B |A **C-C**
A

1152

| 101 | 475 | 475 | 101 |

51 50 25 | 450 | 450 | 25 50 51

DEHYDRATION AXIS

Wearing course-ASPHALTIC CONCRETE (SMA) 5cm
Binding course-GUSSASPHALT 4cm
THERMAL INSULATION
IN SITU CONCRETE SLAB 21cm
PREFABRICATED CONCRETE FLANGE 10-12cm

DEHYDRATION AXIS

JAWOR ⬦ ⬦ SYCÓW

8% | 2% | 2% | 8% | 8% | 1:1.5

59
10 18
2

35 | 135 | 270 | pl 300x15 | 270 | 135 | 270 | 135 | 35 | 35

118 | pl 200x10 | 100 | 126 | 940 | 150

pl 1000x10
1000 | pl 500x40 | 167

100 | 100 | 110 | 50 | 220 | 50 | 110 | 40

540

591 | 447

100

100 | 510 | 30 | 50 | 20

590 | 150

100 | 90 | 100 | 170 | 100 | 85 | 20

545

140 | 270 | 135 | 135 | 270 | 205

A

UNIVERSITAT POLITECNICA DE CATALUNYA		
Enginyeria de la construcció		
DESIGN BY: AGNIESZKA SKALSKA	SIGNATURE:	DATE:
CHECKED BY: JOAN RAMON CASAS	SIGNATURE:	DATE:
PROJECT: ROAD BRIDGE		SCALE: 1:50
TYTUŁ RYSUNKU: CONCEPTION 1: Cross-section of VFT bridge		NUMBER OF DRAWING: Drawing. 1.2

END VIEW

SCALE 1:100

LONGITUDINAL SECTION A-A

SCALE 1:100

JAWOR

SYCÓW

B

C

C

B

ROAD
600

RAILWAY LINE
420

RAILWAY LINE
420

L 75x75x8
2600

L 75x75x8
1500

L 75x75x8
2490

pł 300x15

pł 1100x10

pł 500x40

pł 400x30

fł 300x200

1200
2500

5100

1044

133 133 133

5

200 200

2500

585

100

100

100

90 100 90

280

80

75 130 75

1044

5

400

30

30

522

350

136

441

12 150

150
250

20 50 50 20

523

20

138 274 274 128

100

812

126,30

191 40 43

577

578

43 40 75 100

266

374

1035

374

150 146 60 50 60 100

300

300

100 60 50 60
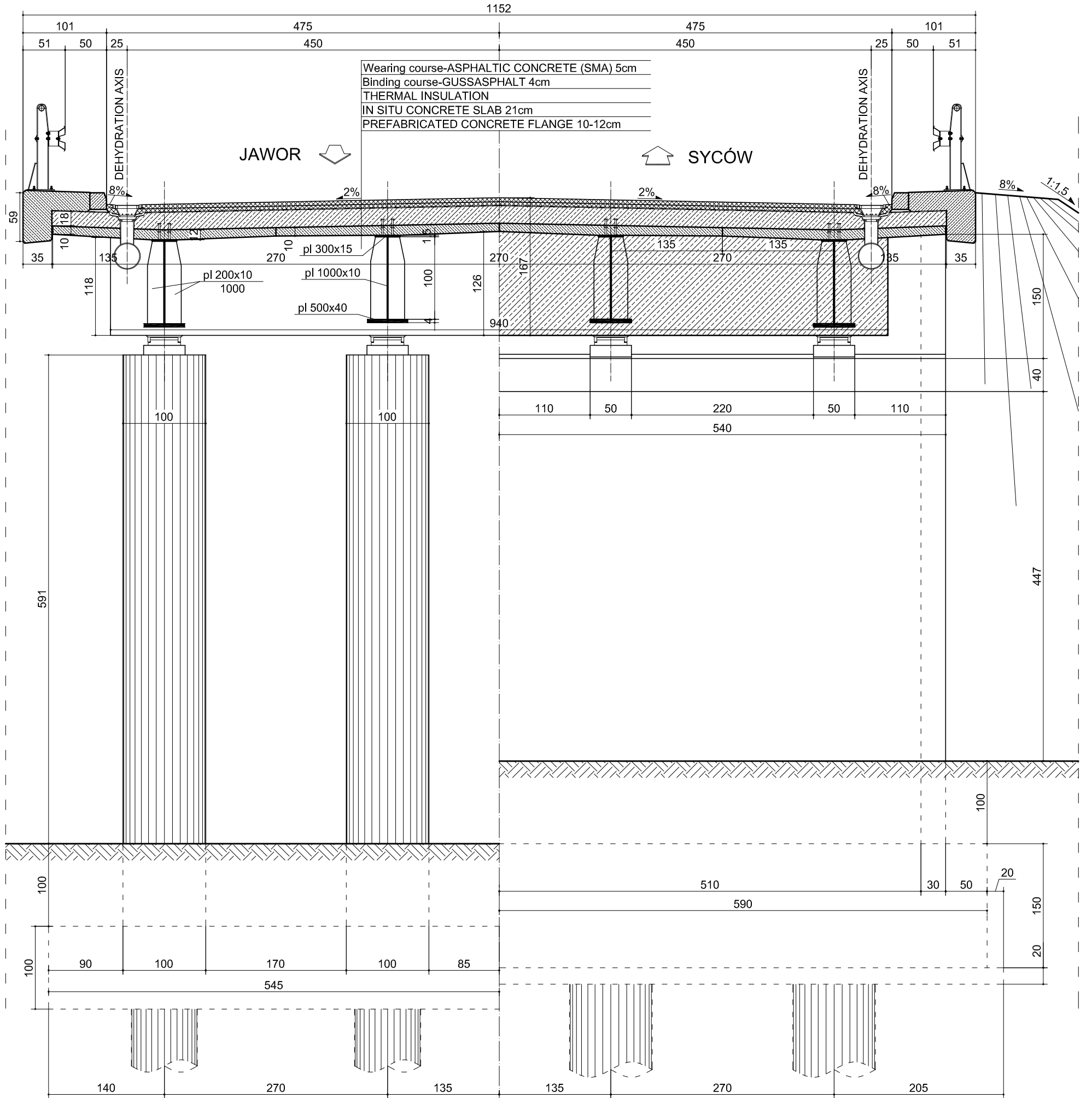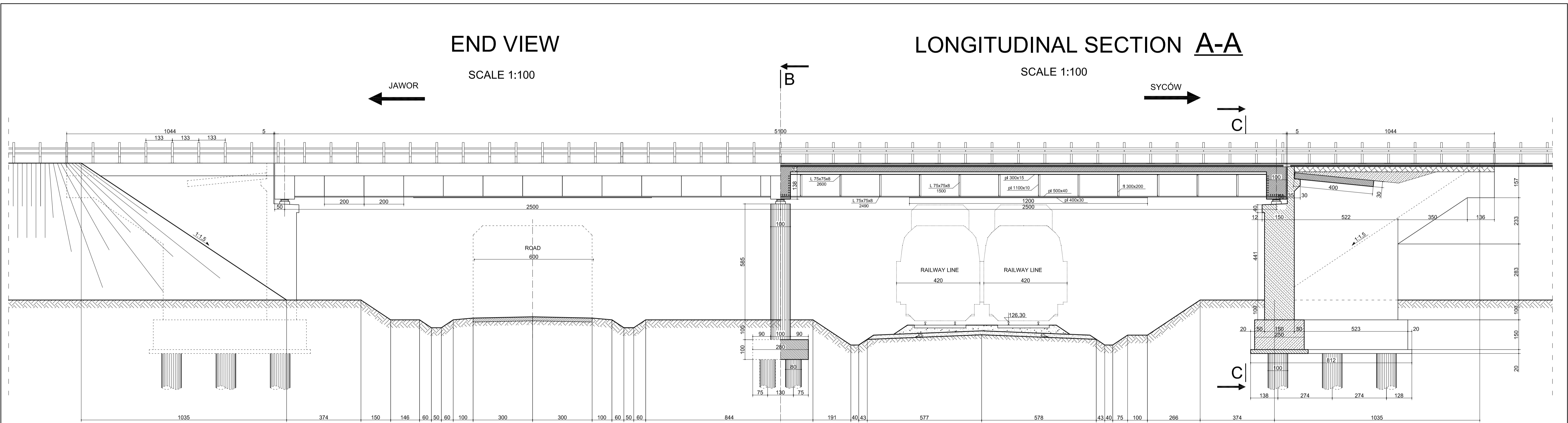
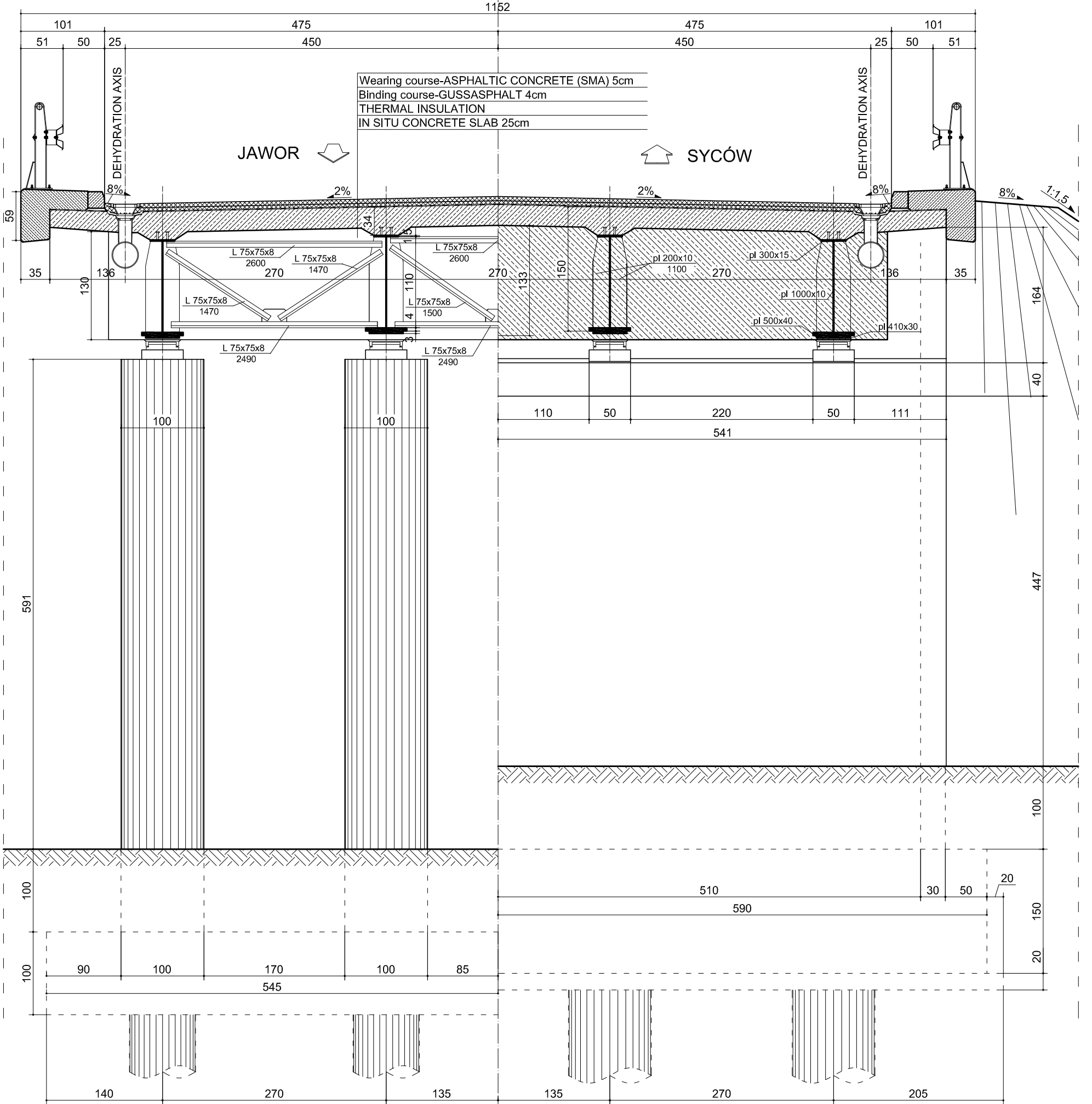844

1035

157

233

283

150

20

1:1,5

1:1,5

UNIVERSITAT POLITECNICA DE CATALUNYA
Enginyeria de la construcció

DESIGN BY:	AGNIESZKA SKALSKA	SIGNATURE:	DATE:
CHECKED BY:	JOAN RAMON CASAS	SIGNATURE:	DATE:
PROJECT:	ROAD BRIDGE		SCALE: 1:100
TYTUŁ RYSUNKU:	CONCEPTION 2: Side view and longitudinal section of composite bridge		NUMBER OF DRAWING: Drawing. 2.1

CROSS-SECTION B-B , C-C

SCALE 1:50

B-B

C-C

A

1152

101 | 475 | 475 | 101
51 | 50 | 25 | 450 | 450 | 25 | 50 | 51

DEHYDRATION AXIS

Wearing course-ASPHALTIC CONCRETE (SMA) 5cm
Binding course-GUSSASPHALT 4cm
THERMAL INSULATION
IN SITU CONCRETE SLAB 25cm

JAWOR

SYCÓW

DEHYDRATION AXIS

8%

2%

2%

8%

8%

1:1.5

59

34

L 75x75x8 2600
L 75x75x8 1470
L 75x75x8 2600

L 75x75x8
L 75x75x8
150

pl 200x10 1100
pl 300x15

pl 1000x10

270

270

133

35 | 136

130

L 75x75x8 1470

110

4

L 75x75x8 1500
L 75x75x8 1500

pl 500x40

pl 410x30

136 | 35

164

L 75x75x8 2490
L 75x75x8 2490

100

100

110 | 50 | 220 | 50 | 111
541

447

591

100

100

510 | 30 | 50 | 20
590

150

20

100

100

90 | 100 | 170 | 100 | 85
545

140 | 270 | 135 | 135 | 270 | 205

A